

**UNIVERSIDADE FEDERAL DO RIO GRANDE DO SUL
INSTITUTO DE QUÍMICA
PÓS-GRADUAÇÃO EM QUÍMICA**

Leliz Ticona Arenas

**SÍNTESE, CARACTERIZAÇÃO E PROPRIEDADES DE XEROGÉIS
HÍBRIDOS ORGANO INORGÂNICOS À BASE DE SÍLICA**

Tese apresentada como requisito parcial para a
obtenção de grau de Doutor em Química

Dr. Edilson Valmir Benvenuti
Orientador
Dra. Tania Maria Haas Costa
Co orientadora

Porto Alegre, Junho 2007

A presente tese foi realizada inteiramente pelo autor, exceto as colaborações as quais serão devidamente citadas nos agradecimentos, no período entre junho de 2003 e maio de 2007, no Instituto de Química da Universidade Federal do Rio Grande do Sul, sob Orientação do professor Doutor Edilson Valmir Benvenuti e Co-orientação da professora Doutora Tania Maria Haas Costa. A Tese foi julgada adequada para obtenção do título de Doutor em Química pela seguinte banca examinadora:

Comissão examinadora:

Com muito carinho

*Aos meus pais, Andrés e Dominga, aos meus irmãos
Edy, Norma, Bertha, Antonio e Andrés, e às minhas
queridas sobrinhas Litha e Karen*

AGRADECIMENTOS

Aos professores Edilson Valmir Benvenuti e Tania Maria Haas Costa pela orientação, apoio desde o início, ajuda incondicional e amizade. Muito Obrigado devo a vocês mais uma vez essa conquista, serei eternamente grata.

Aos professores que contribuirão com o desenvolvimento deste trabalho Celso Camilo Moro, Eder Cláudio Lima, obrigada pelo apoio.

Ao professor Silvio Luis Dias Pereira por toda a sua dedicação e o grande apoio na parte de eletroquímica.

Aos professores do grupo de eletroquímica Denise, Clarisse e Emilse por permitirem utilizar os equipamentos do laboratório assim como contribuir com discussões e esclarecimentos.

Ao CNPQ pela bolsa concedida.

Às minhas amigas e companheiras que participaram na elaboração deste trabalho Tanira, Adriana, Lina, Carol, Clarissa e Núbia.

Às minhas grandes amigas: Andréa, Débora, Jaqueline, Jordana, Marina, Sandra, Camila, Helena, Marluza e Priscila, pelo carinho, incentivo e amizade.

A todos os professores e funcionários do Instituto de Química que, de diferentes maneiras, contribuíram na realização deste trabalho.

A todos, a minha infinita gratidão.

LISTA DE TRABALHOS GERADOS

ARTIGOS

1. Arenas, L.T.; Dias, S. L. P.; Moro, C. C.; Costa, T. M. H.; Benvenuti, E. V.; Lucho, A. M.S; Gushikem, Y. Structure and property studies of hybrid xerogels containing bridged positively charged 1,4-diazoniabicyclo[2.2.2]octane dichloride. *J. Colloid Interface Sci.* **2006**, 297, 244.
2. Arenas, L. T.; Lima E. C.; Santos, A. A.; Vaghetti, J. P.; Costa, T. M. H.; Benvenuti, E. V. Use of statistical design of experiments to evaluate the sorption capacity of 1,4-diazoniabicyclo[2.2.2]octane/silica chloride for Cr(VI) adsorption. *Colloids Surf. A: Physicochem. Engin. Aspects.* **2007**, 297, 240.
3. Arenas, L. T.; Pinheiro, A. C.; Ferreira, J. D; Pereira, V. P.; Gallas, M. R. Costa, T. M. H.; Benvenuti, E. V.; Gushikem, Y. Anisotropic self-organization of hybrid silica based xerogels containing bridged positively charged 1,4-diazoniabicyclo[2.2.2]octane chloride. Submetido, **2007**
4. Arenas, L.T.; Gay, D. S. F.; Dias, S. L. P.; Moro, C. C.; Azambuja, D. S.; Costa, T. M. H.; Benvenuti, E. V.; Gushikem, Y. Brilliant yellow dye immobilized on silica and silica/titania based hybrid xerogels containing bridged positively charged 1,4-diazoniabicyclo[2.2.2]octane: Preparation, characterization and electrochemical properties study. Submetido, **2007**.
5. Arenas, L. T.; Simon, N. M.; Gushikem, Y.; Costa, T. M. H.; Lima, E. C.; Benvenuti, E. V. A water soluble 3-n-propyl-1-azonia-4-azabicyclo[2.2.2]octane chloride silsesquioxane grafted onto Al/SiO₂ surface. Chromium adsorption study. *Eclat. Quim.* **2006**, 31, 53.
6. Arenas, L. T.; Simm, C. W.; Gushikem, Y.; Dias, S. L. P.; Moro, C. C.; Costa, T. M. H.; Benvenuti, E. V. Synthesis of silica xerogels with high surface area using acetic acid as catalyst. *J. Braz. Chem. Soc. Aceito*, **2007**.

TRABALHOS APRESENTADOS EM CONGRESSOS

1. Arenas, L. T.; Pereira, V. P.; Gallas, M. R; Gushikem, Y.; Ferreira, J. D.; Pinheiro, A. C; Costa, T. M. H.; Benvenuti, E. V. Anisotropic organization of silica based hybrid material with the bridged positively charged 1,4-diazoniabicyclo[2.2.2]octane group In: 5th Brazilian MRS Meeting SBPMat, 2006, Florianópolis, S. C. v. E583. p. 176.
2. Simm, C. W.; Arenas, L.T.; Moro, C. C.; Benvenuti, E. V.; Costa, T. M. H. Influência da

- temperatura de gelificação em géis de sílica com elevada área superficial. In: XII Encontro de Química da Região Sul, 2005, Florianópolis, SC. v. QI034.
3. Pinheiro, A. C.; Arenas, L. T.; Ferreira, Núbia do Carmo.; Gushikem, Y.; Dias, S. L. P.; Costa, T. M. H.; Benvenuti, E. V. Obtenção de híbridos contendo o grupo 1,4-diazoniabicyclo [2.2.2] octano em ponte, carregado positivamente In: XIII Encontro de Química da Região Sul, 2005, Florianópolis, SC. v. QI-035.
 4. Simm, C. W.; Arenas, L. T.; Vilar, R. B. C.; Moro, C. C.; Costa, T. M. H.; Benvenuti, E. V. Obtenção de xerogel de sílica com alta área superficial In: 28ª Reunião anual da SBQ, 2005, Poços de Caldas, Livro de Resumos, v.QM. p.159.
 5. Arenas, L. T.; Aguirre, T. A. S.; Gushikem, Y.; Costa, T. M. H., Benvenuti, E. V. Caracterização eletroquímica do xerogel híbrido cloreto de 1,4 dipropil 1,4 diazoniabicyclo[2,2,2]octano silsesquioxano modificado com ferricianeto de potássio. In: XII Encontro de Química da Região Sul, 2004, Guarapuava, PR. v.QI. p.024.
 6. Corrêa, C. P.; Arenas, L. T.; Dias, S. L. P.; Gushikem, Y.; Costa, T. M. H.; Benvenuti, E. V. Híbrido microporoso sílica/celulose com dispersão de fases no nível molecular In: Congresso Latino Americano de Química, 27 Reunião Anual da SBQ, 2004, Salvador, BA. Livro de resumos, v.QM. p.197.
 7. Arenas, L. T.; Aguirre, T. A. S; Moro, C. C.; Costa, T. M. H.; Gushikem, Y.; Benvenuti, E. V. Obtenção do xerogel híbrido tipo ponte, cloreto de 1,4 dipropildiazôniabicyclo[2,2,2]octano silsesquioxano In: Congresso Latino Americano de Química - 27 Reunião Anual da SBQ, 2004, Salvador, BA. Livro de resumos, v. QM. p. 176.
 8. Arenas, L. T.; Aguirre, T. A. S, Lucho, A. M. S.; Gushikem, Y.; Moro, C. C.; Costa, T. M. H. Benvenuti, E. V. Xerogel híbrido tipo Puente, cloruro de 1,4 di propil 1,4 diazobicyclo [2.2.2] octano silsesquioxano In: XXII Congreso Peruano de Química, 2004, Lima, Peru. Libro de resúmenes, v. P-1.
 9. Corrêa, C. P.; Arenas, L. T.; Dias, S. L. P.; Costa, T. M. H.; Gushikem, Y.; Benvenuti, E. V. Acetato de Celulose / Sílica. Síntese e caracterização de um novo material híbrido. In: XI Encontro de Química da Região Sul, 2003, Pelotas., 2003. v.QI-09.

SUMÁRIO

	Pg
Resumo.....	vii
Abstract.....	viii
1- INTRODUÇÃO.....	1
2- OBJETIVOS.....	7
3- REFERÊNCIAS BIBLIOGRÁFICAS.....	8
4- ARTIGOS GERADOS.....	11
4.1- Structure and property studies of hybrid xerogels containing bridged positively charged 1,4-diazoniabicyclo[2.2.2]octane dichloride. <i>Journal of Colloid and Interface Science</i> , 2006 , 297, 244.	
4.2- Use of statistical design of experiments to evaluate the sorption capacity of 1,4-diazoniabicyclo[2.2.2]octane/silica chloride for Cr(VI) adsorption. <i>Colloids and Surfaces A-Physicochemical and Engineering Aspects</i> , 2007 , 297, 240.	
4.3- Anisotropic self-organization of hybrid silica based xerogels containing bridged positively charged 1,4-diazoniabicyclo [2.2.2] otane chloride. Submetido, 2007 .	
4.4- Brilliant yellow dye immobilized on silica and silica/titania based hybrid xerogels containing bridged positively charged 1,4-diazoniabicyclo[2.2.2]octane: Preparation, characterization and electrochemical properties study. Submetido, 2007 .	
4.5- Arenas, L. T.; Simon, N. M.; Gushikem, Y.; Costa, T. M. H.; Lima, E. C.; Benvenuto, E. V. A water soluble 3-n-propyl-1-azonia-4-azabicyclo [2.2.2]octane chloride silsesquioxane grafted onto Al/SiO ₂ surface. Chromium adsorption study. <i>Eclética. Química</i> , 2006 , 31, 53.	
4.6- Synthesis of silica xerogels with high surface area using acetic acid as catalyst. <i>Journal of the Brazilian Chemical Society</i> . Aceito, 2007	

RESUMO

O presente trabalho descreve a síntese, a caracterização e o estudo das propriedades de materiais híbridos nanoestruturados constituídos de sílica e do grupo orgânico 1,4-diazabicyclo[2,2,2]octano (dabco). A síntese desses materiais foi realizada pelo método sol-gel, partindo-se de precursores organosilanos desenvolvidos em nosso laboratório. Foram sintetizados materiais híbridos contendo o grupo orgânico covalentemente ligado à estrutura da sílica na forma pendente, contendo uma carga positiva (1-aza-4-azoniabicyclo[2,2,2]octano) e também materiais contendo o grupo orgânico na forma duplamente carregada, constituindo pontes (1,4-diazonibicyclo[2,2,2]octano).

Para o híbrido que apresenta o grupo orgânico na forma de pontes, foram sintetizadas amostras variando-se o conteúdo orgânico. Nas amostras com baixo conteúdo orgânico (até 3 %) observou-se que o diâmetro dos microporos está relacionado com o tamanho da cadeia desse grupo. Nas amostras com maior conteúdo orgânico a análise por difração de raios X evidenciou uma organização nanoestrutural que apresentou espaçamentos interplanares impostos pelo grupo orgânico positivamente carregado. A presença de birrefringência óptica nos materiais confirmou a existência de organização estrutural anisotrópica. Adicionalmente, as amostras mostraram-se transparentes e termicamente estáveis.

A presença do contra-íon cloreto nos híbridos permitiu seu uso como trocadores aniônicos na adsorção de Cr (IV) de soluções aquosas. Adicionalmente, foi possível imobilizar espécies eletroativas aniônicas, tais como o hexacianoferrato e o corante amarelo brilhante. Foram preparados eletrodos de pasta de carbono modificados com essas amostras e realizados estudos de voltametria cíclica, onde foi observado que essas espécies eletroativas encontram-se fortemente adsorvidas nos poros. O eletrodo de pasta de carbono modificado com uma amostra de híbrido contendo sílica/titânia e corante amarelo brilhante foi utilizado como mediador na eletroxidação do ácido ascórbico, possibilitando o desenvolvimento de um sensor para vitamina C.

Na perspectiva de estudar fatores que afetam as características morfológicas e texturais de materiais resultantes de sínteses em sistemas híbridos, apresenta-se também, a preparação de xerogéis microporosos de sílica, com área superficial elevada, acima de 800 m²g⁻¹. Esses xerogéis foram obtidos estudando-se alguns parâmetros experimentais como a temperatura de gelificação, solvente e catalisadores, sendo que a presença do ácido acético mostrou-se o fator primordial.

ABSTRACT

The present work describes the synthesis, the characterization and the study of properties of the hybrid nanostructured materials constituted by silica and the organic group 1,4-diazabicyclo[2,2,2]octane (dabco). The synthesis of the materials was performed using the sol-gel method, starting from organosilane precursors developed in our laboratory. Hybrid materials with the organic group covalently bonded to silica structure in the pendant form were prepared, containing one positive charge (1-aza-4-azoniabicyclo[2,2,2]octane), and also hybrid materials with the organic group in the double charged form, forming bridges (1,4-diazoniabicyclo[2,2,2]octane).

For the hybrid presenting the organic group in the bridged form, samples varying the organic content were prepared. In the samples with low organic content (up to 3 %) it was observed that the diameter of the micropores was related to the chain length of the organic group. In the samples with high organic content the X-ray diffraction analysis showed nanostructural organization with interplanar distances imposed by the positively charged organic group. The presence of optical birefringence in the materials confirmed the existence of anisotropic structural organization. Additionally the samples were transparent and thermally stable.

The presence of chloride contra-ions in the hybrids afforded their use as anionic exchangers in the adsorption of Cr (VI) from aqueous solutions. Additionally, it was possible to immobilize anionic electroactive species like hexacyanoferrate and brilliant yellow dye. Modified carbon paste electrodes were prepared with these samples and cyclic voltammetry studies were performed. It was observed that these electroactive species are strongly adsorbed in the pores. The carbon paste electrode modified with a hybrid containing silica/titania and brilliant yellow dye was used as mediator in the electrooxidation of ascorbic acid, enabling the development of a sensor for vitamin C.

In the perspective to study the factors that affect morphological and textural characteristics of materials resulting from syntheses in hybrid systems, it was also presented the preparation of silica microporous xerogels with high surface area, above $800 \text{ m}^2 \text{ g}^{-1}$. These xerogels were obtained studying some experimental parameters as gelation temperature, solvent and catalyst, being that the presence of acetic acid was significant.

1- INTRODUÇÃO

O desenvolvimento da ciência dos materiais trouxe importantes contribuições no avanço da tecnologia. A busca constante pela síntese de novos materiais com desempenho e propriedades otimizadas para aplicações inovadoras e o aperfeiçoamento de materiais já existentes é um desafio e um dos motivos da evolução técnica e científica atual.

Nesse contexto, encontra-se a possibilidade de combinar no nível molecular ou nanométrico componentes orgânicos e inorgânicos em um único material, surgindo assim, novos materiais conhecidos como híbridos organo-inorgânicos. A síntese desses materiais híbridos, além de oferecer a oportunidade de combinar em forma sinérgica as propriedades físico-químicas inerentes de seus constituintes, nos permite obter materiais com novas propriedades únicas, resultantes da combinação de seus componentes devido ao tamanho reduzido dos domínios que os compõe. Uma vantagem adicional é também a possibilidade de controlar a forma estrutural e morfológica em escala nanométrica ou molecular^{1,2}.

Em vista do grande potencial desses materiais, associadas ao seu caráter multidisciplinar, pesquisas voltadas a esta área vêm aumentando nos últimos anos e atraindo a atenção tanto de pesquisadores acadêmicos de diferentes áreas como despertando o interesse para uso industrial.

Dentre os híbridos organo-inorgânicos os que têm como suporte inorgânico a sílica tornam-se cada vez mais atrativos. O grande interesse nesses materiais deve-se ao fato deles apresentarem sinergicamente as propriedades da sílica tais como a rigidez, estabilidade mecânica e térmica, associadas com a reatividade do grupo orgânico. Além disso, existe uma maior facilidade em controlar as propriedades microestruturais como porosidade e área superficial, o que tem possibilitando que esses materiais se apresentem potencialmente para aplicações em processos de separação e adsorção²⁻⁴, na construção de sensores químicos⁵, em catálise heterogênea^{3,6}, como dispositivos ópticos^{7,8}, como carregadores de fármacos⁹ e em revestimentos¹⁰⁻¹¹.

O grupo orgânico presente nos híbridos a base de sílica pode encontrar-se, disperso na rede da sílica⁷ ou preso covalentemente formando ligação Si-C. Quando covalente ligado à rede inorgânica, os grupos orgânicos podem ser encontrados na forma pendente^{13,14} ou ainda fazendo parte da rede, formando pontes².

Uma forma de se obter materiais híbridos a base de sílica pode ser a partir da reação de condensação de compostos de silício, como alcóxidos, silicato de sódio ou organossilanos,

em presença de um tensoativo que atue como agente direcionador de estrutura. Os híbridos obtidos por este método são conhecidos como organosílicas mesoporosas organizadas, que se caracterizam principalmente por possuírem um ordenamento geométrico de mesoporos, com uma elevada dispersão do componente orgânico na rede inorgânica e elevada área superficial^{15,16}. Usando-se precursores que apresentam dois pontos de condensação, foi possível obter híbridos do tipo ponte nanoestruturados, com porosidade controlada, e com organização periódica do componente orgânico similar a um cristal. Essa cristalinidade pode proporcionar um melhor desempenho ao material híbrido em várias aplicações, sendo uma das grandes conquistas nesse campo¹⁷⁻²⁰.

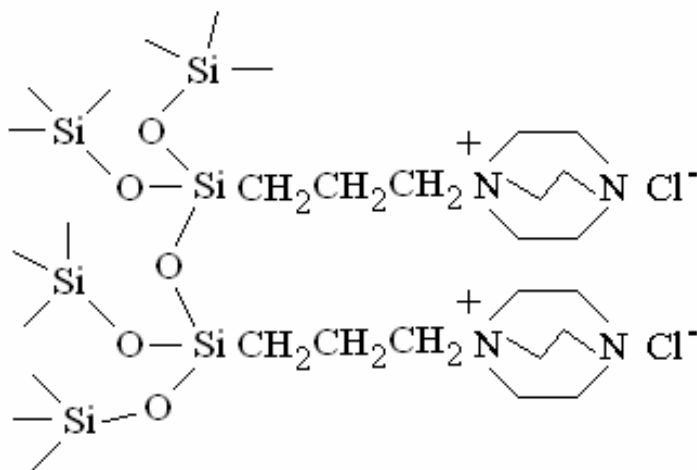
O método sol-gel, baseado em reações de hidrólise e condensação de precursores moleculares é outra estratégia de preparação de híbridos a base de sílica. A baixa temperatura de processamento, geralmente à temperatura ambiente, permite a incorporação de moléculas orgânicas^{7,13,14}, oligômeros, polímeros^{21,22} ou até mesmo biomoléculas na rede inorgânica²³. Como a combinação dos precursores acontece no nível nanométrico ou molecular, existe alta dispersão dos componentes orgânico e inorgânico. Portanto, os materiais obtidos pelo método sol-gel de síntese podem se apresentar homogêneos e com elevada pureza. Outra vantagem desse método é a versatilidade para se obter híbridos com diferentes configurações como monólitos²⁴, membranas²⁵, filmes²⁶, fibras²⁷ e pós²⁸, sendo que as características físico-químicas do sólido resultante podem ser controladas a partir das condições experimentais de síntese. O método sol-gel de síntese também permite a obtenção de híbridos nanoestruturados, com organização anisotrópica sem necessidade de adição de agentes direcionadores de estrutura²⁹, sendo que a organização nanostructural do híbrido está relacionada com a rigidez e a geometria do grupo orgânico³⁰⁻³², assim como, às interações do grupo orgânico no híbrido³²⁻³⁴. Além disso, esse método envolve relativamente baixos custos e simplicidade nos procedimentos experimentais.

Nos anos recentes, os materiais híbridos organo-inorgânicos a base de sílica contendo grupos orgânicos carregados positivamente têm atraído bastante atenção da comunidade científica. Esse interesse decorre das características que esses híbridos apresentam, pois pelo fato de possuírem um contra-íon em sua estrutura, tornam-se potencialmente importantes em diversas áreas tais como no tratamento de águas (como trocadores aniônicos), na separação e adsorção química e no desenvolvimento de sensores. Nesse sentido, o método sol-gel de síntese tem possibilitado a obtenção de novos materiais híbridos catiônicos. Já foram desenvolvidos filmes³⁵⁻³⁸, membranas^{39,40}, partículas^{35,41} e monólitos⁴²⁻⁴⁴ de híbridos

catiônicos com grupos amônio quaternário. Nesses materiais o grupo orgânico contendo o sal de amônio se encontra ligado covalentemente à estrutura da sílica e caracteriza-se por possuir estabilidade térmica e elevada capacidade de troca aniônica. Suas aplicações são, por exemplo, na adsorção e pré-concentração de ânions^{35,36}, como fase estacionária para cromatografia líquida de alta eficiência e eletrocromatografia^{35,43}, como sensores potenciométricos³⁵ e no preparo eletrodos quimicamente modificados³⁸.

Outros híbridos catiônicos também foram desenvolvidos. Materiais contendo o grupo catiônico imidazolio foram utilizados como trocadores aniônicos, na adsorção do ânion ReO_4^- ⁴⁵ e foram também usados como fase estacionária para cromatografia líquida, mostrando eficiência na separação de ânions inorgânicos, aminas e nucleotídeos⁴⁶. Outro híbrido catiônico bastante estudado foi o silsesquioxano contendo o íon piridínio. Além da capacidade de trocar ânions, esse material mostrou habilidade de formar filmes estáveis em substratos porosos, tornando possível sua aplicação na adsorção e pré-concentração de íons metálicos em solução etanólica^{47,48}. Também foi usado como sensor potenciométrico para sacarina⁴⁹, na imobilização de espécies eletroativas como as ftalocianinas tetrasulfonadas, porfirinas e o ânion hexacianoferrato, possibilitando o desenvolvimento de sensores eletroquímicos para o ácido oxálico⁵⁰, hidrazina⁵¹ e o ácido ascórbico⁵². Em recente trabalho, foi sintetizado um novo silsesquioxano contendo o grupo metilpiridínio que foi empregado na adsorção de metais em solução aquosa⁵³.

Recentemente foi sintetizada, em nosso grupo de pesquisa, Grupo de Estado Sólido e Superfícies da UFRGS, uma família de materiais híbridos do tipo silsesquioxano, usando-se o método sol-gel de síntese. Esse híbrido foi obtido com diferentes graus de incorporação do grupo orgânico catiônico, 3-n-propil-1-azônia-4-azabicyclo[2.2.2]octano (dabco silsesquioxano). Este grupo orgânico encontra-se pendente à estrutura da sílica como é mostrado no Esquema 1.



Esquema 1. Híbrido organo-inorgânico cloreto de 3-n-propil-1-azônia-4-azabicyclo [2.2.2] octano silsesquioxano.

As amostras com elevado conteúdo orgânico foram estáveis termicamente e apresentaram propriedades interessantes como solubilidade em água e habilidade de formar filmes sobre superfícies de matrizes porosas⁵⁴. Foram usadas como matrizes o gel de sílica comercial, alumina e sílica modificada com óxido de alumínio (Al/SiO₂). A melhor adesão do híbrido ocorreu na superfície de alumina e Al/SiO₂.

A matriz Al/SiO₂ enxertada com o híbrido mostrou capacidade de adsorver haletos metálicos em solução etanólica⁵⁵, na seguinte ordem CdCl₂ > ZnCl₂ > CuCl₂. Numa situação competitiva este material também mostrou ser mais seletivo para o Cd²⁺.

Uma série de amostras desse híbrido, contendo baixo conteúdo orgânico, mostrou-se insolúvel em água. Além disso, foi observado que sua microestrutura foi drasticamente influenciada pelo aumento do conteúdo inorgânico. Tanto a área superficial específica como a porosidade foram aumentadas. O aspecto físico também foi alterado, sendo que as amostras contendo maior conteúdo orgânico apresentaram uma estrutura compacta enquanto que aquelas com menor incorporação orgânica apresentaram uma superfície rugosa, formada por partículas primárias esferóides⁵⁶. Essa variação na microestrutura mostrou-se um fator importante quando essas amostras foram aplicadas na adsorção do Cd²⁺ em solução aquosa. A amostra com menor conteúdo orgânico adsorveu maior quantidade de Cd²⁺ do que aquela com maior incorporação orgânica⁵⁷. Em outros trabalhos descritos na literatura, o grupo catiônico dabco, quando imobilizado na superfície da sílica mostrou seletividade para o íon perclorato, possibilitando o desenvolvimento de um novo sensor potenciométrico para este íon⁵⁸. Quando

ancorado à superfície de acetato de celulose, modificada com óxido de alumínio, o grupo dabco mostrou habilidade para adsorver Fe^{+3} , Co^{+2} e Cu^{+2} , em solução etanólica⁵⁹.

No presente trabalho, materiais híbridos nanoestruturados a base de sílica foram sintetizados usando-se o método sol-gel de síntese. Os materiais foram caracterizados usando-se várias técnicas visando o conhecimento de suas características físico-químicas. Baseados em suas características foi estudada a viabilidade de aplicação em algumas áreas.

Na primeira etapa do trabalho foi dada continuidade à pesquisa das propriedades de adsorção do híbrido dabcosil sesquioxano, para isso, realizou-se um estudo da capacidade de adsorção do Cr (VI) pelo dabcosil sesquioxano, enxertado na superfície Al/SiO₂, em solução aquosa. O material foi caracterizado e a capacidade de adsorção avaliada mediante isotermas de adsorção, sendo que o sistema obedece à equação de Langumir.

Tendo em vista as importantes aplicações dos híbridos organo-inorgânicos a base de sílica, sobre tudo os que possuem grupos orgânicos carregados positivamente, com o grupo catiônico dabco, a perspectiva de se obter um híbrido contendo o dabco com uma dupla carga catiônica, nos pareceu oportuna. O dabco neste caso se encontraria formando pontes na rede inorgânica, com dois pontos de polimerização. Nesse sentido, realizou-se a síntese do precursor orgânico cloreto de 1,4-bis-(3-trimetoxisililpropil)diazoniabicyclo[2,2,2]octano ((R₂dabco)Cl₂), a partir do qual se obteve um novo material híbrido, contendo esse grupo orgânico catiônico ligado em ponte a rede inorgânica. Foi estudada a influência da presença do grupo orgânico na microestrutura, as suas características e propriedades adsorventes. Também foi avaliado o comportamento eletroquímico do corante amarelo brilhante adsorvido por troca aniônica na superfície do híbrido (R₂dabco)Cl₂/sílica e a influência da adição de titânia à rede inorgânica. A potencialidade de sua utilização como electrocatalisador para a oxidação do ácido ascórbico foi investigada.

Posteriormente, foi obtida uma segunda seqüência de amostras do material híbrido, (R₂dabco)Cl₂/sílica, mudando-se as condições experimentais de síntese, tendo sido possível incorporar maior quantidade de orgânico à rede inorgânica. Na caracterização estrutural foi observada uma organização nanoestrutural nas amostras que apresentam grande quantidade de orgânico. Essas amostras apresentaram propriedades anisotrópicas interessantes.

Foi feito um estudo comparativo de algumas características e propriedades, entre uma amostra do híbrido (R₂dabco)Cl₂/sílica e uma sílica organofuncionalizada pelo método enxerto (*grafting*), com o mesmo grupo orgânico, na mesma quantidade. As características microestruturais das amostras foram bastante distintas. Essas diferenças influenciaram

fortemente as suas propriedades de adsorção de Cr (VI) em meio aquoso. Nessa etapa foi desenvolvido um planejamento estatístico de experimentos.

Considerando a importância que têm os materiais porosos a base de sílica, com alta área superficial, principalmente nas variadas aplicações como suporte de catalisadores e processos de adsorção e separação^{60,61}, nesse trabalho foram estudadas algumas condições experimentais de síntese de géis de sílica em sistemas híbridos, tais como solvente usado, temperatura de gelificação e catalisador ácido utilizado. Foi observado que a adição de ácido acético ao sistema pode resultar em xerogéis de sílica amorfos microporosos com área superficial superior a $800 \text{ m}^2\text{g}^{-1}$.

2- OBJETIVOS

Os Objetivos gerais deste trabalho estão inseridos na proposta do Grupo de Química do Estado Sólido e Superfícies da UFRGS, cujos interesses estão centrados na síntese caracterização e estudo das propriedades de híbridos organo-inorgânicos a base de sílica.

Os objetivos específicos deste trabalho são:

- a) Sintetizar novos precursores organosilanos contendo cadeia carregada positivamente usando 1,4-diazabicyclo[2.2.2]octano (dabco) como reagente de partida.
- b) Desenvolver, a partir dos precursores organosilanos sintetizados, novos materiais híbridos que contenham na rede estrutural cadeia orgânica positivamente carregada contendo o grupo 1,4-diazoniabicyclo[2.2.2]octano.
- c) Determinar as características físico-químicas e explorar a viabilidade de aplicação dos materiais híbridos como adsorventes e sensores eletroquímicos, a partir das propriedades observadas.
- d) Estudar a influência dos parâmetros experimentais de síntese em sistemas híbridos, na preparação de materiais de alta área superficial específica.

3- REFERÊNCIAS BIBLIOGRÁFICAS

1. Sharp, K. G. *Adv. Mater.* **1998**, 10, 1243.
2. Loy, D. A.; Shea, K. J. *Chem. Mater.* **2001**, 13, 3306.
3. Price, P. M.; Macquarrie, D.J. *J. chem. Soc. Dalton Trans.* **2000**, 2, 101.
4. Sanches, C.; Julian, B.; Belleville, P.; Popall, M. *J Mater.Chem.* **2005**, 15, 3559.
5. Walcarius, A. *Chem. Mater.* **2001**, 13, 3351.
6. Ford, D. M.; Simanek, E. E.; Shantz, D. F. *Nanotechnology* **2005**, 16, S458.
7. Costa, T. M. H.; Hoffmann, H. S.; Benvenuti, E. V.; Stefani, V.; Gallas, M. R. *Opt. Mater.* **2005**, 27, 1819.
8. Serwaczak, M.; Wübbenhorst, M. W.; Kucharski, S. *J Sol-Gel Sci Techn.* **2006**, 40, 39.
9. Fagundes, L. B.; Sousa, T. G. F.; Sousa, A.; Silva, V. V.; Sousa, E. M. B. *J. Non-Cryst. Solids.* **2006**, 352, 3496.
10. Zandi-zand, R.; Ershad-langroudi, A.; Rahimi, A. *Prog. Org. Coat.* **2005**, 53, 286.
11. Hofacker, S.; Mechtel, M.; Mager, M.; Kraus, H. *Prog.Inorg. Coat.* **2002**, 45, 159.
12. Chou, T. P.; Chandrasekaran, C. *J. of Sol-Gel Sci. Techn.* **2003**, 26, 321.
13. Gay, D. S. F.; Moro, C. C.; Costa, T. M. H.; Benvenuti, E. V.; Gushikem, Y. *J. Sol-Gel Sci. Technol.* **2005**, 34, 195.
14. Azolin, D. R.; Moro, C. C.; Costa, T. M. H.; Benvenuti, E. V. *J. Non-Cryst. Solids.* **2004**, 337, 201.
15. Wang, W.; Xie, S.; Zhou, W.; Sayari, A.; Hamoudi, S. *Chem. Mater.* **2001**, 13, 3151.
16. Hodgkins, R. P.; García-Bennett, A. E.; Wright, P A. *Microporous Mesoporous Mater.* **2005**, 79, 241.
17. Kapoor, M. P; Inagaki, S. *Bull. Chem. Soc. Jpn.* **2006**, 7, 10.
18. Inagaki, S.; Guan, S.; Ohsuna, T.; Terasaki, O. *Nature.* **2002**, 416, 304.
19. Kapoor, M. P.; Yang, Q.; Inagaki, S. *J. Am. Chem. Soc.* **2002**, 124, 15177.
20. Xia, Y.; Mokaya, R. *J. Phys. Chem. B.* **2006**, 110, 3889.
21. Al-Kandary, S. H.; Ali, A. A. M.; Ahmad, Z. *J. Mater. Sci.* **2006**, 41, 2907.
22. Kickelbick, G. *Prog. Polym. Sci.* **2003**, 28, 83.
23. Avnir, D.; Coradin, T.; Lev, O.; Livage, J. *J. Mater. Chem.*, **2006**, 16, 1013.
24. Avila-Herrera, C.A.; Gómez-Guzmán, O.; Almaral-Sánchez, J. L.; Yáñez-Limón, J.M J.; Muñoz-Saldaña, J.; Ramírez-Bom, R. *J Non-Cryst solids* **2006**, 352, 356.

25. Aparício, M.; Mosa, J.; Duran, A. *J Sol-Gel Sci Techn.* **2006**, 40, 309.
26. Bonilla, B.; Martinez, M.; Mendoza, A. M.; Widmaier, J. M. *Eur. Polymer J.* **2006**, 42, 2977.
27. Yang, Y.; Suzuki, M.; Fukui, H.; Shirai, H.; Kenji, H. *Chem. Mater.* **2006**, 18, 1324.
28. Laranjo, M. T.; Stefani, V.; Benvenuti, E. V.; Costa, T. M. H.; Ramminger, G. O.; Gallas, M. R. *J. Non-Cryst. Solids.* **2007**, 353, 24.
29. Boury, B.; Corriu, R. J. P. *Chem Commun.* **2002**, 8, 795.
30. Ben, F.; Boury, B.; Corriu, R. J. P.; Strat, V. L. *Chem. Mater.* **2000**, 12, 3249.
31. Boury, B.; Ben, F.; Corriu, R. J. P.; Delord, P.; Nobili, M. *Chem. Mater.* **2002**, 14, 730.
32. Cerveau, G.; Corriu, R. J. P.; Framery, E.; Lerouge, F. *Chem. Mater.* **2004**, 16, 3794.
33. Lerouge, F.; Cerveau, G.; Corriu, R. J. P. *J. Mater. Chem.* **2006**, 16, 90.
34. Nam, H.; Boury, B.; Park, S. Y. *Chem. Mater.* **2006**, 18, 5716.
35. Tien, P.; Chau, L-K.; Shieh, Y-Y.; Lin, W-C.; Wei, G-T. *Chem. Mater.* **2001**, 13, 1124.
36. Wei, H.; Collison, M. M. *Anal. Chim. Acta.* **1999**, 397, 113.
37. Liu, A.; Zhou, H.; Honma, I. *Electrochem Commun.* **1999**, 7, 1.
38. Lin, C-L.; Tien, P.; Chau, L-K.; *Electroch. Acta* , **2004**, 49, 573.
39. Wu, C.; Xu, T.; Weihua, Y. *J. Membr. Sci.* **2003**, 216, 269.
40. Kogure, M.; Ohya, H.; Peterson, R.; Hosaka, M.; Kim, J-J.; Mc Fadzen, S. *J. Membr. Sci.* **1997**, 126, 161.
41. Wu, C.; Xu, T.; Weihua, Y. *Eur. Polym. J.* **2005**, 41, 1901.
42. Kanungo, M.; Collinson, M. M. *Langmuir.* **2005**, 21, 82.
43. Lin, T-A.; Li, G-Y.; Chau, L-K. *Anal. Chim. Acta.* **2006**, 576, 117.
44. Ye, F.; Xie, Z.; Wong, K-Y. *Electrophoresis.* **2006**, 27, 373.
45. Lee, B.; Jung Im, H-J.; Luo, H.; Hagaman, E. W.; Dai, S. *Langmuir* **2005**, 21, 5372.
46. Qui, H.; Jiang, S.; Liu, X. *J. Chromatogr A.* **2006**, 1103, 265.
47. Alfaya, R. V. S.; Fujiwara, S. T.; Gushikem, Y.; Kholin, Y. V. *J. Colloid Interface Sci.* **2004**, 269, 32.
48. Fujiwara, S. T.; Gushikem, Y.; Alfaya, V. S. R. *Colloids. Surf A.* **2001**, 178, 135.
49. Alfaya, R. V. S.; Alfaya, A. A. S.; Gushikem, Y.; Rath, S. *Anal. Lett.* **2000**, 33, 2859.
50. Lucho, A. M. S.; Oliveira, E. C.; Pastore, H. O. *J. Electroanal. Chem.* **2004**, 573, 55.
51. Fujiwara, S. T.; Gushikem, Y.; Pessoa, C. A. *Electroanalysis.* **2005**, 17, 783.
52. Alfaya, R. V. S.; Gushikem, Y.; Alfaya A. A. S. *J. Braz. Chem. Soc.* **2000**, 11, 281.

53. Mogosso, H. H.; Panteleimonov, A. V.; Kholin, Y. V.; Gushikem, Y. *J. Colloid Interface Sci.* **2006**, 303, 18.
54. Arenas, L. T.; Langaro, A.; Gushikem, Y.; Moro, C. C.; Costa, T. M. H.; Benvenuti, E. *V. J. Sol-Gel Sci. Technol.* **2003**, 28, 51.
55. Arenas, L. T. Dissertação de Mestrado. Universidade Federal do Rio Grande do Sul, 2003.
56. Arenas, L. T.; Aguirre, T. A. S; Langaro, A.; Gushikem, Y.; Benvenuti, E. V.; Costa, T. M. H.; *Polymer.* **2003**, 44, 5521.
57. Arenas, L. T.; Vaghetti, J. C. P.; Moro, C. C.; Lima, E. C.; Benvenuti, E. V.; Costa, T. M. H.; *Mater. Lett.* **2004**, 58, 895.
58. Fernandes, J. R.; Kubota, L. T.; Gushikem, Y.; Neto, G. O. *Anal. Lett.* **1993**, 26, 2555.
59. Splendore, G.; Benvenuti, E. V.; Kholin, Y. V.; Gushikem, Y. *J. Braz. Chem. Soc.* **2005**, 16, 147.
60. Ishii, R.; Nakatsuji, M.; Ooi, K. *Microporous Mesoporous Mater.* **2005**, 79, 111.
61. Valdé-Sólis, T.; Fuertes, A. B. *Mater. Research Bull.* **2006**, 41, 2187.

4- ARTIGOS

- 4.1- Structure and property studies of hybrid xerogels containing bridged positively charged 1,4-diazoniabicyclo[2.2.2]octane dichloride. *Journal of Colloid and Interface Science*, **2006**, 297, 244.



ELSEVIER

Available online at www.sciencedirect.com

SCIENCE @ DIRECT®

Journal of Colloid and Interface Science 297 (2006) 244–250

 JOURNAL OF
 Colloid and
 Interface Science

www.elsevier.com/locate/jcis

Structure and property studies of hybrid xerogels containing bridged positively charged 1,4-diazoniabicyclo[2.2.2]octane dichloride

Leliz T. Arenas^a, Sílvia L.P. Dias^a, Celso C. Moro^a, Tania M.H. Costa^a, Edilson V. Benvenutti^{a,*}, Alzira M.S. Lucho^b, Yoshitaka Gushikem^b

^a Instituto de Química, Universidade Federal do Rio Grande do Sul, C.P. 15003, 91501-970 Porto Alegre, Rio Grande do Sul, Brazil

^b Instituto de Química, Universidade Estadual de Campinas, C.P. 6154, 13083-970 Campinas, São Paulo, Brazil

Received 6 September 2005; accepted 13 October 2005

Available online 21 November 2005

Abstract

The compound di-3-*n*-propyltrimethoxysilane (1,4-diazoniabicyclo[2.2.2]octane) dichloride, [(MeO)₃Si(CH₂)₃N⁺(CH₂CH₂)₃N⁺(CH₂)₃Si(OMe)₃]Cl₂ was obtained and was used as a precursor reagent to obtain hybrid xerogels where the organic molecule was bonded to a silica framework by reacting the ends of both sides of the precursor reagent. That is, both –Si(OMe)₃ groups react with tetraethylorthosilicate (TEOS) by hydrolysis–condensation reactions. The resulting hybrid xerogels with variable C/Si mole ratios were prepared and analyzed and their textural characteristics determined. The samples prepared presented micropores with diameter 1.5 nm, the chain length of which matched with the estimated length of the organic bridging group. The charged organic bridging groups allow the immobilization of hexacyanoferrate ions by an ion exchange process. The electron transfer process of the hexacyanoferrate anionic complex confined in the pores of the matrices was studied by cyclic voltammetry.

© 2005 Elsevier Inc. All rights reserved.

Keywords: Dabco; Silica-based polymers; Sol–gel; Electrochemical measurements

1. Introduction

Hybrid xerogel materials offer exceptional opportunities to combine the important properties of organic and inorganic materials and also to create entirely new compositions with truly unique properties [1–5]. Of interest has been to prepare hybrid materials where the organic component is bonded to a polymeric silica skeleton framework [6–8].

Recently, the preparation and characterization of a charged hybrid containing 3-*n*-propyl-1-azonia-4-azabicyclo[2.2.2]octane chloride, (MeO)₃Si(CH₂)₃N⁺(CH₂CH₂)₃NCl[–], reacted with TEOS to obtain an organic group bonded to a silica framework [9], as described by Scheme 1, was reported.

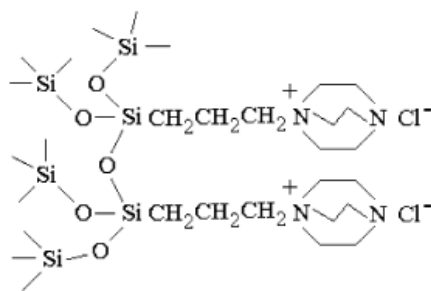
An important characteristic of this xerogel was its high solubility in water and its capacity to form stable thin layer films on various surfaces containing silanol, SiOH, or aluminol, Al–OH,

groups [10]. The solubility observed in this case was dependent on the amount of the organic, material i.e., on the Si/C mole ratios. When the inorganic content in the matrices was augmented a decrease of the solubility was observed [9]. Knowledge of this property led us to prepare a series of insoluble charged hybrid xerogels with potential application as metal adsorbents from aqueous solutions [11,12]. Additionally, previous papers using charged dabco grafted onto silica-gel surfaces showed selectivity to perchlorate ions making it possible to develop a new potentiometric sensor for these ions [13].

In view of the interesting properties of these silica-based xerogels containing charged groups bonded to the silica framework, we undertook to obtain a hybrid where the organic groups are bonded to both nitrogen atoms of the dabco molecule, resulting in a doubly charged species bonded to a silica framework. These positively charged organic groups make possible the use of the materials as anionic exchanger materials [14–16] and as a substrate base for immobilization of electroactive species and thus useful in preparing chemically modified elec-

* Corresponding author. Fax: +55 51 33167304.

E-mail address: benvenutti@iq.ufrgs.br (E.V. Benvenutti).



Scheme 1.

trodes [17]. The important property of these electrodes has been that the devices produced presented improved sensitivity and selectivity, which are very important characteristics of electrochemical sensors [18–20].

In this work, we report the synthesis of di-3-*n*-propyltrimethoxysilane (1,4-diazoniabicyclo[2.2.2]octane) dichloride, which was used as a precursor to obtain the hybrid xerogels, where the organic groups were bonded in a bridged way to a silica framework. Materials with different C/Si mole ratios were prepared and characterized. The hexacyanoferrate anionic complex was adsorbed onto the obtained solids by an ion exchange reaction and their electrochemical behavior studied by cyclic voltammetry. The electron transfer process can reveal how the hexacyanoferrate species are confined in the pores of the matrices obtained [21–23].

2. Materials and methods

2.1. Preparation of the charged precursor

1,4-Diazabicyclo[2.2.2]octano (dabco) (8 mmol), previously sublimed, was dissolved in 20 ml of dimethylformamide. To the resultant solution 3.0 ml (16 mmol) of 3-chloropropyltrimethoxysilane (CPTMS) was added. The mixture was heated for 72 h at reflux temperature (ca. 90 °C), under stirring and argon atmosphere. The white solid obtained was filtered and washed with methyl alcohol and then dried for 2 h in an oven at 90 °C. The resulting solid, named di-3-*n*-propyltrimethoxysilane (1,4-diazoniabicyclo[2.2.2]octane) dichloride, hereafter designated as (R₂dabco)Cl₂ (R = (H₃CO)₃Si(CH₂)₃-), was used as organic precursor for the hybrid xerogel synthesis. The elemental analyses results obtained are C = 27.9 wt% (23.2 mmol g⁻¹); N = 6.5 wt% (4.6 mmol g⁻¹); Cl⁻ = 3.9 mmol g⁻¹.

2.2. Preparation of the bridged hybrid xerogels

The organic precursor dabconia dichloride was dissolved in a mixture of dimethylsulfoxide (DMSO), water, and, hydrofluoric acid (HF) and heated at 60 °C. To this solution tetraethylorthosilicate (TEOS), previously dissolved in ethanol and water, was added. The reaction mixture was allowed to stand for 30 days, open to the atmosphere at a constant temperature of 40 ± 1 °C, for gelation and evaporation of solvent. The resulting xerogel was washed with ethanol and dried in an oven at

Table 1
Synthesis conditions of the hybrid xerogels

Sample	Organic precursor solutions ^a				TEOS solutions ^a		
	(R ₂ dabco)Cl ₂ (mg ^b)	DMSO (ml ^c)	Water (ml ^c)	HF (ml ^c)	TEOS (ml ^c)	ETOH (ml ^c)	H ₂ O (ml ^c)
D1	50	5.0	0.6	0.1	5.0	5.0	1.0
D2	100	5.0	0.6	0.1	5.0	5.0	1.0
D3	100	5.0	0.6	0.1	2.5	2.5	0.2

^a Quantity added in the synthesis.

^b Deviation 1 mg

^c Deviation lower than 1%.

90 °C for 2 h. The experimental conditions are summarized in Table 1.

2.3. Immobilization of potassium hexacyanoferrate

The hybrid xerogel sample (500 mg) was immersed in a 0.5 mol l⁻¹ potassium hexacyanoferrate solution (20 ml) and the mixture was stirred for 3 h at 25 °C. The modified solid was filtered and washed with distilled water and finally dried in an oven at 90 °C for 1 h.

2.4. Elemental analyses

The elemental analyses of the organic groups incorporated into the matrices, were carried out on a CHN Perkin–Elmer M CHNS/O Analyzer, Model 2400. The analyses were made in triplicate.

The ionized chloride was made by immersing the material in HNO₃ solution, under stirring. The chloride ion was potentiometrically analyzed by titration using silver nitrate, with a calomel electrode as reference.

2.5. ¹³C CP MAS analyses

Solid state NMR spectroscopy was performed on a Bruker 300/P spectrometer using MAS (magic angle) with CP (cross-polarization) experiments of a pulse length of 1 ms and recycle delay of 2 s.

2.6. Infrared spectra

Self-supported disks of the materials, having a diameter of 2.5 cm, weighing ca. 100 mg, with a disk sufficiently thin to allow measurements by the transmission technique were prepared. The disks were heated at 120 °C under vacuum (10⁻² Torr) for 1 h. The IR cell used in this work has already been described [24]. The equipment used was a Shimadzu FTIR, Model 8300. The spectra were obtained at room temperature with a resolution of 4 cm⁻¹ and 100 cumulative scans.

2.7. SAXS analyses

The small-angle X-ray scattering data were obtained on Shimadzu XD3A equipment using CuK α radiation source.

The average pore radii of the samples were obtained using the Guinier law [25,26]. This law establishes that the

scattering intensities $I(q)$ are described as $\ln I(q) = \ln I_0 - (R_G^2 q^2)/3$, where R_G is the gyration radii and q is defined as $q = (4\pi \sin \theta)/\lambda$, where θ is the scattering angle and λ the wavelength of the X-rays used. The gyration radii could be calculated by the equation $R_G = (3p)^{1/2}$, where p is the slope of the Guinier plot ($\ln(q)$ vs q^2). Assuming spherical pores, the pore radii were obtained by the equation $R_P = (5/3)^{1/2} R_G$.

2.8. Pores size distribution

The pore size distribution data were obtained by measuring the nitrogen adsorption–desorption isotherms, determined at the boiling point of liquid nitrogen, using a homemade volumetric apparatus connected to a turbomolecular vacuum line system, employing a Hg capillary barometer. The apparatus was frequently checked with an alumina (Aldrich) standard reference (150 mesh, 5.8 nm, and $155 \text{ m}^2 \text{ g}^{-1}$). Prior to the measurements, the xerogel samples were degassed at 120°C in vacuum for 2 h. The data obtained were analyzed using the BJH (Barret, Joyner, and Halenda) method [27].

2.9. Surface areas

The specific surface areas of the previous degassed solids at 120°C , under vacuum, were determined by the BET (Brunauer, Emmett, and Teller) [28] multipoint technique using the volumetric apparatus cited above, using nitrogen as probe.

2.10. Cyclic voltammetric measurements

The cyclic voltammetric measurements were carried out on an Autolab PGSTAT 20 potentiostat–galvanostat. The electrochemical cell system consisted of a working electrode, a reference electrode (saturated calomel electrode, SCE), and a platinum counter electrode. The working electrode was prepared as a carbon paste electrode by mixing in the ratio of 50% (w/w) of graphite/xerogel and a drop of mineral oil.

3. Results and discussion

3.1. Charged precursor $(R_2\text{dabco})\text{Cl}_2$

The reaction that describes the preparation of the precursor reagent $(R_2\text{dabco})\text{Cl}_2$, can be described by the equation represented in Scheme 2. The nucleophilic attack on the RCl by both dabco basic nitrogens results in a doubly $(\text{H}_3\text{C})_3\text{Si}(\text{CH}_2)_3$ -bonded to the quaternary N atoms of bridged dabco.

The ^{13}C CP MAS NMR spectrum of the $(R_2\text{dabco})\text{Cl}_2$ is presented in Fig. 1. The NMR spectrum is consistent with two bonded *n*-propyltrimethoxysilane groups, as represented in Scheme 2 and comparable to similar compounds described in the literature [29,30]. The peaks positions observed (in ppm) are assigned according to the C atoms numbered in the inset Fig. 1 as follows C^1 10.3, C^2 16.2, C^3 45.2, C^4 52.6, and C^5 66.9 [29,30].

The organic content of $(R_2\text{dabco})\text{Cl}_2$ was determined by elemental analyses. The ionized chloride was determined by

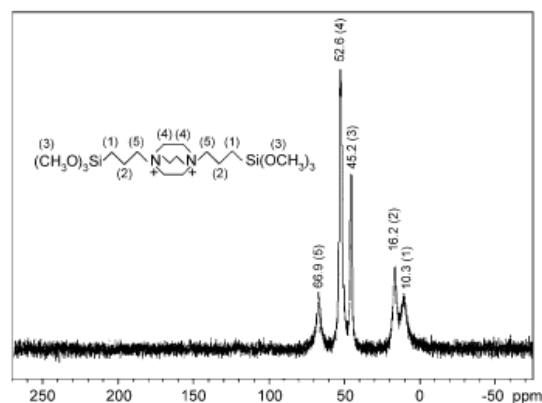
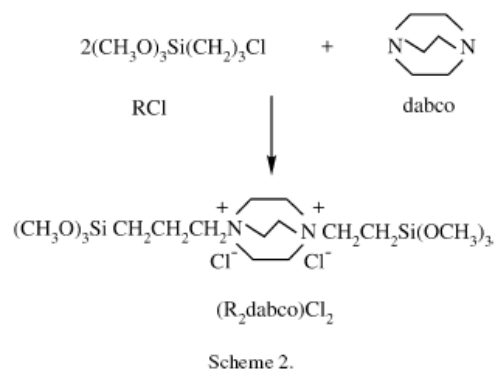
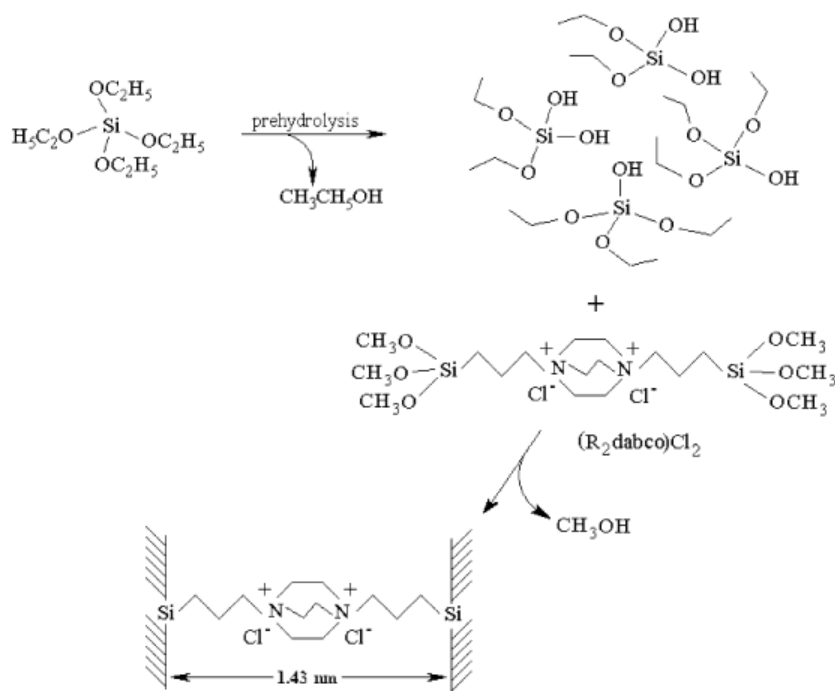


Fig. 1. ^{13}C NMR spectra of di-3-*n*-propyltrimethoxysilane (1,4-diazabicyclo[2.2.2]octane) dichloride $(R_2\text{dabco})\text{Cl}_2$.

potentiometric titration using the standard AgNO_3 as titrant. The elemental analyses obtained were $\text{C} = 27.9 \text{ wt}\%$ (23.2 mmol g^{-1}); $\text{N} = 6.5 \text{ wt}\%$ (4.6 mmol g^{-1}); $\text{Cl}^- = 3.9 \text{ mmol g}^{-1}$. The results are also consistent with a doubly bridged species, as shown in Scheme 2, from which the expected mole ratio is $\text{N}/\text{Cl}^- = 1.0$ and the experimental value is $\text{N}/\text{Cl}^- = 1.2$. Taking into account the reactivity of the methoxy groups bonded to the Si atom in $-\text{Si}(\text{OCH}_3)_3$, it can be expected that partial hydrolysis of the Si–O–C bond can occur during the preparation, therefore, only the relative N elemental analysis value is considered. We observe that the expected N/C mole ratio should be 0.11 against the experimental one of 0.20. This higher value is assigned to the partial hydrolysis of the $\text{Si}(\text{OCH}_3)_3$ group resulting in $\text{Si}(\text{OCH}_3)_{3-n}(\text{OH})_n$, which can also explain the low solubility of $(R_2\text{dabco})\text{Cl}_2$ obtained. The compound prepared can be dissolved only in DMSO/water mixture in the presence of HF and heating, as described in the experimental part. It is important to point out that the presence of nonhydrolyzed methoxy groups is confirmed by the ^{13}C NMR spectrum shown in Fig. 1. On the basis of expected C content (42.4 wt% for non-hydrolyzed compound) a loss of about 14 wt% is estimated for the compound prepared.

3.2. Bridged hybrid xerogels

Starting from $(R_2\text{dabco})\text{Cl}_2$ it was possible to prepare hybrid bridged silica based xerogels with different contents of silica, according to conditions described in Table 1. The reaction equa-



Scheme 3.

Table 2
Elemental analyses for hybrid xerogels

Sample	C (wt%) ^a	N (wt%) ^b	N/C mole ratios ^c
D1	3.89 (3.24) ^d	0.66 (0.47) ^d	0.15
D2	4.06 (3.38)	0.76 (0.54)	0.16
D3	4.61 (3.84)	1.00 (0.71)	0.18

^a Deviation 5%.

^b Deviation 10%.

^c Expected mole ratio: 0.17.

^d In parenthesis: mmol g⁻¹.

tion that describes the preparation of xerogel is represented by Scheme 3. The first step of the preparation consisted in the prehydrolysis of TEOS in water/ethanol solution. The reaction of (R₂dabco)Cl₂ occurs very slowly and the gel is formed by the reaction of CH₃O–Si with ≡Si–OH of the prehydrolyzed TEOS molecules.

The elemental analyses are presented in Table 2. The results of the C, N atoms indicate that in the course of preparations the –CH₂–⁺N≡ bonds were not broken. The N/C ratios obtained are 0.15, 0.16, and 0.18 for D1, D2, and D3, respectively, and the expected N/C mole ratio is 0.17. The calculation of the expected mole ratio was made based on assumption that all RO–Si (R = –CH₃ and –C₂H₅) were hydrolyzed at the end of the reaction process.

Fig. 2 shows the pore size distribution curves and in the inset figure the N₂ adsorption–desorption isotherms. Adsorption in the mesopore region of the isotherms ($P/P_0 > 0.5$) is observable in the curve for D1. This sample showed a single mesopore region with maximum distribution at 4 nm radius, like pure silica xerogel obtained in similar conditions [31]. For the samples

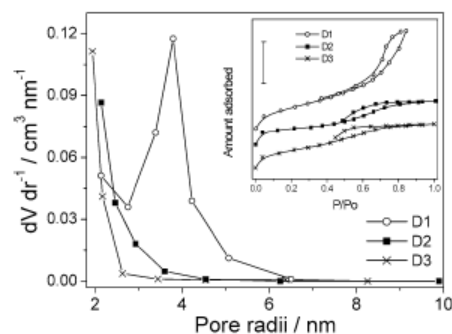


Fig. 2. Pore size distributions for D1, D2, and D3 samples. Inset figure: N₂ adsorption–desorption isotherms. The bar value is 40 mg g⁻¹.

containing lower relative amounts of silica in the matrices, D2 and D3, the pore size distribution curves show the presence of mesopores with radius lower than 2.5 nm. The greater content of organic molecules in these two samples appears to be responsible for the matrices presenting a shift in the pore distribution curves to lower diameter values. Such behavior has already been reported in similar hybrid xerogels where high organic content normally generates matrices presenting pores with lower diameter than pure inorganic matrices [11,32].

The surface areas and pore volumes of the samples obtained from the isotherms are presented in Table 3. We observe that sample D1 presenting the lower organic loading showed the higher area, 570 m² g⁻¹, and for samples D2 and D3 presenting higher organic contents, areas of 290 and 390 m² g⁻¹ were observed, respectively. The presence of a larger amount of SiO₂ in the matrices is presumably the main factor responsible for determining the higher specific surface area for D1. The decrease

Table 3
BET surface area, pore volume and SAXS results

Sample	BET surface area (m ² g ⁻¹)	Pore volume (cm ³ g ⁻¹)	Slope of Guinier curve	Radii of gyration (nm)	Pore diameter (nm)
D1	570 ± 25	0.85 ± 0.04	-0.129	0.62	1.6 ± 0.1
D2	290 ± 26	0.40 ± 0.04	-0.102	0.55	1.4 ± 0.1
D3	390 ± 27	0.29 ± 0.04	-0.155	0.68	1.7 ± 0.1

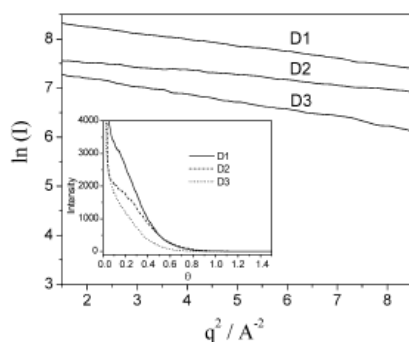


Fig. 3. Guinier plots for D1, D2, and D3 samples. Inset figure: X-ray scattering of the samples.

in surface area from D1 to D2 was accompanied by a proportional decrease in pore volume. From D2 to D3 a decrease in the pore volume was also observed. However, in this case, it was accompanied by an increase in the surface area, suggesting the presence of micropores.

As the BJH method used in this work is suitable for determining pore sizes in the region between diameters 2 and 50 nm [27,33], the pores whose sizes are below this range were obtained by the Guinier law using small-angle X-ray scattering data [25,26]. The Guinier curves are presented in Fig. 3, accompanied by the scattering curves. The Guinier curves were linear in the micropore region for all samples. From the slope of the curves the gyration radii were calculated and assuming spherical pores it was possible to estimate the micropore diameter of these samples. The results are summarized in Table 3. The micropore diameters of samples D1, D2, and D3 were close, between 1.4 and 1.7 nm. Based on the micropore diameter results obtained from SAXS analyses, we propose that the pore structure of the xerogel samples should be imposed by the bridged organic groups, which have an estimated length of 1.43 nm, as illustrated in Scheme 3. It was already reported [34] that the length of the bridge chain is related to the average pore size of the hybrid xerogels. The preparation of crystal-like silica-based hybrid materials with control of anisotropic organization of nanostructure, by using bridged neutral organic groups [35, 36] was also reported.

3.3. Hexacyanoferrate immobilization

The observed porosity allied to the charged chain of the hybrid xerogels made possible the immobilization of hexacyanoferrate anion in the matrix network. The infrared spectra of the hybrids containing immobilized hexacyanoferrate obtained af-

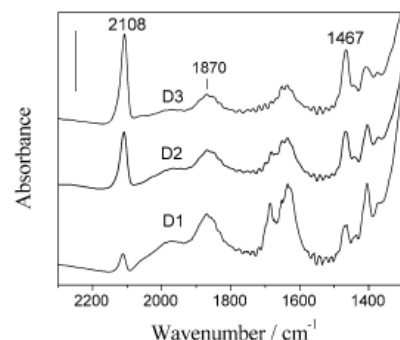


Fig. 4. Infrared spectra of D1, D2, and D3 samples, containing immobilized hexacyanoferrate obtained at room temperature, after heat treatment at 120 °C under vacuum. The bar value is 0.20.

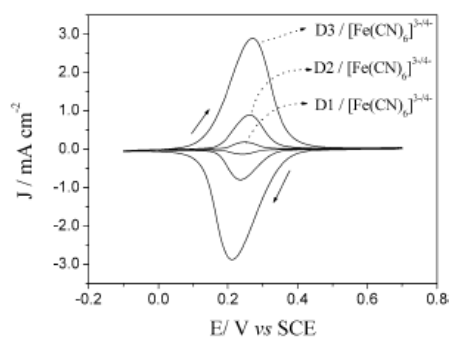
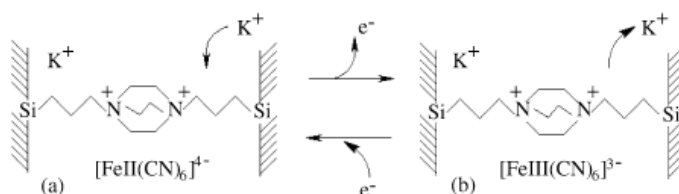


Fig. 5. Cyclic voltammetry curves for [Fe(CN)₆]^{3-/4-} adsorbed on D1, D2, and D3 in 1.0 mol L⁻¹ KCl supporting electrolyte solutions at 25 °C. Scan rate of 1 mV s⁻¹.

ter heat treatment under vacuum at 120 °C for 1 h are presented in Fig. 4. The spectra show a peak in 2108 cm⁻¹ due to the νC–N, confirming its immobilization. In the spectra of Fig. 4, bands due to organic and inorganic moieties of the hybrid xerogels are also observed. The organic component can be identified by the bands at 1460 cm⁻¹ attributed to δCH₂ modes of dabco and propyl chains. The silica is identified by the typical overtone band observed at 1870 cm⁻¹ [37].

3.4. Cyclic voltammetric measurements

From the cyclic voltammetric measurements it was possible to probe the electrochemical behavior of the potassium hexacyanoferrate ion confined in the pores of D1, D2, and D3 samples. The electrode made with the hybrids was submitted to a potential sweep between -0.1 and 0.7 V vs SCE (Fig. 5) with the electrode immersed in a 1.0 mol L⁻¹ KCl supporting electrolyte solution and with a scan rate of 1 mV s⁻¹. The anodic potential, E_{pa} , is observed at 0.27 V and the cathodic potential, E_{pc} , at 0.21 V. The midpoint potential is $E_{pm} = 0.24$ V ($E_{pm} = (E_{pa} + E_{pc})/2$). By integrating the areas under the cathodic or anodic peaks and determining the charge involved in each process, the amount of [Fe(CN)₆]³⁻ confined in each matrix was determined [38]. The amounts of ferricyanide per gram of the material (in μmol g⁻¹) were D1 = 0.87, D2 = 5.5, and D3 = 25.



Scheme 4.

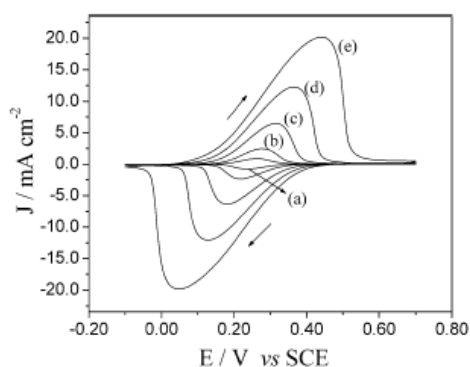


Fig. 6. Cyclic voltammograms for D1/[Fe(CN)₆]^{3-/4-} in different potential scan rates (in mV s⁻¹): (a) 1.0, (b) 2.0, (c) 5.0, (d) 10.0, and (e) 20.0. In 1.0 mol L⁻¹ KCl supporting electrolyte solution at 25 °C.

Fig. 5 also shows that reduction–oxidation is a reversible process at this scan rate since the observed current density ratios at the cathodic and anodic peaks maxima for a scan rate of 1 mV s⁻¹ J_{pa}/J_{pc} are D1 = 0.95, D2 = 1.0, and D3 = 1.0.

By increasing the potential sweeping velocity an increase of ΔE_p ($\Delta E_p = E_{pa} - E_{pc}$) is observed. This result indicates that the electron transfer process on the electrode surface is not sufficiently fast, presumably due to the internal matrix resistance, and thus, the process is not totally reversible (Fig. 6) [38].

However, another process due to the hydrated cation that normally follows the electroactive species when it is adsorbed by an ion exchange process must be considered. In the oxidation–reduction process, as shown in the reaction represented by Scheme 4, the K⁺ ion diffuse into or out of the cavity in order to keep electroneutrality. The process can be rationalized as follow: (a) when the electroactive species is oxidized (anodic potential sweep) K⁺ must move out of the pore and (b) when the potential is reversed, i.e. cathodic potential sweep, the cation K⁺ must diffuse into the pore. The movement of hydrated K⁺ ions into and out of the cavity does not depend on the diameter of the pore, which is too large, near 1.5 nm, in comparison to the hydrated diameter of the ion, 0.24 nm [39], to impose any diffusion barrier. Thus we may conclude that the organic chain forming the bridge inside the pores may be responsible for the high internal resistance inside the matrix cavities.

The interaction of the hexacyanoferrate complex through an electrostatic interaction with the fixed cationic double-charged dabco ion is sufficiently strong to keep the electroactive species confined in the pores. An experiment consisting of cycling the potential for long time and measuring the cathodic and anodic peak current densities for each complete cycle was also carried

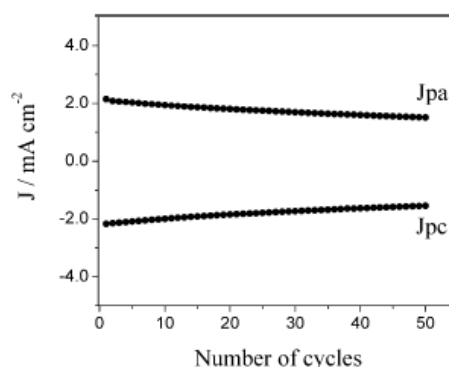


Fig. 7. Current densities plotted against number of oxidation–reduction cycles of carbon paste electrode prepared with D2/[Fe(CN)₆]^{3-/4-}. Scan rate of 10 mV s⁻¹; 1.0 mol L⁻¹ KCl supporting electrolyte at 25 °C.

out. We observe in Fig. 7 that J_{pa} and J_{pc} remain practically unchanged after 50 cycles for experiments carried out at room temperature in 1.0 mol L⁻¹ KCl supporting electrolyte solution. The result is a clear indication that the anionic complex is strongly confined inside the pores of the matrices and it is only slightly leached out during the oxidation–reduction process.

4. Summary

The compound di-3-*n*-propyltrimethoxysilane (1,4-diazoniabicyclo[2.2.2]octane) dichloride was synthesized and it contains a doubly charged organic bridging group and two hydrolyzable –Si(OMe)₃ groups. This compound is used as a precursor reagent to obtain a sequence of silica-based hybrids, containing bridged charged dabco groups. There is a relationship between the organic content and the texture of the material. All samples showed micro- and mesopores. The micropores have pore diameter between 1.4 and 1.7 nm, which matches the estimated chain length of the bridging group, suggesting that the pore structures were imposed on the samples prepared by the bridging length of the organic group.

The ability of the prepared materials to entrap chemical species inside the pores was tested, using hexacyanoferrate as an electroactive probe. The electroactivity of the confined hexacyanoferrate in the matrix was observed by the oxidation and reduction processes inside the pores. The electrochemical responses indicated the species are strongly confined inside the pores, since it was observed only a slightly leaching during the oxidation–reduction process. At low velocity of potential scan the process is reversible, clearly indicating that the electron transfer process can occur inside the pores.

Acknowledgments

We thank CNPq, FAPERGS, and FAPESP for fellowships and financial support.

References

- [1] G. Schottner, *Chem. Mater.* 13 (2001) 3422.
- [2] H.-H. Yang, S.-Q. Zhang, W. Yang, X.-L. Chen, Z.-X. Zhuang, J.-G. Xu, X.-R. Wang, *J. Am. Chem. Soc.* 126 (2004) 4054.
- [3] Y.A. Shchipunov, *J. Colloid Interface Sci.* 268 (2003) 68.
- [4] B.J. Scott, G. Wirnsberger, G.D. Stucky, *Chem. Mater.* 13 (2001) 3140.
- [5] Y. Martínez, J. Retuert, M. Yazdani-Pedram, H. Colfen, *Polymer* 45 (2004) 3257.
- [6] S.H. Phillips, T.S. Haddad, S.J. Tomczak, *Curr. Opin. Solid State Mater. Sci.* 8 (2004) 21.
- [7] G. Kikelbick, *Prog. Polym. Sci.* 28 (2003) 83.
- [8] Y. Khoroshevskiy, S. Komeev, S. Myerniy, Y.V. Kholin, F.A. Pavan, J. Schifino, T.M.H. Costa, E.V. Benvenutti, *J. Colloid Interface Sci.* 284 (2005) 424.
- [9] L.T. Arenas, A. Langaro, Y. Gushikem, C.C. Moro, E.V. Benvenutti, T.M.H. Costa, *J. Sol–Gel Sci. Technol.* 28 (2003) 51.
- [10] G. Splendorea, E.V. Benvenutti, Y.V. Kholinc, Y. Gushikem, *J. Braz. Chem. Soc.* 16 (2005) 147.
- [11] L.T. Arenas, T.A.S. Aguirre, A. Langaro, Y. Gushikem, E.V. Benvenutti, T.M.H. Costa, *Polymer* 44 (2003) 5521.
- [12] L.T. Arenas, J.C.P. Vaghetti, E.C. Lima, C.C. Moro, E.V. Benvenutti, T.M.H. Costa, *Mater. Lett.* 58 (2004) 895.
- [13] J.R. Fernandes, L.T. Kubota, Y. Gushikem, G.O. Neto, *Anal. Lett.* 26 (1993) 2555.
- [14] M. Kogure, H. Ohya, R. Paterson, M. Hosaka, J.-J. Kim, S. McFadzean, *J. Membr. Sci.* 126 (1997) 161.
- [15] G.M. Gray, J.N. Hay, *J. Sol–Gel. Sci. Technol.* 31 (2004) 191.
- [16] W. Cuiming, X. Tongwen, Y. Weihua, *J. Membr. Sci.* 216 (2003) 269.
- [17] C.-L. Lin, P. Tien, L.-K. Chau, *Electrochim. Acta* 49 (2004) 573.
- [18] A. Walcarius, C. Delacote, S. Sayen, *Electrochim. Acta* 49 (2004) 3775.
- [19] M. Darder, M. Colilla, N. Lara, E. Ruiz-Hitzky, *J. Mater. Chem.* 12 (2002) 3660.
- [20] W.S. Cardoso, M.S.P. Francisco, A.M.S. Lucho, Y. Gushikem, *Solid State Ionics* 167 (2004) 165.
- [21] L.T. Kubota, Y. Gushikem, *J. Electroanal. Chem.* 362 (1993) 219.
- [22] S.Q. Liu, H.Y. Chen, *J. Electroanal. Chem.* 528 (2002) 190.
- [23] G.A.P. Zaldivar, Y. Gushikem, E.V. Benvenutti, S.C. de Castro, A. Vasquez, *Electrochim. Acta* 39 (1994) 33.
- [24] J.L. Foschiera, T.M. Pizzolato, E.V. Benvenutti, *J. Braz. Chem. Soc.* 12 (2001) 159.
- [25] A. Guinier, G. Fournet, *Small-Angle Scattering of X-Ray*, Wiley, New York, 1955.
- [26] O. Glatter, O. Kratky, *Small-Angle X-Ray Scattering*, Academic Press, London, 1982.
- [27] E.P. Barret, L.G. Joyner, P.P. Halenda, *J. Am. Chem. Soc.* 73 (1951) 373.
- [28] S. Brunauer, P.H. Emmett, E. Teller, *J. Am. Chem. Soc.* 60 (1938) 309.
- [29] S.S. Hou, P.L. Kuo, *Polymer* 42 (2001) 9505.
- [30] M.E. Davis, C.J. Saldarriaga, *Chem. Soc. Chem. Commun.* (1988) 920.
- [31] T.M.H. Costa, H.S. Hoffmann, E.V. Benvenutti, V. Stefani, M.R. Gallas, *Opt. Mater.* 27 (2005) 1819.
- [32] D.R. Azolin, C.C. Moro, T.M.H. Costa, E.V. Benvenutti, *J. Non-Cryst. Solids* 337 (2004) 201.
- [33] T. Takei, M. Chikazawa, T. Kanazawa, *Colloid Polym. Sci.* 275 (1997) 1156.
- [34] K.J. Shea, D.A. Loy, *Chem. Mater.* 13 (2001) 3306.
- [35] H. Muramatsu, R.J.P. Corriu, B. Boury, *J. Am. Chem. Soc.* 125 (2003) 854.
- [36] B. Boury, F. Ben, R.J.P. Corriu, P. Delord, M. Nobili, *Chem. Mater.* 14 (2002) 730.
- [37] P.D. Maniar, A. Navrotsky, E.M. Rabinovich, J.Y. Ying, J.B. Benziger, *J. Non-Cryst. Solids* 124 (1990) 101.
- [38] A.J. Bard, L. Faulkner, *Electrochemical Methods—Fundamentals and Applications*, Wiley, New York, 2000.
- [39] E.A. Muelwyn-Hughes, *Physical Chemistry*, Pergamon, London, 1961, p. 567.

- 4.2- Use of statistical design of experiments to evaluate the sorption capacity of 1,4-diazoniabicyclo[2.2.2]octane/silica chloride for Cr(VI) adsorption. *Colloids and Surfaces A-Physicochemical and Engineering Aspects*, **2007**, 297, 240.

Use of statistical design of experiments to evaluate the sorption capacity of 1,4-diazoniabicyclo[2.2.2]octane/silica chloride for Cr(VI) adsorption

Leliz T. Arenas, Eder C. Lima*, Araci A. dos Santos Jr., Julio C.P. Vaghetti,
Tania M.H. Costa, Edilson V. Benvenutti

Instituto de Química, Universidade Federal do Rio Grande do Sul, Av. Bento Gonçalves 9500, Caixa Postal 15003, CEP 91501-970 Porto Alegre-RS, Brazil

Received 29 August 2006; received in revised form 15 October 2006; accepted 23 October 2006

Available online 26 October 2006

Abstract

1,4-Diazabicyclo[2.2.2]octane (dabco) silica prepared by grafting (GR-dabco) and sol-gel (SG-dabco) methods were used for removal of Cr(VI) species from aqueous solutions. Full 2^3 factorial designs with two pseudo-central points were carried out in order to achieve the best conditions of batch adsorption procedure for the Cr(VI) anion uptake by the adsorbents. In order to continue the optimizations, central composite surface design was also employed. These two independent statistical designs of experiments led to the following conditions: $m = 30.0$ mg of adsorbent; pH 6.0; t of contact of 180 min to guarantee the equilibration at higher adsorbate concentration. After achieving the best conditions for Cr(VI) adsorption, isotherms of this adsorbate on using the chosen adsorbents were obtained, which were fitted to non-linear Langmuir, Freundlich, and Sips isotherm models. The maximum sorption capacity for Cr(VI) anion adsorption was 63.86 and 79.82 mg g^{-1} for using GR-dabco and SG-dabco, respectively. © 2006 Elsevier B.V. All rights reserved.

Keywords: Cr(VI) adsorption; Modified silica gel; Isotherm models; Statistical design of experiments

1. Introduction

Chromium (VI), in the form of CrO_4^{2-} , $\text{Cr}_2\text{O}_7^{2-}$ and HCrO_4^- , is largely employed in the chemical industry for chrome plating, the manufacture of dyes and pigments, leather tanning, wood preserving, battery, rust and corrosion inhibitors, textiles, rubbers, toner for copying machines and cement-producing plants [1]. Waste streams from all these industries can discharge Cr(VI) into waterways [1] causing severe impact to the environment [2]. In addition, Cr(VI) has been reported to be carcinogen to humans [1,2]. The maximum allowed amount of Cr(VI) in natural waters is only 0.05 mg l^{-1} [1]. In this way, Cr(VI) must be removed from industrial effluents, before being delivered into the environment.

One of the most efficient ways for removing Cr(VI) from aqueous effluents is the adsorption procedure [3]. In this context, in recent years have been constant searches for new adsorbent materials with high metal adsorption capacities and selectivi-

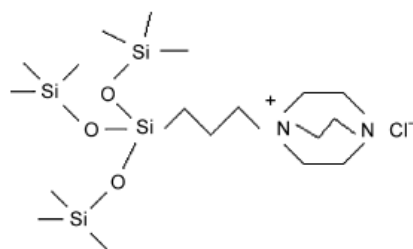
ties [3–8]. In the last years, silica-based materials have been the most extensively kind of adsorbent employed in environmental application studies [9–12]. Chemically modified silica gel is one of the most successful adsorbents, because the silica supports does not swells or shrinks such as the polymeric resin [13], and unmodified natural occurrence materials [3]. The modified silica may be employed in aqueous and organic solvents media [13]; they present good thermal stability [13] and appropriated accessibility of the ions to the adsorbent groups; in addition the modified silica exhibits sorption capacities higher than polymeric resins [9–13], because the number of organic molecules immobilized on the support surface is higher, allowing higher removal of ions from aqueous solution [9–13].

It has been reported that the 1,4-diazabicyclo[2.2.2]octane group (dabco) can be grafted on silica surface by reaction with 3-chloropropyltrimethoxysilane [14,15]. This immobilized pendant group, 3-*n*-propyl-1-azonia-4-azabicyclo[2.2.2]octane chloride (Scheme 1), presents one positively charged group that can act as anion exchanger [14,15].

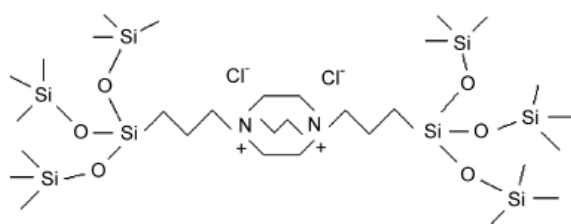
Recently, it has been synthesized the chemically modified silica gel containing a double charged 1,4-diazoniabicyclo[2.2.2]octane chloride group bonded to the silica framework in a bridged way [14], as illustrated in Scheme 2.

* Corresponding author. Tel.: +55 51 3316 7175; fax: +55 51 3316 7304.

E-mail addresses: ederlima@iq.ufrgs.br, profederlima@gmail.com (E.C. Lima).



Scheme 1.



Scheme 2.

This material presented good chemical stability and interesting results as anion exchanger for $[\text{Fe}(\text{CN})_6]^{3-}$ [17]. Therefore, this material could be a promising adsorbent for Cr(VI).

In the present work, it was studied the use of double charged 1,4-diazabicyclo[2.2.2]octane chloride immobilized on silica, prepared by grafting (GR-dabco) and sol-gel (SG-dabco) methods, for removal of Cr(VI) species from aqueous solutions. In order to reduce the total number of experiments to achieve the optimal conditions for adsorption of the Cr(VI) anions, using batch adsorption system with the GR-dabco and SG-dabco adsorbents, statistical designs of experiments were employed.

2. Experimental

2.1. Synthesis of the organic precursor

bis(n-propyltrimethoxysilane)-1,4-diazabicyclo[2.2.2]octane chloride

Firstly, 8 mmol of the 1,4-diazabicyclo[2.2.2]octane (dabco), previously sublimed, was dissolved in dimethylformamide (DMF), afterwards, it was added to 16 mmol of 3-chloropropyltrimethoxysilane (CPTMS). The mixture was stirred for 72 h, under argon atmosphere at 90 °C. The settling down white powder was washed with methanol and dried at 90 °C for 2 h. The resulting solid, bis(*n*-propyltrimethoxysilane)-1,4-diazabicyclo[2.2.2]octane chloride was assigned as $(\text{R}_2\text{dabco})\text{Cl}_2$.

2.2. Synthesis of the grafted material (GR-dabco)

The precursor $(\text{R}_2\text{dabco})\text{Cl}_2$ (3.057 g) was dissolved in a mixture containing 25 ml of formamide, 0.65 ml of water and 0.1 ml of HF (48% weight) at 60 °C. This solution was let for gelation and solvent evaporation during 30 days at 40 °C, just covered without sealing. The obtained water-soluble xerogel was used as

Table 1

Amount of water-soluble xerogel grafted onto silica gel surface

Water-soluble xerogel added (mmol ml^{-1})	Grafted xerogel on silica surface (mmol g^{-1}) ^a
0.015	0.09
0.03	0.12
0.06	0.18
0.09	0.25
0.12	0.28
0.15	0.29

^a Obtained from chloride potentiometric analysis.

reagent precursor for grafting reaction. The solid support used for grafting reactions was the commercial silica gel 100 Merck, with particle size of 0.2–0.5 mm. With the objective to determine the maximum quantity of soluble xerogel can be attained onto silica surface, the grafting reaction was made using several concentrations of water-soluble precursor solutions, showed in Table 1. For each solution (10 ml) it was added 1.0 g of commercial silica. It was let under stirring for 3 h, for adsorption. The resulting solid was filtrated, dried in an oven at 60 °C for 3 h and washed three times with deionized water. Finally the solid was again dried in oven at the same temperature. The quantities of $(\text{R}_2\text{dabco})\text{Cl}_2$ grafted onto commercial silica surface are showed in Table 1. Considering that the saturation plateau was attained at 0.12 mmol ml^{-1} , this condition was employed for obtaining the GR-dabco adsorbent.

2.3. Synthesis of the sol-gel material (SG-dabco)

The precursor $(\text{R}_2\text{dabco})\text{Cl}_2$ (0.504 g) was dissolved in a mixture containing 25 ml of formamide, 1.2 ml of water and 0.1 ml of HF (48% weight) at 60 °C. At this solution, it was drop wise added a freshly prepared solution containing 6.5 ml of tetraethylorthosilicate (TEOS) plus 1.0 ml of water and 7.0 ml of ethanol under stirring. The resulting solution was let for gelation and solvent evaporation during 30 days at 40 °C, just covered without sealing. The obtained solid was washed with ethanol and dried at 90 °C for 2 h. The xerogel that was not water-soluble was assigned as SG-dabco.

2.4. Infrared analysis

Self-supported disks of the materials were prepared having a diameter of 2.5 cm, weighing *ca.* 100 mg, with a disk thickness sufficiently thin to allow the measurements by the transmission technique. The disks were heated at 100 °C, under vacuum (10^{-2} Torr), for 1 h. The IR cell used in this work has already been described [18]. The equipment used was a Shimadzu FTIR, model 8300. The spectra were obtained at room temperature with a resolution of 4 cm^{-1} and 100 cumulative scans.

2.5. Elemental analyses

The elemental analyses of the organic groups, incorporated into the silica matrices, were carried on a CHN Perkin-Elmer

CHNS/O Analyzer, model 2400. The analyses were made in triplicate.

The chloride amount was determined by immersing the material in HNO₃ solution under stirring. The chloride ion was potentiometric determined by a titration using silver nitrate, against calomel electrode as reference electrode.

2.6. N₂ adsorption–desorption isotherms

The nitrogen adsorption–desorption isotherms of previous degassed samples, at 150 °C, were determined at liquid nitrogen boiling point in a homemade volumetric apparatus, with a vacuum line system employing a turbo molecular Edward vacuum pump. The pressure measurements are made using capillary Hg barometer. The specific surface areas of hybrid materials were determined from the BET (Brunauer, Emmett and Teller) multipoint method [19] and the pore size distribution was obtained using BJH (Barret, Joyner, and Halenda) method [20].

2.7. Determination of Cr(VI) species

Measurements of Cr(VI) was made by using a Perkin-Elmer Flame atomic Absorption Spectrometer model Analyst 200 (Boston, MA, United States) using air–acetylene (7.6:4.31 min⁻¹) flame. Hollow cathode lamp of Cr ($\lambda = 357.87$ nm) of the same manufacturer, was used as radiation source.

2.8. Batch adsorption procedure for Cr(VI)

An aliquot of 20.00 ml of 10.00–1000.0 mg l⁻¹ of Cr(VI) were added to a conical plastic tube (117 mm height, 30 mm diameter) containing 30.0–50.0 mg of GR-dabco and SG-dabco. The flasks were capped, in placed horizontally in a Tecnal shaker model TE-240 (Piracicaba-SP, Brazil), and the system was shaken for 30–180 min. Afterwards, the flasks were centrifuged using a FANEM centrifuge model Baby I (São Paulo-SP, Brazil), in order to separate the adsorbent from the aqueous solution, and aliquots of 1–5 ml of the supernatant were properly diluted to 25.0–100.0 ml in calibrated flasks using water. The Cr(VI) final concentrations were determined by FAAS, after multiplying the measured concentration value found in the solution after the adsorption procedure, by the proper dilution factor.

The amounts of Cr(VI) ion uptaken by the adsorbents were given by the following equation:

$$q = \frac{C_0 - C_e}{m} V \quad (1)$$

where q is the amount of Cr(VI) ion uptaken by the adsorbent (mg g⁻¹); C_0 the initial Cr(VI) ion concentration put in contact with the adsorbent (mg l⁻¹), C_e the Cr(VI) ion concentrations (mg l⁻¹) after the batch adsorption procedure, m the mass of adsorbent (g) and V is the volume (l) of Cr(VI) ion put in contact with the adsorbent.

Table 2

Full 2⁴ factorial design with two pseudo-central points for optimization of Cr(VI) adsorption on GR-dabco (A) and SG-dabco (B)

Experiment	Adsorbent	pH	C ₀	t	q (mg g ⁻¹)
1	A	-1	-1	-1	5.7099
2	B	-1	-1	-1	7.4450
3	A	1	-1	-1	1.8848
4	B	1	-1	-1	2.1278
5	A	-1	1	-1	29.0255
6	B	-1	1	-1	30.6958
7	A	1	1	-1	18.5770
8	B	1	1	-1	17.8020
9	A	-1	-1	1	12.5780
10	B	-1	-1	1	15.6980
11	A	1	-1	1	3.1319
12	B	1	-1	1	3.7651
13	A	-1	1	1	29.7540
14	B	-1	1	1	32.1318
15	A	1	1	1	20.4586
16	B	1	1	1	21.6777
17	A	0	0	0	20.4571
18	B	0	0	0	23.7472
19	A	0	0	0	20.7892
20	B	0	0	0	23.4109

Levels

	-1	0	1
Adsorbent	A		B
pH	4.0	6.0	8.0
C ₀ (mg l ⁻¹)	50.0	75.0	100.0
t (h)	30.0	75.0	120.0

Masses of adsorbents were fixed at 30.0 mg.

2.9. Statistical design of experiments

2.9.1. Full factorial design with pseudo-central point

One of the simplest types of factorial designs used in experimental work is one having two levels (2^k) [21–23]. The design determines which factors have important effects on a response as well as how the effect of one factor varies with the level of the other factors (interactions of factors). Effects are differential quantities expressing how a response changes as the levels of one or more factors are changed [21–23]. The determination of interactions of factors can be important for successful system optimization [24,25].

For studying the Cr(VI) adsorption on GR-dabco and SG-dabco, the amounts of adsorbed Cr(VI) ion (q) could depend on the kind of adsorbent (A, GR-dabco; B, SG-dabco), acidity of the medium (pH), initial concentration of the Cr(VI) ion (C_0), the time of contact (t) between the adsorbate and adsorbent. Others variables such as, speed of agitation was kept at 150 strikes/min; and temperature was kept at 25 °C, mass of adsorbent was fixed at 30.0 mg [25]. Full 2⁴ factorial designs with their two pseudo-central points employed were given in Table 2. The factor levels were coded as -1 (low), 0 (central point) and 1 (high) [21–23]. For treatment of data, the Minitab Statistical Software release 14.20 was employed throughout in order to obtain the effects, coefficients, standard error of coefficients, and other statistical parameters of the fitted models.

2.9.2. Central composite response surface design

Response surface methods are used to examine the relationship between one or more response variables and a set of quantitative experimental factors. These methods are often employed after a screening of important factors, usually by performing a previous factorial design. After that, it is necessary to find the factor settings that optimize the response. Designs of this type are usually chosen when the previous factorial design indicated a curvature in the response surface [21–23]. Response surface methods may be employed to [21–23]:

- To find factor settings (operating conditions) that produces the best response.
- To find factor settings that satisfies operating or process specifications.
- To model a relationship between the quantitative factors and the response.

In this work, after performing a screening of the factors with the factorial design for the both adsorbents, response surface analysis statistical procedure [21–23] were employed, in order to achieve the highest amount of the Cr(VI) ions adsorbed by the two adsorbents. The experimental sets were carried out according to Table 3.

2.10. Isotherm modeling

The isotherms models of Langmuir [26], Freundlich [26], and Sips [26] were fitted to describe the equilibrium adsorption.

Table 3
Central composite surface design containing 13 experiments, and two factors (C_0 , t) for optimization of Cr(VI) adsorption conditions on GR-dabco (A) and SG-dabco (B)

Experiment	C_0	t	q (mg g ⁻¹)	
			A	B
1	-1	-1	19.4732	20.9453
2	1	-1	21.6905	25.5564
3	-1	1	18.2146	20.4883
4	1	1	32.0118	45.8665
5	-1	0	19.3682	21.0595
6	1	0	33.6621	41.3808
7	0	-1	20.2743	37.7804
8	0	1	24.5398	30.6750
9	0	0	23.2757	31.9698
10	0	0	24.2681	31.6110
11	0	0	19.8210	33.4964
12	0	0	22.3095	33.7282
13	0	0	18.7828	33.4767

	Levels		
	-1	0	1
C_0 (mg l ⁻¹)	100	150	200
t (min)	30	105	180

The pH was fixed at 4.0, and the mass was fixed at 30.0 mg.

These equations of isotherms were given below:

$$\text{Langmuir isotherm } q = \frac{Q_{\max} K_L C_e}{1 + K_L C_e} \quad (2)$$

where C_e is the supernatant concentration after the equilibrium of the system (mg l⁻¹), K_L the Langmuir affinity constant (l mg⁻¹), and Q_{\max} is the maximum adsorption capacity of the material (mg g⁻¹) assuming a monolayer of adsorbate uptaken by the adsorbent:

$$\text{Freundlich isotherm } q = K_F C_e^{1/n} \quad (3)$$

where K_F is the Freundlich constant related with adsorption capacity [mg g⁻¹ (mg l⁻¹)^{-1/n}] and n is the Freundlich exponent (dimensionless):

$$\text{Sips isotherm } q = \frac{Q_{\max} K_S C_e^{1/n}}{1 + K_S C_e^{1/n}} \quad (4)$$

where K_S is the Sips constant related with affinity constant (mg l⁻¹)^{-1/n}, Q_{\max} the Sips maximum adsorption capacity (mg g⁻¹), and n is the Sips exponent (dimensionless).

In this work, the Langmuir, Freundlich, and Sips isotherms were fitted employing the non-linear fitting method using the software Microcal Origin 7.0. In addition, the model were also evaluated by an error function [27], which measures the differences of the amount of Cr(VI) uptaken by the adsorbent predicted by the models and the actual q measured experimentally:

$$F_{\text{error}} = \sqrt{\frac{\sum_i^p ((q_i \text{ model} - q_i \text{ experimental}) / q_i \text{ experimental})^2}{p}} \quad (6)$$

where $q_i \text{ model}$ is each value of q predicted by the fitted model and $q_i \text{ experimental}$ is each value of q measured experimentally, and p is the number of experiments performed.

3. Results and discussion

3.1. Synthesis and characterization of adsorbent materials

The infrared spectra of the obtained materials are showed in Fig. 1. These spectra are typical of hybrid materials where the organic and inorganic components can be observed. The organic moiety can be identified by the bands at 1465 and 1412 cm⁻¹ assigned as CH₂ bending and the band at 1375 attributed to umbrella bending of CH₃ of remained methoxyl groups of unreacted precursors. The inorganic component is recognized by the typical silica overtone bands with maximum in 1860 cm⁻¹.

The characteristics of the obtained samples are showed on Table 4. The CHN results were higher than that obtained from potentiometric chloride analysis, mainly for the SG-dabco. This difference can be ascribed to the increasing in the carbon contents that led to an incomplete hydrolysis of the precursors during the sol-gel reactions. Therefore, it was considered that the chloride analysis was more suitable to represent the quantity of organic groups incorporated in the silica matrices and consequently the organic content was very similar for both materials.

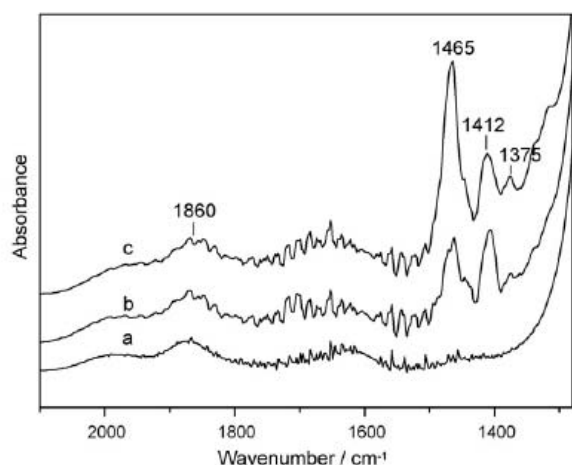


Fig. 1. Absorbance infrared spectra obtained at 25 °C: (a) pure silica; (b) GR-dabco; (c) SG-dabco.

Table 4
Elemental analysis and surface area results

Material	Dabco groups (mmol g ⁻¹)		Surface area (m ² g ⁻¹)	Pore volume (cm ³ g ⁻¹)
	CHN analysis	Cl ⁻ analysis		
Pure silica			310 ± 20	0.76 ± 0.03
GR-dabco	0.41 ± 0.05	0.36 ± 0.02	260 ± 20	0.71 ± 0.03
SG-dabco	0.62 ± 0.06	0.41 ± 0.02	460 ± 25	0.42 ± 0.03

The BET surface area of SG-dabco material was higher than that obtained for GR-dabco material. On the other hand, the pore volume was lower for the SG-dabco material when compared to GR-dabco (Table 4). These results could be explained considering the pore size distribution curves showed in Fig. 2. As can be seen the GR-dabco material presents a large pore diameter distribution curve ranging from 4 to 14 nm while SG-dabco material shown smaller pores with a sharp distribution curve ranging from 2 to 6 nm, with a maximum at 4 nm.

Some comments about the grafting reaction should be pointed out. From the pore size distribution curves it was observed that

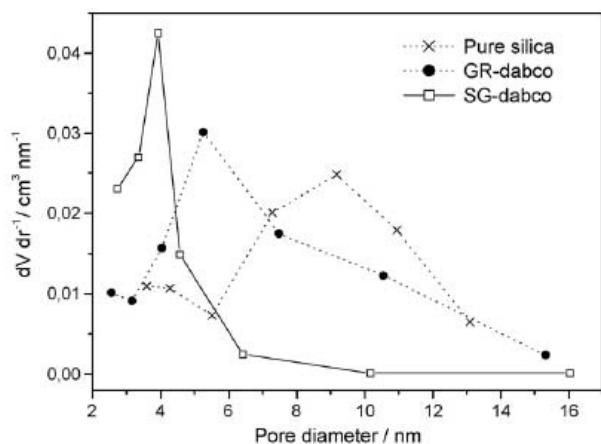


Fig. 2. Pore size distribution curves obtained from BJH method.

the GR-dabco material presented a maximum shifted to lower values of pore diameter when compared to pure silica. This result was observed for grafting reactions when the organics were uniformly dispersed in a presumable monolayer on solid surfaces [18]. The surface area results were in agreement with this explanation, because the monolayer produced a uniform covering of pore surface resulting in a slight decrease in the surface area [16,28].

3.2. Screening of factors for Cr(VI) uptake by GR-dabco and SG-dabco

In order to achieve the highest adsorption capacity of the Cr(VI) by an adsorbent using a batch system, it would require the optimization of several factors, such as, kind of adsorbent, acidity of medium (pH), time of contact between the Cr(VI) and the adsorbent (t), initial Cr(VI) anion concentration (C_0), mass of the adsorbent (m), speed of shaking, etc. The conventional optimization procedure of all those variables is tedious, because any variable (factor) is optimized, by varying just one factor by the time and fixing the others. Then, the best value achieved by this procedure is fixed and other factors will be varied by the time sequentially [24,25]. The disadvantage of this conventional univariate procedure is that the best condition would demand so many experiments to be carried-out [21–25].

In order to reduce the total number of experiments to achieve the highest adsorption capacity of the adsorbents for Cr(VI) adsorption, statistical design of experiments was carried-out. Initially the factors screened were, type of adsorbent (GR-dabco and SG-dabco), acidity of the medium (pH), initial concentration of Cr(VI) (C_0), times of contact (t) between the adsorbents and Cr(VI), for highest ion adsorption using a batch adsorption system. The experiments of Table 2 ($n=20$) were carried-out, obtaining the Cr(VI) anion uptake (q) in milligram per gram of GR-dabco (A) and SG-dabco (B). The definitions of the factors and the levels used in the complete design were presented in Table 2. Main, interaction effect, coefficients of the model, and standard error of each coefficient, and probability for the full 2⁴ factorial designs with two pseudo-central points were presented on Table 5. All main factors and its interactions which presented probability (P) lower than 0.05 were significant at 95% of confidence level. The pseudo-central points carried out in duplicate were useful to obtain the standard error of the coefficients. The probability results showed that the pseudo-central points were significant presenting, $P=0.001$, at 5% of probability level. It meant that it was detected a curvature of the factors when the levels were changed from the lower level (–) going to the higher level (+), passing through the central point (0). Therefore for a complete optimization of the batch adsorption procedure a surface analysis design would be required in order to achieve a better comprehension of the sorption system. In addition, the fit model presented square correlation coefficients (R^2) of 0.9988, fitting very well the statistical model.

The positive values of effects meant that an increase in their levels led to an increase in the Cr(VI) uptake by the adsorbents (q), on the other hand, the negative values of the effects,

Table 5
Factorial fits: q vs. adsorbent, pH, C_0 and t

Term	Effect	Coefficient	SE of coefficient	P
Constant		15.779	0.2219	0.000
Main factors				
Ads	1.614	0.807	0.1985	0.027
pH	-9.202	-4.601	0.2219	0.000
C_0	18.473	9.236	0.2219	0.000
t	3.241	1.620	0.2219	0.005
Interaction of two factors				
Ads \times pH	-0.948	-0.474	0.2219	0.122
Ads \times C_0	-0.155	-0.077	0.2219	0.750
Ads \times t	0.560	0.280	0.2219	0.297
pH \times C_0	-1.571	-0.786	0.2219	0.038
pH \times t	-1.080	-0.540	0.2219	0.093
$C_0 \times t$	-1.260	-0.630	0.2219	0.066
Interaction of three factors				
Ads \times pH \times C_0	0.047	0.023	0.2219	0.923
Ads \times pH \times t	0.036	0.018	0.2219	0.940
Ads \times $C_0 \times t$	0.116	0.058	0.2219	0.811
pH \times $C_0 \times t$	1.979	0.989	0.2219	0.021
Interaction of four factors				
Ads \times pH \times $C_0 \times t$	0.285	0.143	0.2219	0.566
Central point (cp)		6.322	0.4963	0.001

Estimated effects and coefficients for q (coded units). Full 2^4 factorial design with two pseudo-central points for optimization of Cr(VI) uptake by GR-dabco and SG-dabco. The effects and coefficients are given in coded units. SE, standard error of coefficient; Ads, adsorbent; cp, central point; S , standard deviation; R^2 , squared correlation factor. $S=0.887720$; $R^2=0.9988$.

led to a diminution of the response (q), when their levels were increased.

The amount of the adsorbate uptaken by both adsorbents could be expressed as the following equation:

$$q_{\text{Cr(VI)}} = 15.779 + 0.807 \times \text{Ads} - 4.601 \times \text{pH} + 9.236 \times C_0 + 1.620 \times t - 0.786 \times \text{pH} \times C_0 + 0.989 \times \text{pH} \times C_0 \times t \quad (R^2 = 0.9988) \quad (7)$$

Being the values of the factors coded and its levels valid only to the levels described on Table 2.

The ranking of importance of each factor and interaction in the global processes of batch adsorption procedure will depend on the numeric value of the coefficient of each factor or its interaction in absolute value [3,24].

Analyzing the values of Table 5, it can be inferred that initial Cr(VI) concentration (C_0) was most important variable of the overall adsorption process. The positive value of its coefficient meant that increasing the concentrations of the adsorbate would lead a remarkable increase in the amount of Cr(VI) uptaken by both adsorbents (q), because at 100.0 mg l^{-1} of initial concentration of Cr(VI), the amount uptaken by both adsorbents were not level off. Therefore, in order to achieve the highest amount uptaken of the adsorbate, higher concentrations of Cr(VI) should be explored in the further statistical design of experiments.

The second important factor in the overall optimization of the batch adsorption procedure was the pH of the solutions. The

increase of the pH up to 8.0 led to a remarkable decrease of the Cr(VI) anion uptake by the both adsorbents, because at this pH value, the surface of adsorbents material could present an excess of negative charge, precluding the electrostatic attraction between the positive dabco groups with the Cr(VI) anions [16].

The third important factor to the overall optimization of the batch adsorption processes for Cr(VI) was the time of contact between the adsorbents and the adsorbate. Increasing contact times from 30 to 120 min led to an augmentation of the response (q). Probably for low contact times, the batch adsorption system did not reach the equilibrium. Higher times of contact should be explored in further statistical design of experiments in order to optimize this factor.

The fourth important contribution to the overall optimization of the batch adsorption processes for Cr(VI) uptake was the interactions of three factors (pH \times $C_0 \times t$) which was more significant than the main factor type of adsorbent. Only the achievement of this result, justifies the use of the statistical design of experiments over the conventional univariate process of optimization of the system. This information would not be acquired in a univariate optimization of the adsorption system. The positive value of the coefficient of this interaction meant that an increase in the pH associated with an increase in the initial Cr(VI) concentration connected to an increase in the contact time, led to an increase of the response (q). This synergistic effect would not be easily detected in a univariate optimization of the system.

In the ranking of overall optimization of the batch adsorption system, the kind of adsorbent was classified as fifth important factor. The positive value of the coefficient of adsorbent meant that the SG-dabco presented a slight higher adsorption capacity when compared to GR-dabco. As the organic group quantity was similar for both samples, this difference should be attributed to the higher surface area of SG-dabco in relation to GR-dabco.

The last important contribution to overall optimization of the batch adsorption system was the interaction of two factors pH \times C_0 which presented a negative coefficient, indicating that an increase in the pH associated with an increase in the initial concentration of the adsorbate, would lead to a diminution of the response (q).

By performing a response optimization Eq. (7) having as a target the highest adsorption capacity of the adsorbents for Cr(VI) uptaken using a batch adsorption system, the best conditions achieved were: pH 4.0; $C_0 = 100.0 \text{ mg l}^{-1}$; $t = 120 \text{ min}$. In the further experiments the pH will be kept constant at 4.0, and the C_0 and t will be explored at other levels for each adsorbent.

3.3. Surface analysis

After performing a screening of factors using a full 2^4 factorial design, a central composite response surface design (containing 13 experiments, divided in four cube points, four axial points and five central points) were carried out according to experiments described in Table 3, in order to achieve the highest amount of Cr(VI) uptaken by GR-dabco and SG-dabco adsorbents. The levels of the chosen factors were set based on the

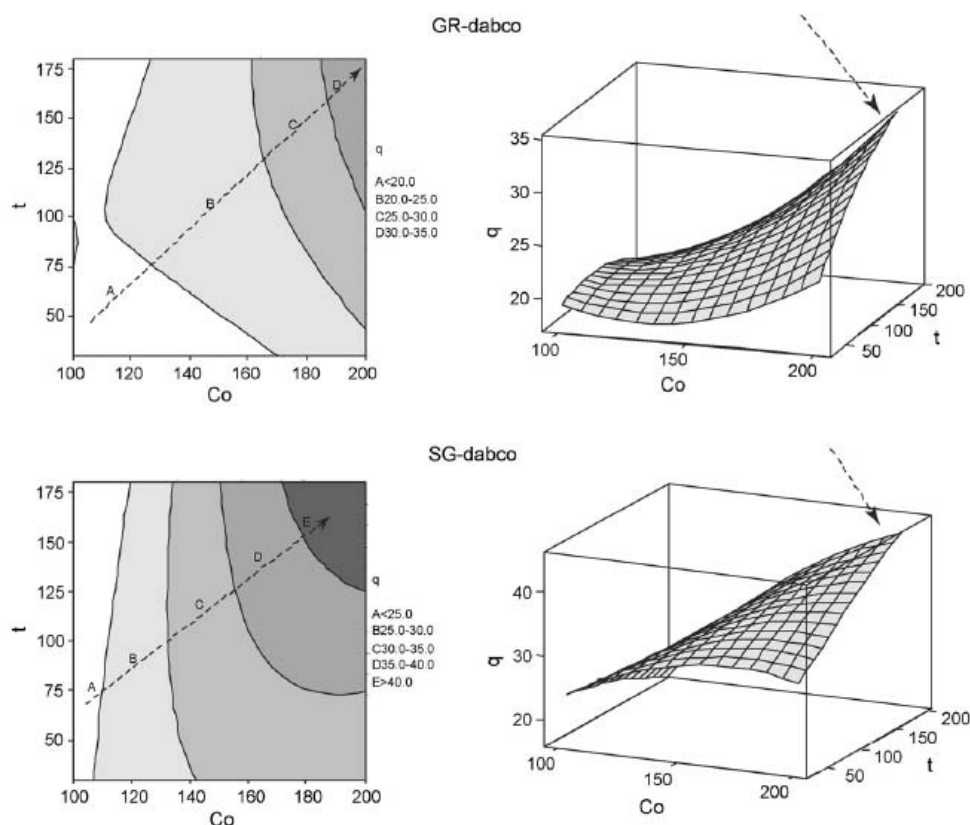


Fig. 3. Contour plot (left) and surface plots (right) for Cr(VI) uptake using GR-dabco and SG-dabco as adsorbents. The response q is expressed in mg/g , C_0 is expressed in mg l^{-1} and t is expressed in min. The arrows indicate the increasing of q at the several regions.

previous factorial design described above, increasing the initial Cr(VI) concentration up to 200.0 mg l^{-1} ; and varying the contact time up to 180 min and fixing the pH at 4.0.

In Fig. 3 were shown the contour plots of the response (q) for time of contact between the adsorbate and adsorbents and also the surface plots, for the optimization of Cr(VI) adsorption on GR-dabco and SG-dabco used as adsorbents. As can be seen, the highest Cr(VI) uptake by the both adsorbents occurred for times of contact of 180 min and for higher metallic ion concentration. It also can be noted that the saturation of the both adsorbents did not occurred when the initial concentration employed was 200.0 mg l^{-1} .

Base on the two set of statistical design of experiments for the GR-dabco and SG-dabco as adsorbents, it could establish the following conditions:

- The ideal pH for obtaining the maximum amount of Cr(VI) uptaken by the adsorbents was 4.0.
- The ideal time of contact between the adsorbents and adsorbate was 180 min to guarantee the equilibration.
- The saturation of the adsorbents did not occurred when the initial concentration of Cr(VI) was up to 200.0 mg l^{-1} . In order to obtain the maximum amount of the Cr(VI) anion uptaken by the adsorbents, isotherm curves should be obtained, using the best conditions optimized by the statistical design of experiments.

- The amount of Cr(VI) uptaken by SG-dabco is slightly higher than that adsorbed by GR-dabco. This was attributed to the higher surface area of SG-dabco when compared to the GR-dabco material.

The total number of experiments carried-out to get all this information was only 23 for each adsorbent studied (1st facto-

Table 6
Isotherm parameters

Isotherm	GR-dabco	SG-dabco
Langmuir		
Q_{\max} (mg g^{-1})	63.86	79.82
K_L (l mg^{-1})	0.00372	0.00375
R^2	0.9913	0.9919
Function error, F_{error}	0.07915	0.1313
Freudlich		
K_F ($\text{mg g}^{-1} (\text{mg l}^{-1})^{-1/n}$)	2.097	2.716
n	2.119	2.139
R^2	0.9586	0.9811
Function error, F_{error}	0.3195	0.3874
Sips		
Q_{\max} (mg g^{-1})	60.42	79.82
K_S ($(\text{mg l}^{-1})^{-1/n}$)	0.00263	0.00375
n	0.9209	1.000
R^2	0.9918	0.9919
Function error, F_{error}	0.09912	0.1313

Table 7
Comparison of different adsorbents for Cr(VI) uptaken

Adsorbent	Characteristic	q_{\max} (mg g ⁻¹)	Reference
<i>Auracaria angustifolia</i> wastes	Treatment with water boiling	125.0	[3]
Activated carbon	Prepared from sugarcane bagasse	11.4	[29]
Coconut shell charcoal	Biosorbent treated with HNO ₃	10.88	[30]
Coconut shell charcoal	Biosorbent treated with H ₂ SO ₄	4.05	[30]
Coconut shell charcoal	Without treatment	2.18	[30]
Hazelnut shell	Biosorbent treated with H ₂ SO ₄	17.7	[31]
Chitosan	Modified chitosan	153.8	[32]
Sugar beet pulp	Composite of biosorbent with Fe(OH) ₃	5.12	[33]
Olive stones	Particle size 1.0–1.5 mm	0.012	[34]
<i>Yohimbe</i> bark	Particle size 1.0–1.5 mm	42.5	[34]
Grape stalks	Particle size 1.0–1.5 mm	59.8	[34]
Cork	Particle size 1.0–1.5 mm	0.022	[34]
Oil shale	Activated carbo-aluminosilicate treated with H ₂ SO ₄	92.0	[35]
Waste crab shell	Treated with HCl	28.1	[36]
Palygorskite clay	Industrial clay	58.5	[37]
Commercial polymeric resin	Lewatit MP 62 (pH 5.0)	20.80	[38]
Commercial polymeric resin	Lewatit M 610 (pH 5.0)	21.32	[38]
Dabco immobilized silica gel	Obtained by grafting process	63.86	This work
Dabco immobilized silica gel	Obtained by sol–gel process	79.82	This work

rial design, 10 experiments per adsorbent; 2nd response surface analysis, 13 experiments for each adsorbent).

3.4. Adsorption isotherms for Cr(VI) uptake on GR-dabco and SG-dabco

In Table 6 were presented the values of the parameters of the Langmuir [26], Freundlich [26], and Sips [26] models of isotherms. In order to evaluate which model was best fitted, the error function was measured. How lower is the error function, lower will be the difference of the q calculated by the model from the experimental q measured. For GR-dabco adsorbent, the Langmuir isotherm model presented lower error function, even though the R^2 values of Sips model was better than the Langmuir one. Therefore it can be inferred that just analyzing the R^2 of the fitting is not the unique parameter that should be take into account to verify the best fitting of isotherm model. On the other hand, for SG-dabco, the Sips isotherm model presented the same parameters values of Langmuir isotherm model, since the n Sips exponent value was 1.000. In addition, by analyzing this table, it can also be verified that the SG-dabco presented a higher sorption capacity than GR-dabco for Cr(VI) adsorption, confirming the data of statistical design of experiments performed earlier. Also, it can be inferred that with exception of Freundlich model, all the isotherms presented a behavior similar to Langmuir isotherm.

3.5. Comparison of different adsorbents for Cr(VI) adsorption

In Table 7 was presented a comparison of several adsorbents employed for Cr(VI) uptaken. As can be seen from Table 7, the adsorbents employed in this work (GR-dabco and SG-dabco) presented higher adsorption capacity when compared

with several different adsorbents. From 19 different adsorbents presented on this table, only three of them presented higher sorption capacity than GR-dabco and SG-dabco, indicating that these adsorbents could be successfully employed for removal of Cr(VI) species from aqueous solutions.

4. Conclusion

Two sets of statistical design of experiments were successfully employed for optimizing the best conditions to attaining the maximum amount of Cr(VI) adsorption using GR-dabco and SG-dabco as adsorbents and employing only 23 experiments for each adsorbent. The decrease of the number of experiments using statistical design of experiments is the fastest and statistically correct procedure to optimize a desired procedure. These two independent statistical designs of experiments led to the following conditions: pH 4.0; t of contact of 180 min to guarantee the equilibration at higher adsorbates concentration; the saturation of the adsorbents did not occurred when the initial concentration of Cr(VI) was up to 200.0 mg l⁻¹; the amount of Cr(VI) uptaken by SG-dabco is slightly higher than that adsorbed by GR-dabco.

After optimizing, the conditions, isotherms of Cr(VI) adsorbed on the GR-dabco and SG-dabco were carried-out. These isotherms were suitably fitted to non-linear Langmuir, and Sips isotherm models.

The SG-dabco adsorbent presented higher adsorption capacity for the adsorption of Cr(VI), taking into account the Langmuir and Sips maximum adsorption capacity (Q_{\max}), reinforcing the data obtained previously with the statistical design of experiments. Therefore, the use of statistical tools helps to adjust the variables to obtain the maximum adsorption capacity and also brings an overview of the parameters of adsorption isotherm.

Acknowledgements

The authors are grateful to Ministério de Ciência e Tecnologia (MCT), to Conselho Nacional de Desenvolvimento Científico e Tecnológico (CNPq), and to Fundação de Amparo à Pesquisa do Estado do Rio Grande do Sul (FAPERGS) for financial support and fellowships. We also thank to Perkin-Elmer for donating impact beads utilized in the nebulizer of Analyst 200 spectrometer.

References

- [1] Toxicological Profile for Chromium, U.S. Department of Health and Human Services, Public Health Service, Agency for Toxic Substances and Disease Registry, Atlanta, 2000.
- [2] M.H. Yu, *Environmental Toxicology—Biological and Health Effects of Pollutants*, 2nd ed., CRC Press, Boca Raton, 2005.
- [3] J.L. Brasil, R.R. Ev, C.D. Milcharek, L.C. Martins, F.A. Pavan, A.A. dos Santos Jr., S.L.P. Dias, J. Dupont, C.P.Z. Norena, E.C. Lima, *J. Hazard. Mater.* 133 (2006) 143.
- [4] R.A. Shawabkeh, *J. Colloid Interf. Sci.* 299 (2006) 530.
- [5] H. Seki, A. Suzuki, H. Maruyama, *J. Colloid Interf. Sci.* 281 (2005) 261.
- [6] M.Y. Arica, G. Bayramoglu, *Colloid Surf. A* 253 (2005) 203.
- [7] E. Oguz, *Colloid Surf. A* 252 (2005) 121.
- [8] N. Sankaramakrishnan, A. Dixit, L. Iyengar, R. Sanghi, *Bioresour. Technol.* 97 (2006) 2377.
- [9] S.V.M. de Moraes, J.L. Brasil, C.D. Milcharek, L.C. Martins, M.T. Laranjo, M.R. Gallas, E.V. Benvenuti, E.C. Lima, *Spectrochim. Acta Pt. A* 62 (2005) 398.
- [10] S.V.M. de Moraes, M.M. Tisott, C.D. Milcharek, J.L. Brasil, T.M.H. Costa, M.R. Gallas, E.V. Benvenuti, E.C. Lima, *Anal. Sci.* 21 (2005) 573.
- [11] J.L. Brasil, L.C. Martins, R.R. Ev, J. Dupont, S.L.P. Dias, J.A.A. Sales, C. Airoidi, E.C. Lima, *Int. J. Environ. Anal. Chem.* 85 (2005) 475.
- [12] J.C.P. Vaguetti, J.L. Brasil, T.M.H. Costa, E.C. Lima, E.V. Benvenuti, *Eclét. Quím.* 30 (2005) 43.
- [13] C. Airoidi, R.F. Farias, *Quim. Nova* 23 (2000) 496–503.
- [14] L.T. Arenas, J.C.P. Vaghetti, C.C. Moro, E.C. Lima, E.V. Benvenuti, T.M.H. Costa, *Mater. Lett.* 58 (2004) 895.
- [15] G. Splendore, E.V. Benvenuti, Y.V. Kholin, Y. Gushikem, *J. Braz. Chem. Soc.* 16 (2005) 147.
- [16] L.T. Arenas, N.M. Simon, Y. Gushikem, T.M.H. Costa, E.C. Lima, E.V. Benvenuti, *Eclét. Quím.* 31 (2006) 53.
- [17] L.T. Arenas, S.L.P. Dias, C.C. Moro, T.M.H. Costa, E.V. Benvenuti, A.M.S. Lucho, Y. Gushikem, *J. Colloid Interf. Sci.* 297 (2006) 244.
- [18] J.L. Foschiera, T.M. Pizzolato, E.V. Benvenuti, *J. Braz. Chem. Soc.* 12 (2001) 159.
- [19] S. Brunauer, P.H. Emmett, E. Teller, *J. Am. Chem. Soc.* 60 (1938) 309.
- [20] E.P. Barret, L.G. Joyner, P.P. Halenda, *J. Am. Chem. Soc.* 73 (1951) 373.
- [21] The Statistic homepage, <http://www.statsoft.com/textbook/stathome.html>, Experimental Design link, website visited on May 26, 2006.
- [22] D.C. Montgomery, *Design and Analysis of Experiments*, 5th ed., John Wiley and Sons, New York, 2001.
- [23] G.E.P. Box, W.G. Hunter, J.S. Hunter, *Statistics for Experimenters—An Introduction to Design, Data Analysis and Model Building*, John Wiley and Sons, New York, 1978.
- [24] F.A. Pavan, Y. Gushikem, A.C. Mazzocato, S.L.P. Dias, E.C. Lima, *Dyes Pigm.* 72 (2007) 256.
- [25] E.C. Lima, B. Royer, J.C.P. Vaghetti, J.L. Brasil, N.M. Simon, A.A. dos Santos Jr., F.A. Pavan, S.L.P. Dias, E.V. Benvenuti, E.A. da Silva, *J. Hazard. Mater.* 140 (2007) 211–220.
- [26] B. Volesky, *Hydrometallurgy* 71 (2003) 179.
- [27] J.C.Y. Ng, W.H. Cheung, G. McKay, *Chemosphere* 52 (2003) 1021.
- [28] J.M.D. Cónsul, I.M. Baibich, E.V. Benvenuti, D. Thiele, *Quim. Nova* 28 (2005) 393.
- [29] M. Valix, W.H. Cheung, K. Zhang, *J. Hazard. Matter.* 135 (2006) 395.
- [30] S. Babel, T.A. Kurniawan, *Chemosphere* 54 (2004) 951.
- [31] G. Cimino, A. Passerini, G. Toscano, *Water Res.* 34 (2000) 2955.
- [32] V.M. Boddu, K. Abburu, J.L. Talbott, E.D. Smith, *Environ. Sci. Technol.* 37 (2003) 4449.
- [33] H.S. Altundogan, *Process Biochem.* 40 (2005) 1443.
- [34] N. Fiol, I. Villaescusa, M. Martínez, N. Miralles, J. Poch, J. Serarols, *Environ. Chem. Lett.* 1 (2003) 135.
- [35] R.A. Shawabkeh, *J. Colloid Interf. Sci.* 299 (2006) 530–536.
- [36] H. Niu, B. Volesky, *Hydrometallurgy* 71 (2003) 209.
- [37] J.H. Potgieter, S.S. Potgieter-Vermaak, P.D. Kalibantonga, *Miner. Eng.* 19 (2006) 463.
- [38] F. Gode, E. Pehlivan, *J. Hazard. Mater.* 119 (2005) 175.

- 4.3- Anisotropic self-organization of hybrid silica based xerogels containing bridged positively charged 1,4-diazoniabicyclo [2.2.2]octane chloride. Submetido, **2007**.

Anisotropic self-organization of hybrid silica based xerogels containing bridged positively charged 1,4-diazoniabicyclo[2.2.2]octane chloride group

Leliz T. Arenas^a, Adriana C. Pinheiro^a, Juliana D. Ferreira^b, Vitor P. Pereira^b, Márcia R. Gallas^c, Yoshitaka Gushikem^d, Tania M. H. Costa^a, Edilson V. Benvenutti^{a}.*

^a = LSS, Instituto de Química, UFRGS, CP 15003, 91501-970, Porto Alegre - RS, Brazil.

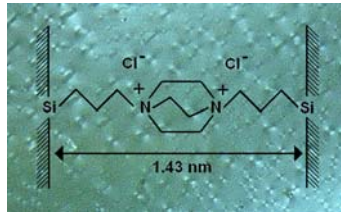
^b = Instituto de Geociências, UFRGS, CP 15001, 91501-970, Porto Alegre, RS, Brazil.

^c = LAPMA, Instituto de Física, UFRGS, CP 15051, 91501-970, Porto Alegre, RS, Brazil.

^d = Instituto de Química, UNICAMP, CP 6154, 13083-970 Campinas, SP, Brazil.

Corresponding Author Edilson V. Benvenutti
ebenvenutti@gmail.com
benvenutti@iq.ufrgs.br
Phone: 55 51 33167209
Fax: 55 51 33167304

TOC Graphic and Summary

<p>Leliz T. Arenas, Adriana C. Pinheiro, Juliana D. Ferreira, Vitor P. Pereira, Márcia R. Gallas, Yoshitaka Gushikem, Tania M. H. Costa, Edilson V. Benvenuto*.</p> <p>Anisotropic self-organization of hybrid silica based xerogels containing bridged positively charged 1,4-diazoniabicyclo[2.2.2]octane chloride group</p>	<p>Hybrid silica based xerogels containing double charged bridged group were prepared. The materials show ordered structure imposed by the charged dabco group and the interplanar distance obtained by XRD matches with the length of this group. The higher organic grade samples showed birefringence properties.</p>	
---	--	--

Abstract

Anisotropic self-organized hybrid silica based xerogels were obtained. The ordered structure was imposed by the double charged 1,4-diazoniabicyclo[2.2.2]octane chloride group bonded in a bridged way. This was confirmed by the presence of well defined X-ray diffraction peaks corresponding to an interplanar distance with the same length estimated for the organic bridged groups. The material was characterized by elemental analysis using CHN technique and the chloride ion was analyzed by a potentiometric titration. C^{13} and Si^{29} CP MAS solid state NMR spectroscopy and thermogravimetric analysis were also performed. The material that can be obtained in the form of powders and transparent monoliths or films, is thermally stable up to 260 °C and the more organic concentrated samples presented birefringence properties.

Introduction

The search for new materials for new applications, with optimized properties and performance, as well as the enhancement of existent materials are challenges for materials science research. In this context, it comes up the possibility to combine organic and inorganic components, at molecular or nanometric level, generating new materials which are known as hybrid organic inorganic.¹⁻⁷

One of the methods used to obtain these hybrid materials is the sol-gel, which allows combining in a synergic form, the physicochemical properties of the original components. Additionally it is possible to monitor the morphological characteristics starting from the synthesis conditions.⁸⁻¹⁰ An important class of hybrid materials presents silica as inorganic component due to its properties such chemical inertness, mechanical rigidity, optical transparency, swelling resistance, thermal stability and others. Furthermore, the slow reactivity of the silicon in sol-gel precursors allows tailoring materials that can be employed in several applications as adsorbents,¹¹⁻¹² electrochemical sensors,¹³ catalysts¹⁴⁻¹⁵ and optical devices.^{16,17} In these materials the organic component can be covalently bonded in a pendant or in a bridged form. The varied in length, rigidity, geometry and functionality of the organic bridged group provides an opportunity to modulate properties such regular pore structure, thermal stability, optical transparency, chemical resistance and hydrophobicity.^{18,19} Self organization in nano and microstructural level have been also observed in some hybrid materials by using X-ray diffraction and light polarized microscopy. In these cases the ordered structure was imposed by the rigidity²⁰⁻²⁴ or arrangement produced by interactions between the organic groups.^{25,26}

Recently it was reported the synthesis of hybrids containing charged organic groups like quaternary ammonium, pyridinium and dabconium halides, which showed interesting properties like thermal stability, water solubility, ability to form films over inorganic surfaces.²⁷⁻³¹ Due to these characteristics they can be used as anion-exchangers, stationary phase for chromatography and electrochemical devices.³¹⁻³⁵ The possibility to form ordered nanostructures using charged organic groups such quaternary ammonium, imidazolium or protonated amine groups was also explored in few works.³⁶⁻³⁸

Recently we synthesized the organofunctionalized silica containing the double

charged 1,4-diazoniabicyclo[2.2.2]octane chloride group bonded to the silica framework in a bridged way. This material presented good chemical stability and the pore size was imposed by the chain length of the bridged organic group.³⁹ Interesting results as anion exchanger for hexacyanoferrate allowed its use as matrix for immobilization of electroactive species that were used in cyclic voltammetry studies.³⁹ It was also suitable as adsorbent for Cr (VI).⁴⁰ Although the interesting properties, the organic content was not higher than 5 % w/w. Aiming to explore new properties or to amplify the existing ones, it was prepared a new sample series of these hybrid xerogels, varying the synthesis conditions, planning to increase the organic content.

Experimental

Synthesis of the organic precursor di-3-n-propyltrimethoxysilane (1,4-diazoniabicyclo[2.2.2]octane) dichloride

Firstly, the 1,4-diazabicyclo[2.2.2]octane (dabco), previously sublimed, was dissolved in dimethylformamide (DMF), afterwards, it was added the 3-chloropropyltrimethoxysilane (CPTMS) in the stoichiometric ratio of 1:2. The mixture was stirred for 72 h, under argon atmosphere at 90 °C. The settling down white powder was washed with methanol and dried at 90 °C for 2 h. This resulting solid, di-3-n-propyltrimethoxysilane (1,4-diazoniabicyclo[2.2.2]octane) dichloride was assigned as $(R_2dabco)Cl_2$.

Synthesis of the sol-gel material

Starting from the organic precursor $(R_2\text{dabco})\text{Cl}_2$, a sample series of hybrid silica based xerogels, containing different organic amounts, was synthesized according Table 1. For each sample, an organic precursor solution containing $(R_2\text{dabco})\text{Cl}_2$ dissolved in a mixture of 25 ml of formamide, water and 0.1 ml of HF (48 %) at 60 °C was prepared. At this solution, it was added, dropping under stirring, a freshly prepared inorganic precursor solution containing tetraethylorthosilicate (TEOS), water and 7.0 ml of ethylic alcohol. The resulting solutions were let to gelation and solvent evaporation during 30 days at 40 °C, just covered without sealing. The obtained solids were washed with ethylic alcohol and dried at 90 °C for 2 h.

Elemental analyses

The elemental analyses of the organic groups present in the hybrid xerogels, were carried on a CHN Perkim Elmer M CHNS/O Analyzer, model 2400. The analyses were made in triplicate.

The ionized chloride amount was made by immersing the material in HNO_3 solution, under stirring. The chloride ion was potentiometric analyzed by a titration using silver nitrate, and calomel electrode as reference.

C^{13} and Si^{29} CP MAS analyses

Solid state NMR spectroscopy was performed on a Bruker 300/P spectrometer using the MAS (Magic angle) with CP (Cross-polarization). The C^{13} experiments were obtained using pulse length of 1 ms and recycle delay of 2 s while the Si^{29} measurements were made utilizing pulse length of 2.5 ms and recycle delay of 1 s

X-ray diffraction

X-ray diffraction patterns of the powdered samples were obtained with a Siemens Diffractometer model D500 using $\text{Cu K}\alpha$ as radiation source.

Optical measurements

The optical images of the xerogel samples were obtained using a microscope with cross polarized light Leica DMLP, coupled to photographic camera.

Birefringence measurements

For the determination of birefringence (Δ), the xerogel samples were fixed with commercial glue (Araldite) on a glass plate. Afterwards the samples were polished with diamond paste until to obtain a uniform thickness lower than 50 μm . The Δ values were obtained by using the Michel-Lévy Interference Color Chart.^{41,42}

Thermogravimetric analysis

Thermogravimetric analysis were carried out on a Shimadzu modelo TGA-50 system from room temperature to 800 °C at a heating rate of 20 °C min^{-1} in argon atmosphere. The samples were powdered in an agate mortar before the analysis.

Results and Discussion

The synthesis of the organic precursor di-3-n-propyltrimethoxysilane (1,4-diazoniabicyclo[2.2.2]octane) dichloride ($\text{R}_2\text{dabcoCl}_2$) was already reported.³⁹ It was characterized by CP MAS C^{13} and its structure is presented in the Scheme 1.

Scheme 1

The reactive methoxy groups can be partially or totally hydrolyzed as represented in the Scheme 2.

Scheme 2

Starting from the organic precursor a sample series of hybrid silica based xerogels, containing different organic amounts, was synthesized, according to Table 1. The physical aspect of a typical xerogel, sample X60, is presented in Figure 1. It is possible to see the transparency so much in the sample of the left, a film as in the sample of the right, a monolith.

The C^{13} CP MAS NMR spectra of the hybrid xerogel samples are presented in the Figure 2. The peak at 9,9 ppm was due to carbon bonded to silicon, the peak at 16.1 ppm was assigned to the central carbon of the propyl groups, the peak at 45.1 ppm was assigned to the carbons of methoxy groups and the peaks 52.0 and 66.9 were attributed to the carbons bonded to the quaternary nitrogen, from the dabco and propyl groups, respectively.^{43,44} The CP MAS spectra of hybrid xerogel samples match with the spectrum of the organic precursor assigned as $(R_2dabco)Cl_2$, that was already synthesized and characterized in a previous paper.³⁹ These results confirm the formation of the hybrid xerogel containing the organic group di-3-n-propyltrimethoxysilane (1,4-diazoniabicyclo[2.2.2]octane) dichloride.

The Si^{29} CP MAS NMR spectra of the hybrid xerogel samples are presented on the Figure 3. It is clearly observed two different peak regions, the first region that presents chemical shifts between -50 and -80 ppm is due to T units and the second region with shifts between -80 and -120 ppm is due to Q units. According to literature T units are formed by silicon atoms bonded to carbon atoms and organic groups and Q units are silicon atoms of the siloxane and silanol atoms.⁴⁵⁻⁴⁷ The peaks assignments are showed in the Table 2. For X100 sample, where only the organic precursor $(R_2dabco)Cl_2$ was added, the spectrum shows just T species, revealing the existence of $C-Si^*(OSi)_3$ (T^3 units) $C-Si^*(OR)(OSi)_2$ (T^2 units) and $C-Si^*(OR)_2(OSi)$ (T^1 units). These results are evidences that a fraction of silicon atoms was not completely hydrolyzed. The samples where the inorganic precursor TEOS was added, show also peaks due to the Q units, $(SiO)_2Si^*(OH)_2$, $(SiO)_3Si^*OH$ and $(SiO)_4Si^*$ (Table 2). These Q peaks became more visible with the increasing of the inorganic component content (Figure 3).

The organic content of the organic precursor $(R_2dabco)Cl_2$ and hybrid xerogel samples (X05 – X100) was estimated by using CHN elemental analysis, potentiometric chloride analysis and also thermogravimetric analysis. The results are presented in the Table 3. From the elemental analysis it can be observed that a

sample series containing different organic content was attained. Even considering the differences in each technique, the results are in accordance with the planned syntheses, having an increase in the organic content with the amount of the organic precursor added. It was also observed in all the techniques that occurred saturation in the organic content for the more concentrated samples. Additionally the values attained in the chloride analysis are consistent with the theoretical value of 13.9 % calculated for the proposed structure of the organic precursor $(R_2\text{dabco})\text{Cl}_2$ (Scheme 1). This result confirms the formation of xerogels containing double charged dabco groups.

The Thermogravimetric curves are shown in Figure 4. From 150 up to 650 °C the weight loss was attributed mainly to decomposition of organics and also dehydroxylation reactions of the silanol groups. This loss was more significant above 260 °C showing the formation of hybrid materials thermally stable up this temperature. This thermal stability for dabco groups immobilized in this hybrid material is important because enlarge the possibility of applications, considering that this substance sublime at room temperature. Differential curves, obtained from TGA results are shown in Figure 5. It is possible to observe more clearly that the samples with low organic content, X05 and X15, present high thermal stability for organics. Additionally the peak areas increase with the organic content.

Figure 6 shows the X-ray diffraction results for the sample series. All the diffraction curves show a large peak, with angle 2 theta near 20°, characteristic of amorphous silica materials.⁴⁸ However, with the increasing of the organic content, two additional peaks were observed, starting from the X60 sample. The presence of these peaks, assigned **d1** and **d2** with angle 2 theta 6.2° and 12.5° respectively, is very important because indicates the existence of organized structure imposed by the presence of the charged organic groups. The interplanar distance **d** related to these peaks was calculated using the Bragg law, resulting in 1.43 nm and 0.71 nm, respectively. This interplanar distance of 1.43 nm matches with the length of the organic bridged groups estimated in previous works,³⁹ as represented in Scheme 3. Considering the peak **d2**, although it is not well defined as **d1**, the interplanar distance value corresponds to a half of the **d1** distance. It is important to observe that besides of the organized structure imposed by the organic groups, it can be seen the

presence of a fraction of amorphous silica visible through the large peak at 2 theta, near 20°.

Scheme 3

The samples were analyzed by optical microscopy using natural light at different magnifications and they appeared to be homogeneous with few micrometric bubbles and cracks formed during the gelation process. The samples X60, X70, X80, X90 e X100, with higher organic content presented a first order birefringence with constant values between 0.001 and 0.002, while the samples X05, X15 and X40 did not show this characteristic. In Figure 7 it is showed typical images of the hybrid xerogel obtained at natural and polarized light at different angles, confirming the birefringence property. The existence of the birefringence is an evidence of the anisotropic organization in these hybrid xerogel samples. It was already reported anisotropic organization in bridged hybrid xerogels, where the organization was imposed by the structural rigidity or arrangement of the organics.²⁰⁻
²⁶ In our case the organization is supposed to be imposed by the charge of the organic groups, which are electrostatic oriented when the organic concentration is high in the sol-gel synthesis.

Conclusions

The synthesis of a sample series of hybrid silica based xerogels containing the 3-n-propyl-1,4-diazoniabicyclo[2.2.2]octane chloride double charged group varying the organic content from 15 to 50 % w/w was performed. The hybrid material that can be presented in form of powders, and transparent films or monoliths, is thermally stable up to 260 °C. The samples with higher organic content showed birefringence property indicating the presence of anisotropic organization. These samples also showed X-ray diffraction peaks with interplanar distance of 1.43 nm. This value matches with the length of the organic bridged group. Therefore it was obtained a self-organized hybrid material, where the ordered structure was imposed by the bridged charged dabconium group.

Acknowledgements

We thank to CNPq, FAPERGS and FAPESP for fellowships and financial support.

References

1. Schubert, U.; Gao, Y.; Kogler, F. R.; *Prog. Solid State Chem.* **2007**, *35*, 161.
2. Zhao, L.; Loy, D. A.; Shea, K. J. *J. Am. Chem. Soc.* **2006**, *128*, 14250.
3. Ramos, G.; Belenguer, T.; Levy, D. *J. Phys. Chem.* **2006**, *110*, 24780.
4. Minoofar, P. N.; Hernandez, R.; Chia, S.; Dunn, B.; Jeffrey I. Zink, J. I.; Franville, A.-C. *J. Am. Chem. Soc.* **2002**, *124*, 14388.
5. Gao, Y.; Choudhury, N. R.; Matison, J.; Schubert, U.; Moraru, B. *Chem. Mater.* **2002**, *14*, 4522.
6. Chaker, J. A.; Santilli, C. V.; Pulcinelli, S. H.; Dahmouche, K.; Briois V.; Judeinstein, P. *J. Mater. Chem.*, **2007**, *17*, 744.
7. Marina T. Laranjo, M. T.; Stefani, V.; Benvenutti, E. V.; Costa, T. M. H.; Ramminger, G. O.; Gallas, M. R. *J. Non-Cryst. Solids* **2007**, *353*, 24.
8. Collinson M. M. *Critical Rev. Anal. Chem.* **1999**, *29*, 289.
9. Schubert, U.; Husing, N.; Lorenz, A. *Chem. Mater.* **1995**, *7*, 2010.
10. Gay, D. S. F.; Gushikem, Y.; Moro, C. C.; Costa, T. M. H.; Benvenutti, E. V. *J. Sol-Gel Sci. Technol.* **2005**, *34*, 189.
11. Pavan, F. A.; Lucho, A. M.S.; Gonçalves, R. S.; Costa, T. M. H.; Benvenutti, E. V. *J. Colloid Interface Sci.* **2003**, *263*, 688.
12. Passos, C. G.; Ribaski, F. S.; Simon, N. M.; Santos Jr., A. A.; Vaghetti, J. C. P.; Benvenutti, E. V.; Lima, E. C. *J. Colloid Interface Sci.* **2006**, *302*, 396.
13. Walcarius, A. *Chem. Mater.* **2001**, *13*, 3351.
14. Price, P. M.; Macquarrie, D. J. *J. Chem. Soc. Dalton Trans.* **2000**, *2*, 101.
15. Ford, D. M.; Simanek, E. E.; Shantz, D. F. *Nanotechnology* **2005**, *16*, S458.
16. Costa, T. M. H.; Hoffmann, H. S.; Benvenutti, E. V.; Stefani, V.; Gallas, M. R.; *Opt. Mater.* **2005**, *27*, 1819.
17. Serwaczak, M.; Ubbenhorst, M. W.; Kucharski, S. *J Sol-Gel Sci Techn.* **2006**, *40*, 39.
18. Shea, K. J.; Loy, D. A. *Acc. Chem. Res.* **2001**, *34*, 707.
19. Loy, D. A.; Shea, K. J. *Chem. Mater.* **2001**, *13*, 3306.
20. Ben, F.; Boury, B.; Corriu, R. J. P.; Strat, V. L. *Chem. Mater.* **2000**, *12*, 3249.

-
21. Boury, B.; Ben, F.; Corriu, R. J. P.; Delord, P.; Nobili, M. *Chem. Mater.* **2002**, *14*, 730.
 22. Muramatsu, H.; Corriu, R. J. P.; Boury, B. *J. Am. Chem. Soc.* **2003**, *125*, 854.
 23. Vergnes, A.; Nobili, M.; Delord, P.; Cipelletti, L.; Boury, B.; Corriu, R. J. P. *J. Sol-Gel Sci. Technol.* **2003**, *26*, 621.
 24. Kapoor, M. P.; Yang, Q.; Shinji, I. *Chem. Mater.* **2004**, *16*, 1209.
 25. Cerveau, G.; Corriu, R. J. P.; Framery, E.; Lerouge, F. *Chem. Mater.* **2004**, *16*, 3794.
 26. Lerouge, F.; Cerveau, G.; Corriu, R. J. P. *J. Mater. Chem.* **2006**, *16*, 90.
 27. Arenas, L. T.; Langaro, A.; Gushikem, Y.; Moro, C. C.; Benvenuti, E. V.; Costa, T. M. H. *J. Sol-Gel Sci. Technol.* **2003**, *28*, 51.
 28. Arenas, L. T.; Aguirre, T. A. S.; Langaro, A.; Gushikem, Y.; Benvenuti, E. V.; Costa, T. M. H. *Polymer* **2003**, *44*, 5521.
 29. Alfaya, R. V.S.; Fujiwara, S. T.; Gushikem, Y.; Kholin, Y. V. *J. Colloid Interface Sci.* **2004**, *269*, 32.
 30. Splendore, G.; Benvenuti, E. V.; Kholin, Y. V.; Gushikem, Y. *J. Braz. Chem. Soc.* **2005**, *16*, 147.
 31. Tien, P.; Chau, L. K.; Shieh, Y. Y.; Lin, W. C.; Wei, G. T. *Chem. Mater.* **2001**, *13*, 1124.
 32. Auler, L. M. L. A.; Silva, C. R.; Collins, K. E.; Collins, C. H. *J. Chromatogr. A* **2005**, *1073*, 147.
 33. Arenas, L. T.; Simon, N. M.; Gushikem, Y.; Costa, T. M. H.; Lima, E. C.; Benvenuti, E. V. *Eclat Quim.* **2006**, *31*, 53.
 34. Lucho, A. M. S.; Oliveira, É. C.; Pastore, H. O.; Gushikem, Y. *J. Electroanal. Chem.* **2004**, *573*, 55.
 35. Kanungo, M.; Collinson, M. M. *Langmuir* **2005**, *21*, 827.
 36. Lee, B.; Jung Im, H-J.; Luo, H.; Hagaman, E. W.; Dai, S.; *Langmuir* **2005**, *21*, 5372.
 37. Wong, E. M.; Markowitz, M. A.; Qadri, S. B.; Golledge, S. L.; Castner, D. G.; Gaber, B. P. *Langmuir* **2002**, *18*, 972.
 38. Kaneko, Y.; Iyi, N.; Kurashima, K.; Matsumoto, T.; Fujita, T.; Kitamura, K. *Chem. Mater.* **2004**, *16*, 3417.

39. Arenas, L. T.; Dias, S. L. P.; Moro, C. C.; Costa, T. M. H.; Benvenuti, E. V.; Lucho, A. M. S.; Gushikem, Y. J. *J. Colloid Interface Sci.* **2006**, 297, 244.
40. Arenas, L. T.; Lima, E. C.; Santos A. A.; Vaghetti, J. C. P.; Costa, T. M. H.; Benvenuti, E. V. *Colloids Surf. A* **2007**, 297, 240.
41. Nikon's MicroscopyU website. In <<http://www.microscopyu.com/articles/polarized/michel-levy.html>> Acess in May 02, 2007.
42. Kerr, P. F. *Optical Mineralogy*, McGraw-Hill Book Company: New York, 1977, p 492.
43. Hou, S. S.; Kuo, P. L. *Polymer* **2001**, 42, 9505.
44. Davis; M. E.; Saldarriaga, C. J. *J. Chem. Soc. Chem. Commun.* **1988** 920.
45. Sassi, Z.; Bureau, J. C.; Bakkali, A; *Vibrat. Spectrosc.* **2002**, 28, 299.
46. Oviatt, H. W.; Shea, K. J.; Small, J. H.; *Chem. Mater.* **1993**, 5, 943.
47. Dabrowski, A.; Barczak, M.; Stolyarchuk, N. V.; Melnyk, I.V.; Zub, Yu. L. *Adsorption* **2005**, 11, 501.
48. Hoffmann, H. S.; Staudt, P. B.; Costa, T. M. H.; Moro, C. C.; Benvenuti, E. V. *Surf. Interface Anal.* **2002**, 33, 631.

Table 1: Synthesis conditions of the xerogel samples

Xerogel sample	(R ₂ dabco)Cl ₂ molar %	Organic precursor solution		Inorganic precursor solution	
		(R ₂ dabco)Cl ₂ mmol	H ₂ O ml	TEOS mmol	H ₂ O ml
X5	5	0,90	1,00	17,10	0,30
X15	15	2,25	0,90	12,75	0,30
X40	40	4,80	0,75	7,20	0,30
X60	60	3,60	0,55	2,40	0,10
X70	70	4,20	0,70	1,80	0,10
X80	80	4,80	0,50	1,20	0,10
X90	90	5,40	0,50	0,60	0,10
X100	100	6,00	0,65	0,00	0,00

Table 2: Si²⁹ CP MAS NMR analysis

Chemical shift / ppm		assignment
-50.1	T ¹	C-Si*(OR) ₂ (OSi)
-59.0	T ²	C-Si*(OR)(OSi) ₂
-68.5	T ³	C-Si*(OSi) ₃
-91.4	Q ²	(SiO) ₂ Si*(OH) ₂
-101.3	Q ³	(SiO) ₃ Si*(OH)
-110.7	Q ⁴	(SiO) ₄ Si*

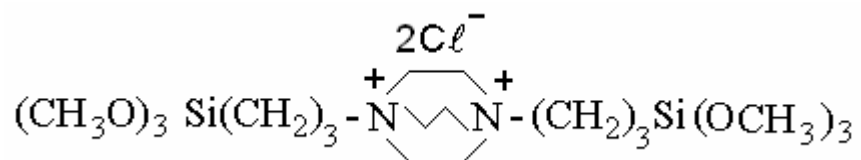
Table 3: Elemental analyses and organic content of the hybrid xerogels.

Sample	CHN analysis (w/w %)	Chloride analysis (w/w %) ^a	TGA analysis (w/w %) ^b
X05	14.9	2.7	23.7
X15	26.4	7.0	31.6
X40	39.4	9.4	40.0
X60	39.7	11.5	42.2
X70	40.1	12.4	42,4
X80	41.6	12.1	44.7
X90	41.8	12.1	48.2
X100	43.4	12.8	48.2
(R ₂ dabco)Cl ₂	50.1	12.6	53

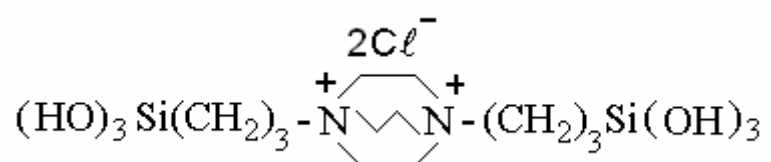
^a Obtained from potentiometric analysis;

^b Weight loss from 150 to 650 °C.

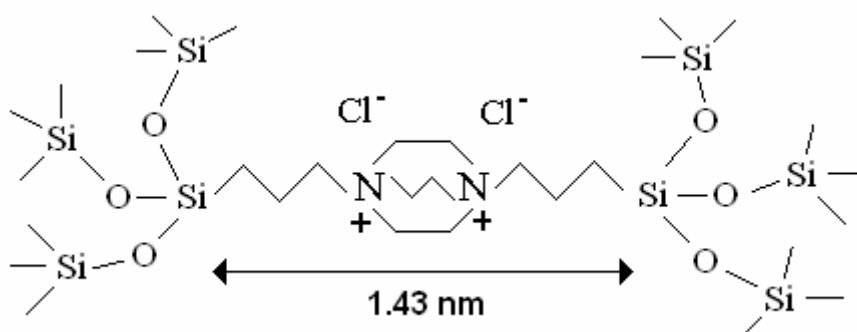
Scheme 1



Scheme 2



Scheme 3



Captions for Figure

Figure 1: Picture of the X60 hybrid xerogel sample.

Figure 2: C^{13} CP MAS spectra of hybrid xerogel samples.

Figure 3: Si^{29} CP MAS spectra of hybrid xerogel samples.

Figure 4: Thermogravimetric curves of hybrid xerogel samples.

Figure 5: Thermogravimetric differential curves of xerogel samples.

Figure 6: X-ray diffratograms of xerogel samples.

Figure 7: Images of the xerogel sample X60, obtained in normal light (a) and polarized light (b) 0° , (c) 20° , (d) 45° , (e) 90° and (f) 180° . The width of each image is 1.0 mm.

Fig 1.

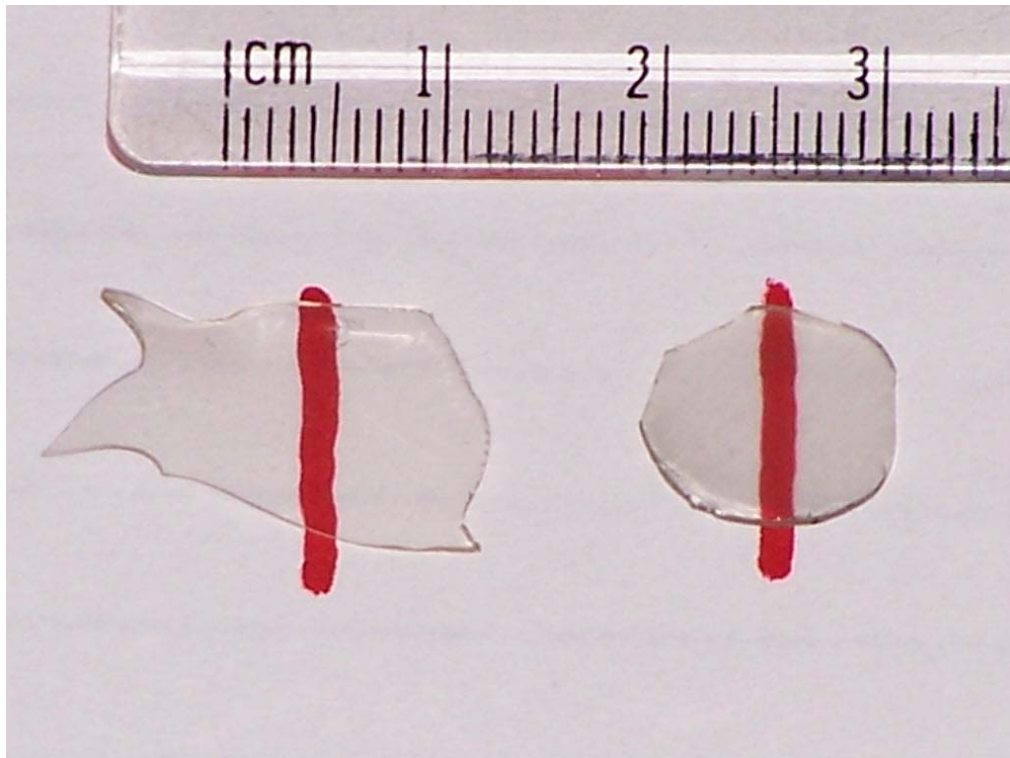


Fig 2

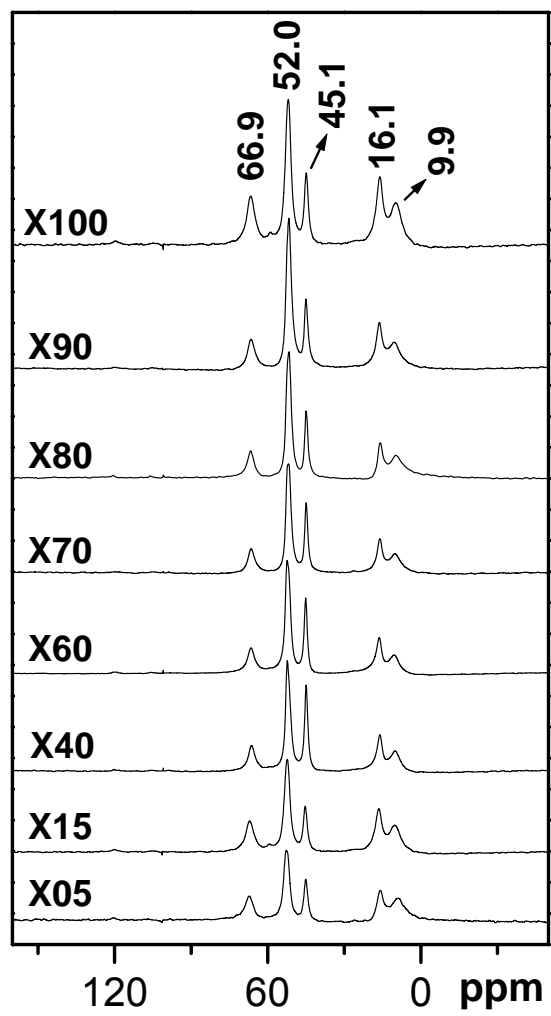


Fig 3

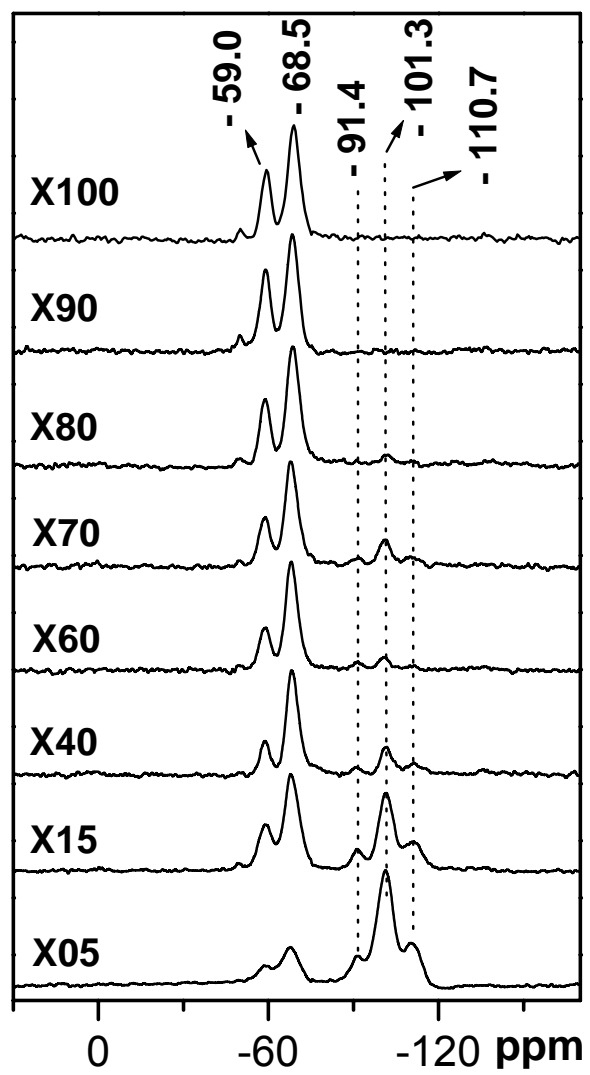


Fig 4

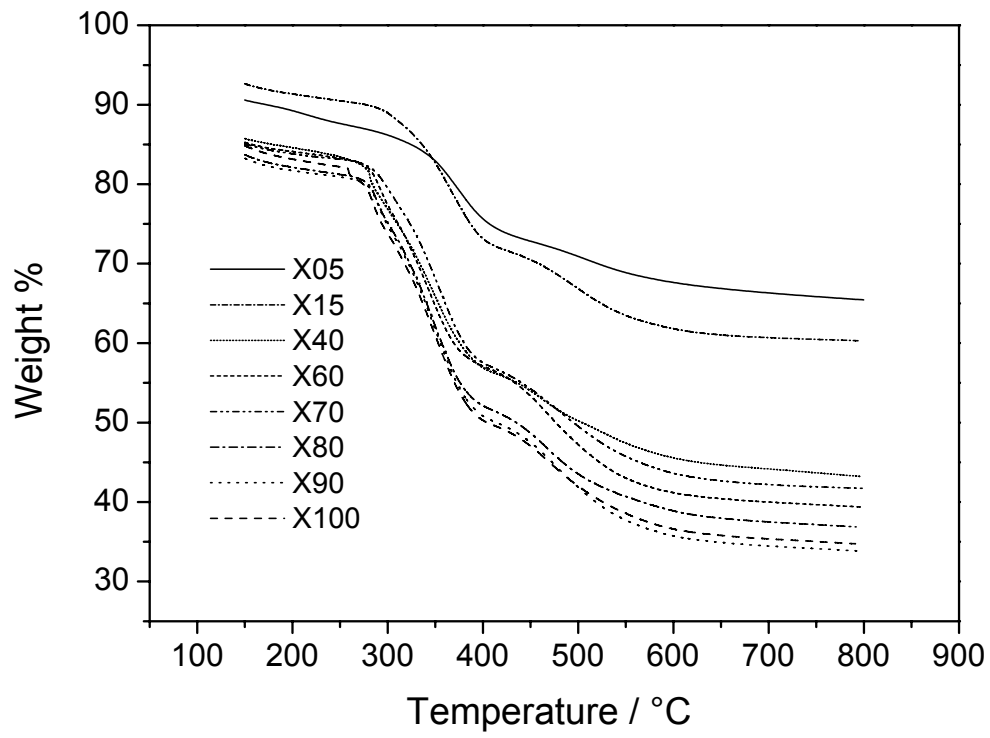


Fig 5

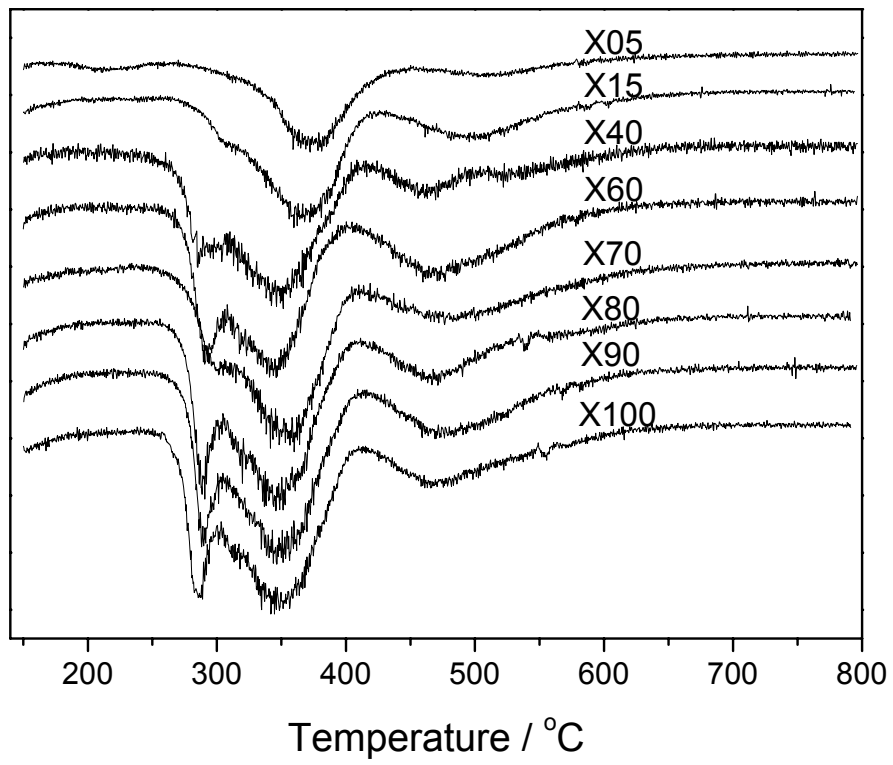


Fig 6

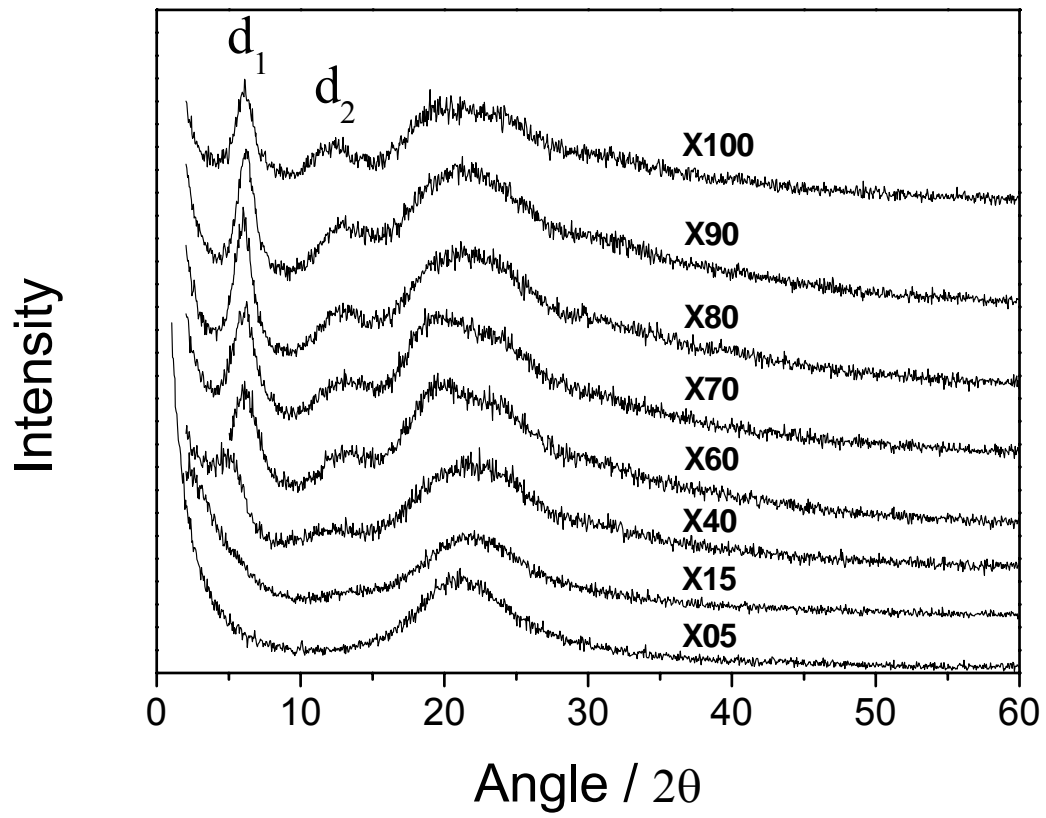
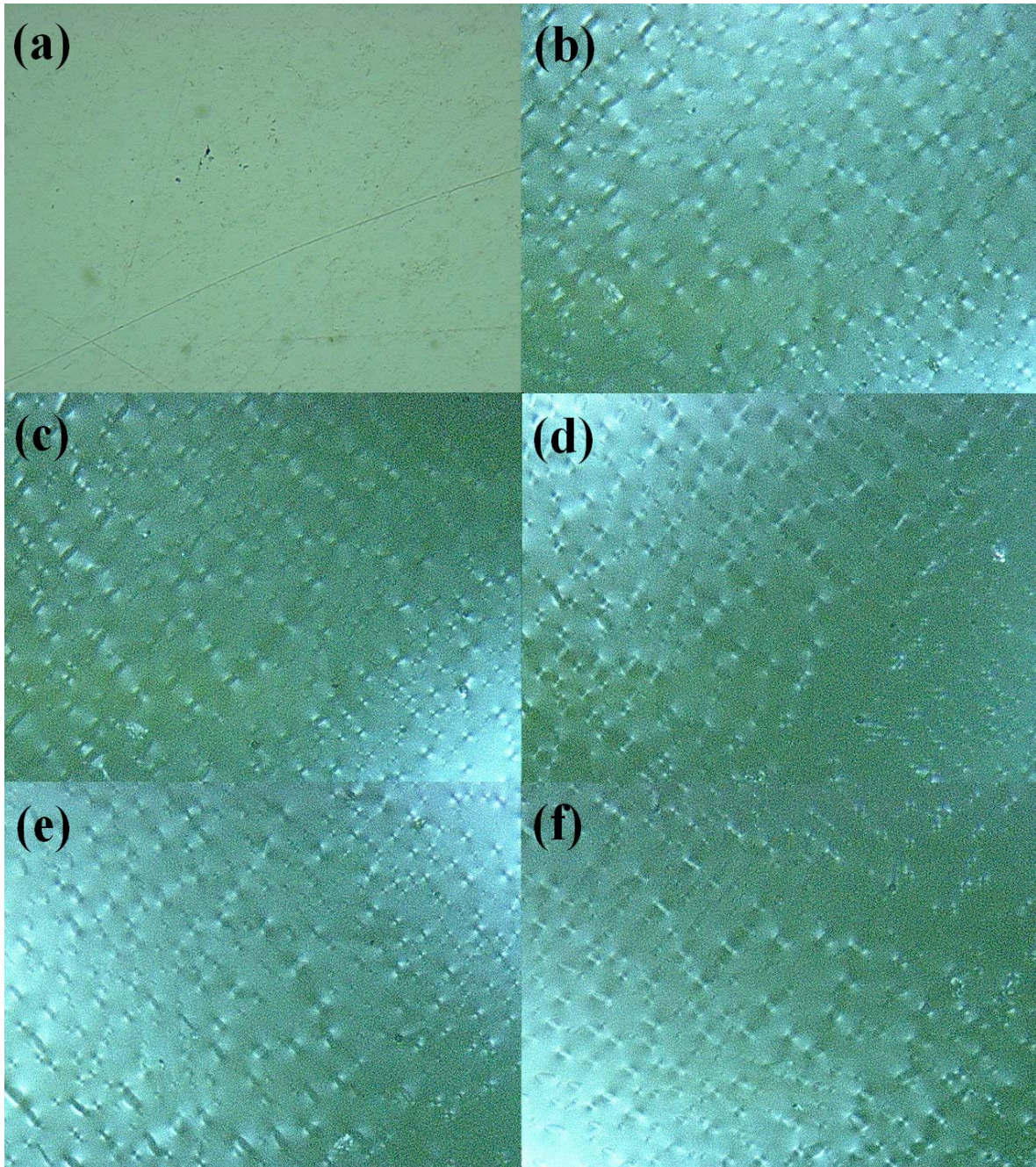


Fig 7



- 4.4- Brilliant yellow dye immobilized on silica and silica/titania based hybrid xerogels containing bridged positively charged 1,4-diazoniabicyclo[2.2.2]octane: Preparation, characterization and electrochemical properties study. Submetido, **2007**.

Brilliant yellow dye immobilized on silica and silica/titania based hybrid xerogels containing bridged positively charged 1,4-diazoniabicyclo[2.2.2]octane: Preparation, characterization and electrochemical properties study.

Leliz T. Arenas, Débora S. F. Gay, Celso C. Moro, Silvio L. P. Dias, Denise S. Azambuja, Tania M. H. Costa, Edilson V. Benvenutti*

Instituto de Química, Universidade Federal do Rio Grande do Sul, CP 15003, 91501-970 Porto Alegre - RS, Brazil.

Yoshitaka Gushikem

Instituto de Química, Universidade Estadual de Campinas, CP 6154, 13083-970 Campinas, SP, Brazil

* Corresponding Author Edilson V. Benvenutti
benvenutti@iq.ufrgs.br
Phone: 55 51 33167209
Fax: 55 51 33167304

Abstract

Silica and silica/titania based hybrid xerogels containing the double charged 1,4-diazoniabicyclo[2.2.2]octane group bonded in a bridged way were obtained. The hybrids were characterized by infrared spectroscopy and CHN analyses for the identification and determination of organic content. N₂ adsorption-desorption isotherms and SEM were applied to study morphological and textural aspects. The hybrid materials presented anion-exchange properties that allowed their use as adsorbent for brilliant yellow anionic dye. These modified materials were used to prepare carbon paste electrodes for cyclic voltammetric measurements, where the brilliant yellow, for the first time, was applied as electroactive species. The pH solution has no effect on the anodic peak potential and anodic peak current in the values range between 2.0 and 7.0. The electrode response was invariant under various oxidation-reduction cycles showing that the system is chemically very stable. A carbon paste electrode of the (R₂dabco)BY/SiO₂/TiO₂ material was used to study the electrocatalytic oxidation of ascorbic acid by cyclic voltammetric and chronoamperometric techniques.

Keywords: sol-gel, brilliant yellow, organofunctionalized silicas, ascorbic acid, vitamin C.

Introduction

The development of silica based organic-inorganic hybrid materials is now a wide field of investigation. These materials combine in a single one the mechanical stability of rigid inorganic framework with the chemical behavior of the organic component. A major appeal of such research activities is probably linked to a synergistic effect carrying advanced properties to the hybrid materials, which can even be improved in comparison to the own unique properties of each component [1-8]. The presence of the heteroatoms in the inorganic oxide matrix can enlarge the possibilities of interesting characteristics [9-12].

Among the varieties of explored hybrid materials, those that possess positively charged organic groups with exchangeable anions, have recently drawn particular interest. Some applications like stationary phase for chromatography [13-16] and for immobilization of electroactive species that allow preparing chemically modified electrodes have been proposed [17-21].

In previous papers, we have synthesized the silica based hybrid xerogel containing the bridged double charged 1,4-diazoniabicyclo[2.2.2]octane group (Figure 1(a)). This material presented good chemical stability and appropriate porosity to adsorb, by anion exchange reactions, hexacyanoferrate [21] and chromate [22].

The brilliant yellow (BY) is an anionic azo dye (Figure 1(b)), which is expected to be immobilized in the pores of the charged hybrid xerogels by anion exchange. In previous studies, it was reported that this dye can be used as optical sensor for pH, for ammonia and urea determination [23,24], as photometric indicator for magnesium [25], and also in electrochemical synthesis of polypyrrol films [26]. However, the behavior of this dye as electroactive species adsorbed on a porous solid matrix has not been investigated.

In the present work, the preparation of silica based hybrid xerogel containing the double charged 1,4-diazoniabicyclo[2.2.2]octane group bonded in a bridged way is reported. The influence of the titania on the matrix of the hybrid material was investigated. The hybrid materials were used to adsorb BY dye by anion exchange, and its electrochemical behavior was also described in this work. The electrodes made with BY dye immobilized on hybrid xerogels, were tested in electron-mediated process for electrocatalysis of the ascorbic acid.

Experimental

Synthesis of the organic precursor 1,4-bis-(3-trimethoxysilypropyl)diazoniabicyclo [2.2.2]octane chloride

Firstly, 8 mmol of the 1,4-diazabicyclo[2.2.2]octane (dabco), previously sublimed, was dissolved in 20 ml dimethylformamide (DMF), afterwards, it was added to 16 mmol of 3-chloropropyltrimethoxysilane (CPTMS). The mixture was stirred for 72 h, under argon atmosphere at 70 °C. The white solid obtained was filtered and washed with methyl alcohol and then dried at 70 °C for 2 h. These resulting solid, 1,4-bis-(3-trimethoxysilypropyl)diazoniabicyclo[2.2.2]octane chloride was designated as (R₂dabco)Cl₂.

Preparation of the bridged hybrid xerogels

The organic precursor (R₂dabco)Cl₂ (50 mg) was dissolved in a mixture of dimethylsulfoxide (DMSO) (5 ml), water (0.6 ml), and hydrofluoric acid 48% (HF) (0.1 ml), heated at 60 °C. To this solution tetraethylorthosilicate (TEOS), previously dissolved in ethanol (5 ml) and water (1.0 ml), was added and stirred for 10 min. The reaction mixture was allowed to stand for 30 days, at 40 ± 1 °C, for gelation and evaporation of solvent. The resulting material was designated as (R₂dabco)Cl₂/SiO₂. The hybrid containing the titania was prepared using the same procedure. However, the titanium isopropoxide (0.32 ml) previously dissolved in ethanol (3 ml) was added dropwise to the sol-gel system. Additionally, the mixture was stirred for 20 min and was allowed to stand for 30 days, at 40 ± 1 °C, for gelation and evaporation of solvent. This xerogel material was then designated as (R₂dabco)Cl₂/SiO₂/TiO₂. The hybrid xerogel materials were then comminuted, washed with ethanol and finally dried in an oven at 90 °C for 2 h.

Brilliant Yellow dye immobilization on bridged hybrid xerogels

The bridged hybrid xerogel samples (500 mg) were immersed in a 1.0 x 10⁻³ mol l⁻¹ brilliant yellow (BY) solution (20 ml) and the mixture was shaken for 3 h at 25 °C. The modified solid was filtered and washed with distilled water and ethanol, finally it was dried in an oven at 60 °C for 2 h. The resulting solids were designated as (R₂dabco)BY/SiO₂ and (R₂dabco)BY/SiO₂/TiO₂.

Elemental analysis

The elemental analyses of the organic groups incorporated in the matrices were carried on a CHN Perkim Elmer M CHNS/O Analyzer, model 2400. The analyses were made in triplicate.

Infrared analysis

Self-supporting disks of the xerogels, with a diameter of 2.5 cm, weighing *ca.* 100 mg were prepared. The disks were heated in a temperature of 100 °C for 1 h, under vacuum (10^{-2} Torr). The IR cell used in this work presents two sections, an oven that consists of an electrical filament on the external wall of the cell and another section with two KBr windows for submitting the sample to the infrared beam, using a mobile support. The two sections are pressed together using a viton o-ring. The sample can be heated, under vacuum and then moved to the infrared beam for analysis without exposition to the external environment [27]. The equipment used was a Shimadzu FTIR, model 8300. The spectra were obtained at room temperature with a resolution of 4 cm^{-1} , with 100 cumulative scans.

Diffuse reflectance analysis

UV visible spectra of hybrid xerogels were obtained on a Cary 5G UV-Vis NIR spectrophotometer using the diffuse reflectance accessory.

N₂ adsorption-desorption isotherms

The nitrogen adsorption-desorption isotherms of previous degassed xerogels at 100 °C, were determined at liquid nitrogen boiling point in a homemade volumetric apparatus, with a vacuum line system employing a turbo molecular Edward vacuum pump. The pressure measurements are made using capillary Hg barometer. The specific surface areas of hybrid materials were determined from the BET (Brunauer, Emmett and Teller) multipoint method [28]. And the pore size distribution was obtained using BJH (Barret, Joyner, and Halenda) method [29].

Scanning Electron Microscopy

The hybrid materials were analyzed by scanning electron microscopy (SEM) in Jeol equipment, model JEOL JSM 6060, with 20kV and magnification of 20000 and 60000x. The

average diameter and standard deviation of the primary particles were determined by using the Quantikov software [30].

EDS analysis

The EDS image was obtained for $(R_2\text{dabco})\text{Cl}_2/\text{SiO}_2/\text{TiO}_2$ material dispersed on a double faced conducting tape on an aluminum support and coated with a thin film of gold using a Baltec SCD 050 Sputter Coater apparatus. The micrograph was obtained using a Jeol Scanning Electron Microscope, model JSM 5800, connected a secondary electron detector and X-ray energy dispersive spectrometer (EDS) for elemental mapping in a Noran Instrument. The image was obtained with a magnification of 1200x.

Electrochemical study

The homogeneous carbon paste electrode was prepared, in an agate mortar, by mixing hybrid xerogels containing the immobilized dye (5.0 mg) with graphite powder (15.0 mg) and a drop of mineral oil (Nujol). Afterwards, the mixture was pressed into a 1 mm depth and 0.5 cm diameter glass cavity fused at the end of a glass tube and arranged with a copper wire serving as an external electric contact. The cyclic voltammetric and chronoamperometric measurements were carried out on a Radiometer model DEA 332 potentiostat-galvanostat. The electrochemical cell system, consisted in a working electrode (carbon paste electrode), in a reference electrode (saturated calomel electrode, SCE) and a platinum contra-electrode.

Electrochemical impedance spectroscopy (EIS) essays were performed using an AUTOLAB PGSTAT 30/FRA 2, in the 10 kHz - 10 mHz frequency range with a sinusoidal voltage amplitude of 10 mV.

Electrocatalytic oxidation of ascorbic acid

The electrocatalytic oxidation of ascorbic acid (H_2AA) on the electrode $(R_2\text{dabco})\text{BY}/\text{SiO}_2/\text{TiO}_2$ was initially investigated by means of cyclic voltammetry over the range from -300 up to 600 mV vs SCE by addition of 1.0 ml of 0.1 mol l^{-1} ascorbic acid solution, in an electrochemical cell containing 20 ml of the 1.0 mol l^{-1} KCl solution, at room temperature. The scan rate was de 20 mV s^{-1} .

For amperometric technique all the measurements were carried out under argon atmosphere. A standard aqueous solution acid 0.01 mol l^{-1} was prepared. In an electrochemical cell filled with 20 ml 1.0 mol l^{-1} KCl solution at pH 6.0, a fixed volume (50

μl) of the standard solution was successively added. The potential fixed to carry out the experiment was 180 mV vs SCE for 50 s. The current values were interloped in an amperometric analytical curve.

Ascorbic acid in vitamin C tablets from three different suppliers was analyzed. The tablets (~ 1 g) were dissolved in deionized and degassed water and the volume completed to 200 ml (solution A). The amperometric curves were obtained by adding successive aliquots of 50 μl of solution A into a cell filled with 20 ml of 1.0 mol l^{-1} KCl at pH 6.0. In commercial juices, ascorbic acid was determined by using similar procedure. To check the performance of the electrode response, the quantity of ascorbic acid in tablets and in juices was also determined by standard iodometry procedure [31].

Results and discussion

Characteristics of the materials

The infrared spectra of the bridged hybrid xerogel are showed in Figure 1, where the organic and inorganic components can be observed. The organic moiety can be identified by the bands at 1467 cm^{-1} that correspond to the CH_2 bending of dabco and propyl groups. The inorganic component can be identified by the typical silica overtone bands with maximum in 1860 cm^{-1} . The amount of organic groups immobilized was estimated by using the CHN elemental analysis. The values obtained were 0.24 and 0.19 mmol of organic groups per gram of hybrid xerogel, for $(\text{R}_2\text{dabco})\text{Cl}_2/\text{SiO}_2$ and $(\text{R}_2\text{dabco})\text{Cl}_2/\text{SiO}_2/\text{TiO}_2$, respectively (Table 1).

Figure 3(a) shows the SEM image of the $(\text{R}_2\text{dabco})\text{Cl}_2/\text{SiO}_2/\text{TiO}_2$ hybrid xerogel and Fig. 3(b) shows the corresponding EDS Ti mapping image. The blue points in Figure 3(b) are emission lines of Ti $\text{K}\alpha$ at 4.5 KeV [32]. Considering the magnification used, it can be seen that the TiO_2 is homogenously dispersed in the sub-micrometric level. Additionally from the X-ray diffraction analysis it was not observed any titania crystalline phase. The Ti/Si atomic ratio determined by EDS analysis was 0.07 (Table 1).

The SEM analysis with magnification of 20000 and 60000x are shown in Figure 4. In the image for $(\text{R}_2\text{dabco})\text{Cl}_2/\text{SiO}_2/\text{TiO}_2$ (Figure 4b) it is possible to observe that the xerogel has globular morphology with primary particles with diameter of 80 ± 26 nm, that are joined

together to form agglomerates with diameter of 270 ± 72 nm. It is also important to observe in this image the presence of macropores. The Figure 4a shows the $(R_2dabco)Cl_2/SiO_2$ hybrid xerogel image. For this xerogel the agglomerates are smaller with diameter of 170 ± 51 nm and they are more closely packed, presenting primary particles with diameter of 60 ± 13 nm.

Figure 5 shows the pore size distribution curves obtained by BJH method and the inserted figure shows the N_2 adsorption-desorption isotherms. The xerogels exhibit type IV-like isotherms with H2 hysteresis, typical of the mesoporous materials [33,34]. Moreover for the $(R_2dabco)Cl_2/SiO_2/TiO_2$ xerogel, at very low relative pressure ($P/P_0 < 0.2$) the isotherm exhibits high adsorption, implying the presence of micropores. In the pore size distribution curve for the $(R_2dabco)Cl_2/SiO_2$ xerogel is observed a single mesopore region with maximum distribution at 7.6 nm diameter and for the $(R_2dabco)Cl_2/SiO_2/TiO_2$ xerogel is observed the presence of pores with diameter lower than 4 nm. This result suggests that the addition of titania produces a reduction in the pore diameter considering this region below 15 nm, on the other hand also causes the formation of macropores already observed in the SEM images.

The BET surface areas and pore volume of the hybrid xerogels are summarized in Table 1. Both xerogels exhibited the same value for surface areas, $570 \text{ m}^2 \text{ g}^{-1}$. Although the $(R_2dabco)Cl_2/SiO_2/TiO_2$ have presented micropores, which would contribute to a higher surface area value, it also presented a higher particle size and higher agglomerate diameter that present a lower contribution to surface area. On the other hand the $(R_2dabco)Cl_2/SiO_2$ xerogel presented mesopores contribution to surface area and lower particle size and agglomerate diameter having a major contribution to surface area. This ensemble of tendencies caused at last, coincidentally the same value of surface area. The higher value of pore volume for $(R_2dabco)Cl_2/SiO_2/TiO_2$ was interpreted considering the presence of macroporosity on this material, observed on SEM images, which was not observed for $(R_2dabco)Cl_2/SiO_2$ xerogel.

Immobilization of dye brilliant yellow

Figure 6 shows the UV/visible diffuse reflectance spectra for hybrid xerogels after the immobilization of the BY dye. It is also presented, in Figure 6, the spectrum of BY dye solution used for its immobilization. The spectrum of the BY solution displayed bands with maxima near 250 and 400 nm, which was assigned as $\pi - \pi^*$ and $n - \pi^*$ electronic transitions, respectively, due to the azobenzene group of the BY dye [35]. Both transitions are observed in the $(R_2dabco)BY/SiO_2$ spectrum, but with a broadening that can be attributed to the light

scattering typical of solid samples and also due to some dye aggregation [26,35,36]. The (R₂dabco)Cl₂/SiO₂ xerogel did not show any optical electronic absorption in the whole wavelength range studied, which confirms that the features in the UV-visible spectrum of (R₂dabco)BY/SiO₂ are exclusively due to the BY dye contribution. The spectrum for the (R₂dabco)Cl₂/SiO₂/TiO₂ xerogel displayed typical absorption edge by the band gap transition of the titanium species highly dispersed [36,37]. This result is in accordance with EDS analysis discussed above. In the (R₂dabco)BY/SiO₂/TiO₂ spectrum, it is possible to observe the band gap transition and also a broad band with maximum near 400 nm due to the BY dye presence.

The amount of BY dye immobilized on hybrids was determined with spectrophotometric method. The values found were 18 μmol g⁻¹ for (R₂dabco)BY/SiO₂ material and 7 μmol for (R₂dabco)BY/SiO₂/TiO₂ material. The lower amount of BY dye immobilized on (R₂dabco)BY/SiO₂/TiO₂ can be interpreted considering two factors: i) the lower organic content of the adsorbent charged groups in this material, obtained by CHN analysis (see Table 1); ii) and the size of the pores. The (R₂dabco)Cl₂/SiO₂ material presents mesopores with diameter between 6 and 8 nm, while (R₂dabco)Cl₂/SiO₂/TiO₂ material presents predominantly pores with lower diameter, hindering the BY dye diffusion. Thus the quantity of BY dye adsorbed in this material should be lower.

Cyclic voltammetry studies

Figure 7 shows the cyclic voltammograms for (R₂dabco)BY/SiO₂ and (R₂dabco)BY/SiO₂/TiO₂ electrodes. The midpoint potentials, E_m were calculated as [E_m = (E_{pa} + E_{pc})/2], where E_{pa} and E_{pc} are the anodic and cathodic peak potentials, respectively. The values were 129 mV for (R₂dabco)BY/SiO₂ and 95 mV for (R₂dabco)BY/SiO₂/TiO₂ material. This observed difference in the midpoint potential was interpreted considering variations in the composition and microstructures of the hybrid xerogels. In the case of (R₂dabco)BY/SiO₂/TiO₂ material it is due to the presence of titanium in the matrix that produces a displacement for lower values. On the other hand, the presence of the BY dye dimmers or aggregates can not be discarded in the (R₂dabco)BY/SiO₂ material that presents a higher BY dye loading than the other one. It was already reported that the presence of dimmers or aggregates can produce displacement of midpoint potentials for more positive values (Figure 6) [38]. In the Figure 7 it is also possible to observe that the peak current densities, J_{pa} and J_{pc}, for the (R₂dabco)BY/SiO₂ electrode are larger than for the

(R₂dabco)BY/SiO₂/TiO₂ electrode. This fact suggests that a larger amount of BY dye was immobilized in the (R₂dabco)Cl₂/SiO₂ according to the results discussed above.

Figure 8 shows the chemical stability of the electrodes even after several redox cycles were performed. The BY dye impregnated at the electrode surface could be leached from the electrode during several oxidation and reduction cycles. As can be seen, after 120 cycles for the (R₂dabco)BY/SiO₂ and (R₂dabco)BY/SiO₂/TiO₂ electrodes, the current density of the anodic and cathodic peaks kept practically constant, using 1.0 mol l⁻¹ KCl as supporting electrolyte solution and pH 6.0, showing that the BY dye was not leached out from the matrix surfaces owing to their large affinities. This fact suggest a strong electrostatic interaction between the anion SO₃⁻ of the BY dye molecule and the bridged cationic dabco group of the hybrid materials.

Figure 9 shows cyclic voltammetry curves of the (R₂dabco)BY/SiO₂ e (R₂dabco)BY/SiO₂/TiO₂ electrodes obtained in a scan rate range between 2 and 50 mV s⁻¹ using 1.0 mol l⁻¹ KCl supporting electrolyte solution. The results show that on increasing the scan rate, the separation of the peak potential, $\Delta E = E_{pa} - E_{pc}$, increases lightly, indicating that the velocity of the electron transfer is not sufficiently fast, presumably due to the internal matrix resistance, and thus, the process is not totally reversible. In addition, it should be taken into account in the oxidation-reduction process a difficulty of the diffusion of the contra-ion through the interface electrode-solution in order to keep the electroneutrality. Plotting the peak current density, J_p, against the square root of the scan rates, v^{1/2}, a linear correlation is obtained (inserted in Figure 9) similar to that observed for a diffusion controlled process of the electroactive species on the surface of the electrode [39,40].

Table 2 shows the behavior of (R₂dabco)BY/SiO₂ and (R₂dabco)BY/SiO₂/TiO₂ electrodes with the sweep speed with more details. It can be observed that the current density ratios J_{pa}/J_{pc} in all of experiments is larger than 1 revealing again that the process is not totally reversible [39]. Also it can be seen in the Table 2 that the ΔE obtained values are smaller for (R₂dabco)BY/SiO₂/TiO₂ electrode than those obtained for the (R₂dabco)BY/SiO₂ electrode, in the range of sweeping rate studied. This behavior also can be attributed to the presence of titanium in the matrix of (R₂dabco)BY/SiO₂/TiO₂ material. Metallic oxides such as titanium oxide are known to present high conductivity properties to mediate the electron transfer in chemically modified electrodes [40,41].

The presence of the titanium in the framework of (R₂dabco)BY/SiO₂/TiO₂ hybrid xerogel decreases the ΔE about two times when compared to the obtained value for

(R₂dabco)BY/SiO₂, favoring the more reversible system in the interval scan rate studied. These results suggest that the diffusion of the contra-ion is fast on the (R₂dabco)BY/SiO₂/TiO₂ electrode. When the scan rate is low, electrode process is controlled by mass diffusion. When the potential is scanned at a low rate, the electrode reaction could reach completion, and the cyclic voltammogram exhibit nearly reversible features. When the potential is scanned at higher rates, the electrode reaction could not reach completion in time: hence, the cyclic voltammogram exhibits quasi-reversible or irreversible feature, hence this electrode process is controlled by both, the electrode reaction and mass diffusion [39].

The pH effects on the electrode response (Figure 10) was studied because it can affects the midpoint potential, E_m , and also the anodic and cathodic current density, limiting the use of the electrodes in a pH range where does not exist variation in these parameters [42]. The (R₂dabco)BY/SiO₂ and (R₂dabco)BY/SiO₂/TiO₂ modified electrodes response were investigated in the pH range between 2.0 and 7.0, using 1.0 mol l⁻¹ KCl as supporting electrolyte solution. In this pH range, E_m , J_{pa} and J_{pc} are not affected, staying practically constant. The results obtained suggest that for (R₂dabco)BY/SiO₂ and (R₂dabco)BY/SiO₂/TiO₂ electrodes the organic dye is entrapped in the host matrix, protected against the change of the external pH solution [43].

EIS Measurements

The EIS technique was used to evaluate the conducting character of the (R₂dabco)BY/SiO₂ and (R₂dabco)BY/SiO₂/TiO₂ electrodes. The EIS measurements were performed in potentiostatic mode. Based upon the voltammetric results the applied potential were fixed at 152 mV and 135 mV for (R₂dabco)BY/SiO₂ and (R₂dabco)BY/SiO₂/TiO₂ electrodes, respectively. The Bode plots given in Figure 11 for both electrodes are similar, presenting two time constants the first one at the middle frequency range with a maximum phase angle around -40° related to diffusional process and another at lower frequencies with a maximum phase angle around 80° ascribed to a capacitive behavior, these spectra are characteristics of diffusion controlled processes, which occur slower than the charge-transfer reaction [44]. The EIS experimental spectra were analyzed using an equivalent electric circuit (EC). The proposed EC is given in the insert of Figure 11 including two time constants. In this EC, R_s represents the ohmic resistance between the reference and the working electrode, C_1 the double layer capacitance and R_1 the charge transfer resistance. The diffusional Warburg impedance, W , was included in the EC to taking into account diffusion processes

which take place at the electrode surface. The CPE is a constant phase element and its impedance is expressed as [39]:

$$Z_{CPE} = [Q (j\omega)^n]^{-1}$$

The CPE represents a capacitor for $n = 1$, a resistor when $n = 0$ and if $n = 0.5$, the CPE is associated with a diffusion process. The experimental data were found to be sufficiently well fitted by the transfer functions of this EC with an error of less than 10%. The simulated data are given in Table 3. As can be seen the charge transfer resistance at the $(R_2\text{dabco})\text{BY}/\text{SiO}_2/\text{TiO}_2$ electrode is $105.3 \Omega \text{ cm}^{-2}$ and that of $(R_2\text{dabco})\text{BY}/\text{SiO}_2$ is $155.2 \Omega \text{ cm}^{-2}$. These results confirm the voltammetric results which shown that titanium oxide enhances the conductivity properties of the modified electrode.

Electrooxidation of ascorbic acid (H_2AA)

Although the BY dye amount immobilized on $(R_2\text{dabco})\text{BY}/\text{SiO}_2/\text{TiO}_2$ has been lower than the titania free material, the electrode made with $(R_2\text{dabco})\text{BY}/\text{SiO}_2/\text{TiO}_2$ showed better reversibility conditions and sensibility to ascorbic acid. Thus, it was chosen for electrocatalytic studies. Figure 12 shows the cyclic voltammetric curves obtained using the $(R_2\text{dabco})\text{Cl}_2/\text{SiO}_2/\text{TiO}_2$ and $(R_2\text{dabco})\text{BY}/\text{SiO}_2/\text{TiO}_2$ carbon paste electrode systems. The measurements were made at pH 6.0 with $5.7 \times 10^{-3} \text{ mol l}^{-1}$ ascorbic acid solution accomplished under argon atmosphere to avoid the oxidation of H_2AA . The anodic potential peak is not observed for $(R_2\text{dabco})\text{Cl}_2/\text{SiO}_2/\text{TiO}_2$, in the absence of H_2AA (curve a). Under similar conditions, but in the presence of H_2AA , it was observed an anodic potential peak at 390 mV vs SCE, corresponding to the oxidation of ascorbic acid (curve b). However, using the $(R_2\text{dabco})\text{BY}/\text{SiO}_2/\text{TiO}_2$ electrode, an increase in the current density was evidenced with the addition of the ascorbic acid, at the same potential of BY oxidation (curves c and d). Therefore, the catalytic electrooxidation of the ascorbic acid for $(R_2\text{dabco})\text{BY}/\text{SiO}_2/\text{TiO}_2$ electrode, occurs in approximately 250 mV below of the observed value for the $(R_2\text{dabco})\text{Cl}_2/\text{SiO}_2/\text{TiO}_2$ electrode without BY dye electron mediator.

Figure 13 shows the ascorbic acid oxidation on the $(R_2\text{dabco})\text{BY}/\text{SiO}_2/\text{TiO}_2$ electrode surface, immersed in 1.0 mol l^{-1} KCl solution, at pH 6.0, in the absence (curve a) and in the presence ascorbic acid at different concentrations (curves b-g). It was observed an increase in the anodic current peak density, as the ascorbic acid concentration was successively increased

from 9.9×10^{-4} a $5.7 \times 10^{-3} \text{ mol l}^{-1}$ (linear correlation, $R = 0.9988$). It is an indication of a catalytic oxidation of ascorbic acid mediated by $(\text{R}_2\text{dabco})\text{BY}/\text{SiO}_2/\text{TiO}_2$ electrode.

Amperometric detection

In order to check the potential of using this electrode made with $(\text{R}_2\text{dabco})\text{BY}/\text{SiO}_2/\text{TiO}_2$ as sensor for ascorbic acid, chronoamperometry experiments were undertaken. First, amperometric studies were performed in order to determine the best potential to be applied. The potential was chosen by measuring the density of the catalytic currents for a solution containing $5.7 \times 10^{-3} \text{ mol l}^{-1}$ H_2AA solution, pH 6.0, 25 °C and under atmosphere of argon. The potential was fixed at 180 mV in the subsequent experiments.

Figure 14 shows the amperometric curve obtained for addition of 50 μl of the 0.01 mol l^{-1} H_2AA solution in 20 ml of 1.0 mol l^{-1} KCl supporting electrolyte solution into the electrochemical cell keeping fixed $E_{\text{pa}} = 180 \text{ mV}$, pH 6.0. The average response time (inserted Figure), measured after various substrate additions in the electrochemical cell was 1.0 s.

In the range of ascorbic acid concentrations between 2.5×10^{-5} and $2.4 \times 10^{-4} \text{ mol l}^{-1}$ a linear correlation was observed (Figure 15), demonstrated by the equations $J = (2.54 \pm 0.06)[\text{H}_2\text{AA}] + (3.42 \pm 8.77)$, where J is variation of current density (mA cm^{-2}), with a linear correlation $R = 0.998$ for $n = 10$. The achieved detection limit (3 standard deviation of the blank divided by the slope of calibration curve) was $15.3 \mu\text{mol l}^{-1}$, quantification limit (10 standard deviation of the blank divided by the slope of calibration curve) was $50 \mu\text{mol l}^{-1}$, and sensitivity $2.54 \text{ mA cm}^{-2} \text{ l } \mu\text{mol}^{-1}$.

An experiment to determine the concentration of ascorbic acid in commercial pharmaceutical tablets and process juices using the $(\text{R}_2\text{dabco})\text{BY}/\text{SiO}_2/\text{TiO}_2$ electrode was performed. The result obtained of this commercial ascorbic acid samples was presented on Table 4. As can be observed, the results obtained indicate that the carbon paste electrode modified with $(\text{R}_2\text{dabco})\text{BY}/\text{SiO}_2/\text{TiO}_2$ presents good performance with low detection limit and high sensitivity, showing the potentiality to be utilized with electrochemical sensor for determination of ascorbic acid in commercial samples.

Conclusion

Amorphous hybrid silica and silica/titania based xerogels containing the double charged bridged 1,4-diazoniabicyclo[2.2.2]octane chloride group were obtained. The materials present the same surface area value, $570 \text{ m}^2\text{g}^{-1}$, however the $(\text{R}_2\text{dabco})/\text{SiO}_2$ had predominantly mesopores while $(\text{R}_2\text{dabco})/\text{SiO}_2/\text{TiO}_2$ material was micro and macroporous. These materials show anion exchange properties that allowed the immobilization of brilliant yellow dye, which was used, for the first time, as electroactive species in the preparation of carbon paste electrodes for cyclic voltammetric measurements. The charge transfer resistance for $(\text{R}_2\text{dabco})\text{BY}/\text{SiO}_2$ and $(\text{R}_2\text{dabco})\text{BY}/\text{SiO}_2/\text{TiO}_2$ electrodes were 155.2 and $105.3 \text{ } \Omega \text{ cm}^{-2}$, respectively, evidencing that titanium oxide enhances the conductivity properties of the modified electrode. The modified electrode showed chemical stability for various oxidation-reduction cycles. From the study of pH effects on the electrode response, it was deduced that in the $(\text{R}_2\text{dabco})/\text{SiO}_2$ and $(\text{R}_2\text{dabco})/\text{SiO}_2/\text{TiO}_2$ materials the organic dye is entrapped in the matrix held by an electrostatic interactions and protected against the change of the external pH solution, allowing its use in a large pH range. The electrode response time for ascorbic acid was very fast, about 1 s. The carbon paste electrode modified with $(\text{R}_2\text{dabco})\text{BY}/\text{SiO}_2/\text{TiO}_2$ shows good potentiality to be utilized as electrochemical sensor for determination of ascorbic acid in commercial products.

Acknowledgements

We thank to CNPq, FAPERGS and FAPESP for fellowships and financial support. We also thank the CME-UFRGS for the use of the SEM.

References

1. K.G. Sharp, *Adv. Mater.* 15 (1998) 1243.
2. M.A. Wahab, H. Kim, C.S. Ha, *Micropor. Mesopor. Mater.* 69 (2004) 19.
3. U. Schubert, N. Husing, A. Lorenz, *Chem. Mater.* 7 (1995) 2010.
4. G. Kickelbick, *Prog. Polym. Sci.* 28 (2003) 83.
5. K.J. Shea, D.A. Loy, *Chem. Mater.* 13 (2001) 3306.
6. B. Boury, F. Ben, R.J.P. Corriu, P. Delord, M. Nobili, *Chem. Mater.* 14 (2002) 730.
7. L.T. Arenas, A. Langaro, Y. Gushikem, C.C. Moro, E.V. Benvenutti, T.M.H. Costa, 28 (2003) 51.
8. M.T. Laranjo, V. Stefani, E.V. Benvenutti, T.M.H. Costa, G.O. Ramminger, M.R. Gallas, *J. Non-Cryst. Solids* 353 (2007) 24.
9. C.L. Lin, M.Y. Yeh, C.H. Chen, S. Sudhakar, S.J. Luo, Y.C. Hsu, C.Y. Huang, K.C. Ho, T.Y. Luh, *Chem. Mater.* 18 (2006) 4157.
10. E. Pabón, J. Retuert, R. Quijada, A. Zarate, *Micropor. Mesopor. Mater.* 67 (2004) 195.
11. S.V.M. Moraes, C.C. Moro, T.M.H. Gallas, M.R. Costa, E.V. Benvenutti, *High Press. Res.* 26 (2006) 11.
12. S.V.M. Moraes, J.B. Passos, P. Schossler, E.B. Caramão, C.C. Moro, T.M.H. Costa, E.V. Benvenutti, *Talanta* 59 (2003) 1039.
13. T.A. Lin, G.Y. Li, L.K. Chau, *Anal. Chim. Acta* 576 (2006) 117.
14. H. Qiu, S. Jiang, X. Liu, *J. Chromatogr. A*, 1103 (2006) 265–270.
15. L. M. L. A. Auler, C. R. Silva, K. E. Collins, C. H. Collins, *J. Chromatogr. A*, 1073 (2005) 147
16. K. Kurata, J. Ono, A. Dobashi, *J. Chromatogr. A*, 1080 (2005) 140.
17. C.L. Lin, P. Tien, L.K. Chau, *Electrochim. Acta*, 49 (2004) 573.
18. A. Liu, H. Zhou, I. Honma, *Electrochem Commun.* 7 (2005) 1.
19. R.V.S. Alfaya, Y. Gushikem, A.A.S. Alfaya, *J. Braz. Chem. Soc.* 11 (2000) 281.
20. M. Kanungo, M. M. Collinson, *Langmuir* 21 (2005) 827.
21. L.T. Arenas, S.L.P. Dias, C.C. Moro, T.M.H. Costa, E.V. Benvenutti, A.M.S. Lucho, Y. Gushikem, *J. Colloid Interface Sci.* 297 (2006) 244.
22. L.T. Arenas, E.C. Lima, A.A. Santos, J.C.P. Vaghetti, T.M.H. Costa, E.V. Benvenutti, *Colloids Surf. A.* 297 (2007) 240.
23. M. Mascini, *Sens. Actuators B.* 29 (1995) 121.

24. Y. Egawa, R. Hayashida, J. Anzai, *Anal. Sci.* 22 (2006) 1117.
25. M. Taras, *Anal. Chem.* 20 (1948) 1156.
26. C. Eiras, V. Zucolotto, O. N. Oliveira, D. Gonçalves, *Synthetic Metals* 135-136 (2003) 161.
27. J.L. Foschiera, T.M. Pizzolato, E.V. Benvenuti, *J. Braz Chem. Soc.* 12 (2001) 159.
28. S. Brunauer, P.H. Emmett, E. Teller, *J. Am. Chem. Soc.* 60 (1938) 309.
29. E.P. Barret, L.G. Joyner, P.P. Halenda, *J. Am. Chem. Soc.* 73 (1951) 373.
30. L.C.M. Pinto, PhD Thesis, Universidade de São Paulo, IPEN, 1996.
31. A. M. Castellani, Y. Gushikem, *J. Colloid Interface Sci.* 230 (2000) 195.
32. O. Zenebon, N.S. Pascuet, *Métodos Físico-Químicos para Análise de Alimentos*, Instituto Adolfo Lutz, Brasília, 2005, p169.
33. K.S.W. Sing, D.H. Everett, R.A.W. Haul, L. Moscou, R.A. Pierotti, J. Rouquérol, T. Siemieniewska, *Pure Appl. Chem.* 57 (1985) 603.
34. S.J. Gregg, K.S.W. Sing, *Adsorption, Surface Area and Porosity*, Academic Press, London, 1982, Ch 3 and 4.
35. V.M. Zucolotto, N.M.N. Barbosa, J.J. Rodrigues, C.J.L. Constantino, S.C. Zílio, C.R. Mendonça, R.F. Aroca, O.N. Oliveira, *J. Nanosci. Nanotech.* 4 (2004) 1.
36. J. Aguado, R. Grieken, M.J. López-Muñoz, J. Marugán, *Appl. Catal. A.* 312 (2006) 202.
37. X. Gao, S. R. Bare, J.L.G. Fierro, M. A. Banares, I.E. Wachs, *J. phys chem B.* 102 (1998) 5653.
38. E.S. Ribeiro, S.S., Rosatto, Y. Gushikem, L.T. Kubota, *J. Solid State Electrochem.* 7 (2003) 665.
39. A.J. Bard, L. Faulkner, *Electrochemical Methods - Fundamentals and Applications*, Wiley, New York, 2000
40. L.T. Kubota, Y. Gushikem, *J. Electroanal. Chem.* 362 (1993) 219.
41. S.L.P. Dias, Y. Gushikem, E.S. Ribeiro, E.V. Benvenuti, *J. Electroanal. Chem.* 253 (2002) 64.
42. S. Shahrokhian, M. Karimi, *Electrochim. Acta.* 50 (2004) 77.
43. F. A. Pavan, E. S. Ribeiro, Y. Gushikem, *Electroanalysis* 17 (2005) 625.
44. G.W. Walter, *Corros. Sci.* 26 (1986) 681.

Table 1. Elemental analysis and surface area results

Hybrid xerogel	Dabco groups / $\pm 0.04 \text{ mmol g}^{-1}$ ^a	Ti/Si atomic Ratio ^b	Surface area / $\pm 25 \text{ m}^2 \text{ g}^{-1}$	Pore volume / $\pm 0.04 \text{ cm}^3 \text{ g}^{-1}$
(R ₂ dabco)Cl ₂ /SiO ₂	0.24		570	0.52
(R ₂ dabco)Cl ₂ /SiO ₂ /TiO ₂	0.19	0.07	570	0.83

^a = Obtained from CHN analysis.

^b = Obtained from the EDS analysis.

Table 2. Cyclic voltammetry in different rate scan for (R₂dabco)BY/SiO₂ and (R₂dabco)BY/SiO₂/TiO₂ electrodes.

Electrode	$v /$ mV s^{-1}	$E_{pa} /$ mV	$E_{pc} /$ mV	E_m	ΔE	$J_{pa} /$ $\mu\text{A cm}^{-2}$	$J_{pc} /$ $\mu\text{A cm}^{-2}$	$J_{pa} /$ J_{pc}
(R ₂ dabco)BY/SiO ₂	5	128	109	118.5	19	62.5	-50.3	1.2
	10	134	104	119.0	30	114.3	-91.4	1.3
	20	150	106	128.0	44	212.1	-170.0	1.2
	30	159	97	128.0	62	296.4	-227.5	1.3
	40	167	89	128.0	78	367.9	-287.9	1.3
	50	181	82	131.5	99	428.6	-339.3	1.3
(R ₂ dabco)BY/SiO ₂ /TiO ₂	5	88	77	82.5	11	24.6	-21.8	1.1
	10	99	88	93.5	11	46.1	-36.1	1.3
	20	101	73	87.0	28	85.0	-66.8	1.3
	30	107	73	90.0	34	108.6	-90.7	1.2
	40	99	57	78.0	42	136.1	-110.7	1.2
	50	89	41	65.0	48	150.7	-128.9	1.2

v = scan rate, E_{pa} e E_{pc} = anodic and cathodic potential peak, E_m = midpoint potential, $\Delta E = E_{pa} - E_{pc}$, J_{pa} e J_{pc} = anodic and cathodic current peak density.

Table 3. Fitting parameters of the equivalent circuit proposed to simulate the experimental data shown in Figure 11.

Electrode	$R_s /$ $\Omega \text{ cm}^2$	$C /$ $\mu\text{F cm}^{-2}$	$R_1 /$ $\Omega \text{ cm}^2$	$W /$ $\Omega^{-1} \text{ cm}^{-2}$ $\times 10^{-3}$	$Q /$ F cm^{-2} $\times 10^{-3}$	n
(R ₂ dabco)BY/SiO ₂	3.20	13.4	155.3	4.16	5.5	0.97
(R ₂ dabco)BY/SiO ₂ /TiO ₂	3.64	0.36	105.3	3.39	3.2	0.96

Table 4. Vitamin C amount in tablets and in processed juices from different suppliers.

Sample	Declared amount / g	(R ₂ dabco)BY/SiO ₂ /Ti O ₂ electrode / g	Standard method / g
A	1.0	0.983 ± 0.008	0.982 ± 0.002
B	1.0	1.038 ± 0.006	1.037 ± 0.001
C	2.0	1.934 ± 0.007	1.931 ± 0.013
Orange juice*	0.3	0.315 ± 0.006	0.313 ± 0.001

* per liter of process juice

Captions for Figures

Figure 1: Chemical structures of hybrid xerogels contained a double charged of the 1,4-diazoniabicyclo[2.2.2]octane chloride group (a) and structure of brilliant yellow dye (BY) (b).

Figure 2. Infrared spectra obtained at room temperature after been heated up to 100 °C, for 1 h. a) $(R_2dabco)Cl_2/SiO_2$; b) $(R_2dabco)Cl_2/SiO_2/TiO_2$.

Figure 3. SEM image of $(R_2dabco)Cl_2/SiO_2/TiO_2$ hybrid xerogel (a), and the corresponding energy-dispersive scanning (EDS) image of titanium (b). The magnification was 1200x.

Figure 4. SEM image of hybrid xerogels: a) $(R_2dabco)Cl_2/SiO_2$; b) $(R_2dabco)Cl_2/SiO_2/TiO_2$. The magnification was 20000 and 60000x.

Figure 5. Pore size distributions for $(R_2dabco)Cl_2/SiO_2$ and $(R_2dabco)Cl_2/SiO_2/TiO_2$ xerogels. Inset figure: N_2 adsorption–desorption isotherms.

Figure 6. UV/visible absorption spectra for BY solution and UV/visible diffuse reflectance spectra for $(R_2dabco)Cl_2/SiO_2$, $(R_2dabco)BY/SiO_2$, $(R_2dabco)Cl_2/SiO_2/TiO_2$ and $(R_2dabco)BY/SiO_2/TiO_2$ samples.

Figure 7. Cyclic voltammograms curves for the $(R_2dabco)BY/SiO_2$ and $(R_2dabco)BY/SiO_2/TiO_2$ electrodes in 1.0 mol l⁻¹ KCl supporting electrolyte solution, temperature of 25 °C and scan rate at 20 mV s⁻¹.

Figure 8. Peak currents density for (A) $(R_2dabco)BY/SiO_2$ and (B) $(R_2dabco)BY/SiO_2/TiO_2$ electrodes, as function of number of redox cycles under scan rate at 20 mV s⁻¹, pH 6.0, in 1.0 mol l⁻¹ KCl solution.

Figure 9. Cyclic voltammograms obtained at different scan rates (2, 5, 8, 10, 20, 30, 40, 50 mV s⁻¹) for $(R_2dabco)BY/SiO_2$ and $(R_2dabco)BY/SiO_2/TiO_2$ electrodes. Supporting electrolyte: 1.0 mol l⁻¹ KCl solution. Plot of the cathodic and anodic peak currents density, J_{pc} and J_{pa} , against the square root of the scan rates, $v^{1/2}$, and (inset on Figure 9).

Figure 10. Plot the solution pH against E_m , J_{pa} and J_{pc} for the $(R_2dabco)BY/SiO_2$ (A) and the $(R_2dabco)BY/SiO_2/TiO_2$ (B) electrodes. In KCl 1.0 mol l^{-1} at pH 6.0 and scan rate of 20 mV s^{-1} .

Figure 11. Bode plots for the $(R_2dabco)BY/SiO_2$ and $(R_2dabco)BY/SiO_2/TiO_2$ electrodes at 135mV and 152mV, respectively. Insert: Equivalent circuits (EC) used to fit the EIS data.

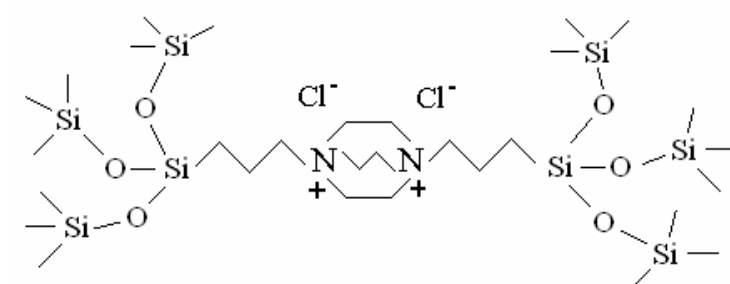
Figure 12. Cyclic voltammograms obtained with $(R_2dabco)Cl_2/SiO_2/TiO_2$ and $(R_2dabco)BY/SiO_2/TiO_2$ in KCl 1.0 mol l^{-1} at pH 6.0, under atmosphere of argon and scan rate of 20 mV s^{-1} : a) $(R_2dabco)Cl_2/SiO_2/TiO_2$ in the absence of the H_2AA , b) $(R_2dabco)Cl_2/SiO_2/TiO_2$ in presence of $5.7 \times 10^{-3} \text{ mol l}^{-1}$ of H_2AA , c) $(R_2dabco)BY/SiO_2/TiO_2$ in the absence of the H_2AA , d) $(R_2dabco)BY/SiO_2/TiO_2$ in presence of $5.7 \times 10^{-3} \text{ mol l}^{-1}$ of H_2AA .

Figure 13. Cyclic voltammetric for the $(R_2dabco)BY/SiO_2/TiO_2$ electrode, (a) in the absence of ascorbic acid and after successively addition of 200 μl de H_2AA $0,1 \text{ mol l}^{-1}$ in 20 mL of 1.0 mol l^{-1} KCl solution, resulting in the following concentration: (b) 9.9×10^{-4} , (c) 2.0×10^{-3} , (d) 2.9×10^{-3} , (e) 3.8×10^{-3} , (f) 4.8×10^{-3} e (g) $5.7 \times 10^{-3} \text{ mol l}^{-1}$. Conditions: pH 6.0, under atmosphere of argon and scan rate of 20 mV s^{-1} .

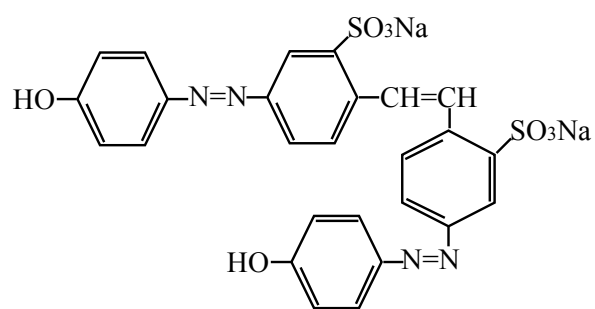
Figure 14. Chronoamperograms obtained after successive addition of 50 μl of the 0.01 mol l^{-1} ascorbic acid in 20 ml of 1.0 mol l^{-1} KCl supporting electrolyte solution, fixed potential in 180 mV and under atmosphere of argon. Figure inserted show response of electrode in detail.

Figure 15. Plote of current density in function of concentration of ascorbic acid. Calibration curve obtained of experiments show in Figure 14.

Figure 1



(a)



(b)

Figure 2

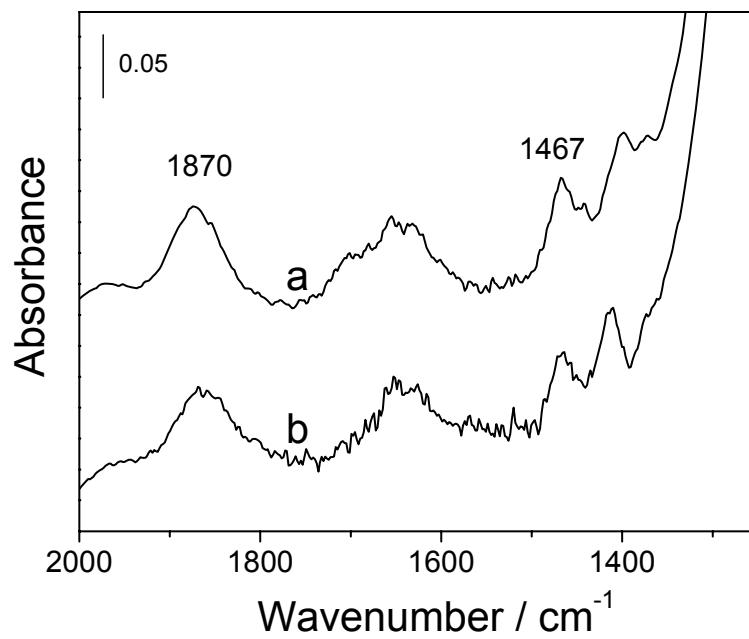


Figure 3

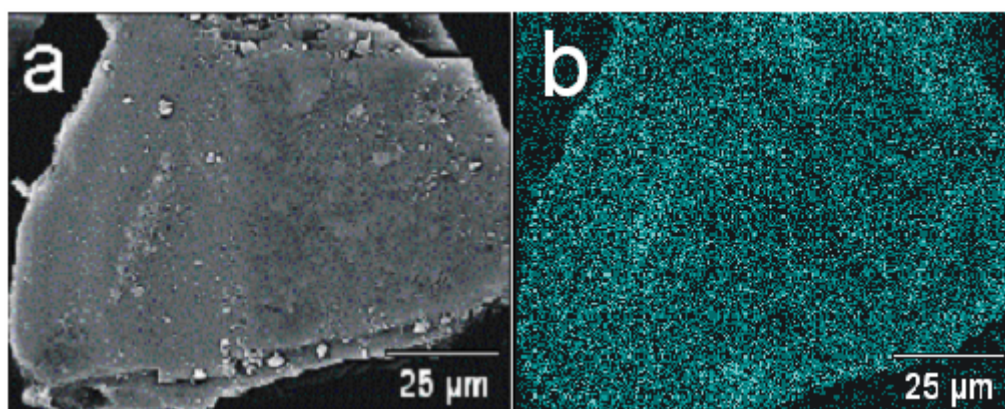


Figure 4

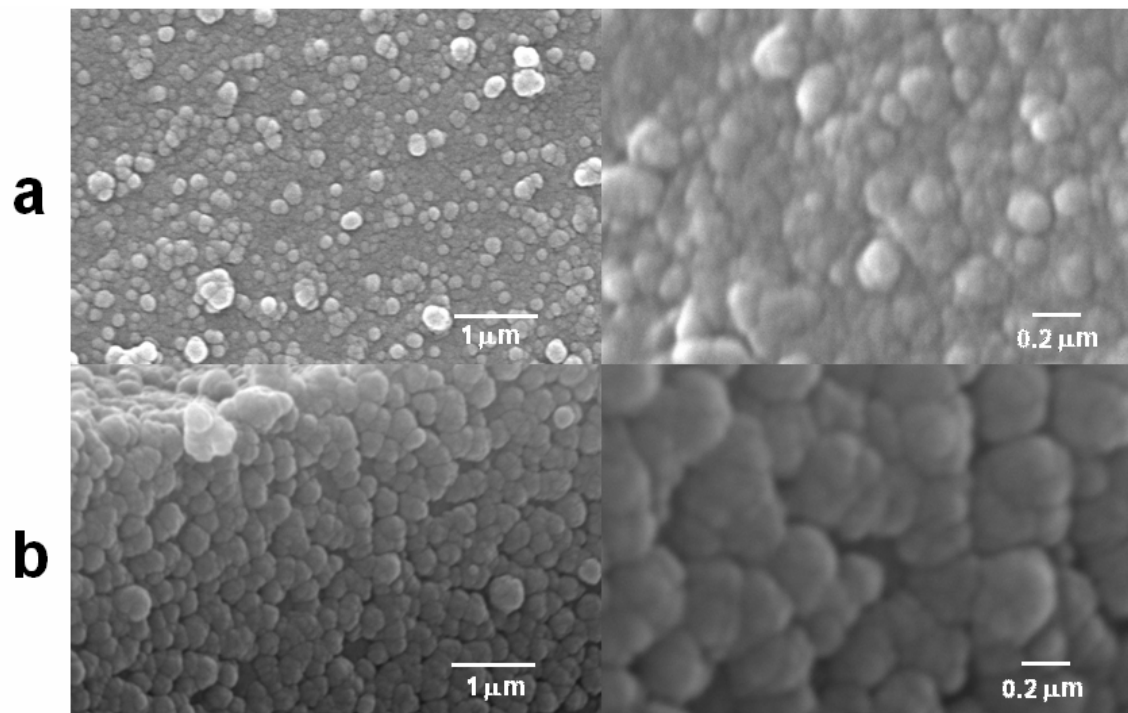


Figure 5

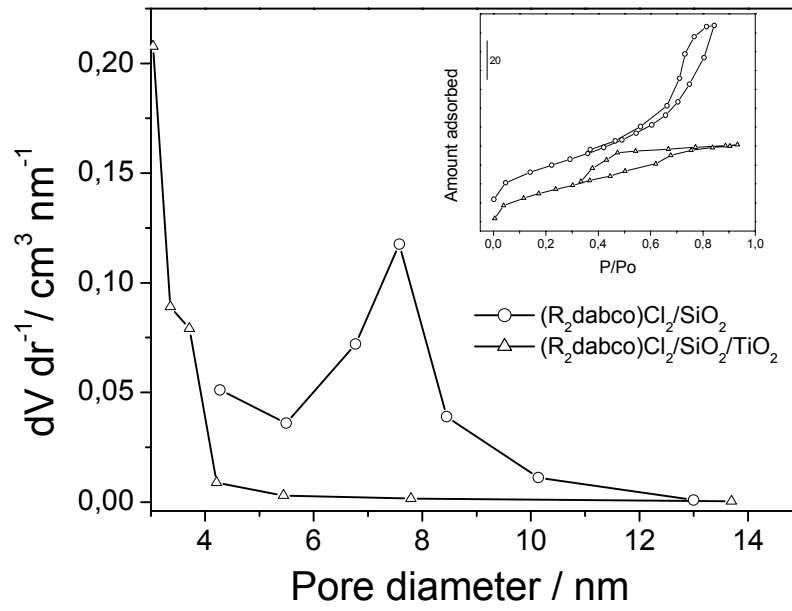


Figure 6

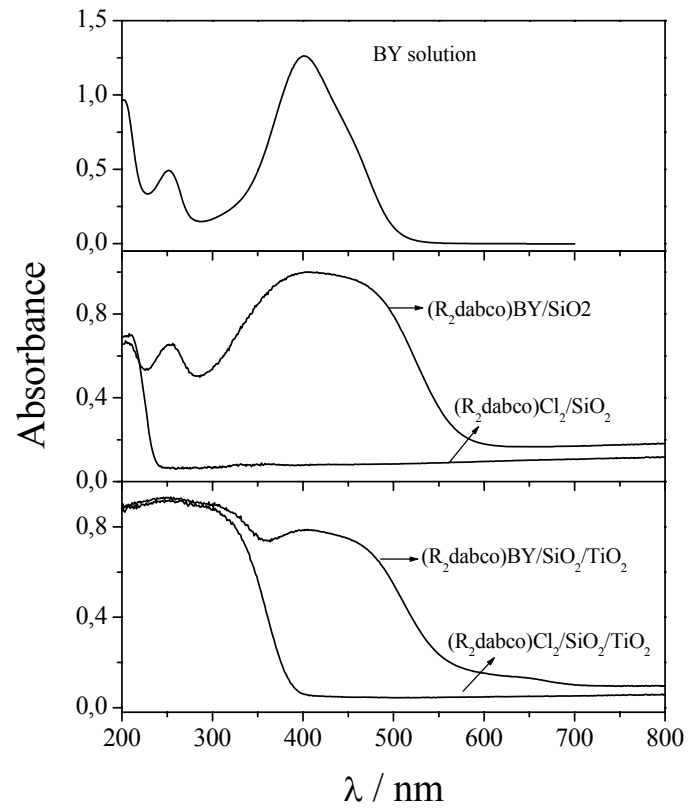


Figure 7

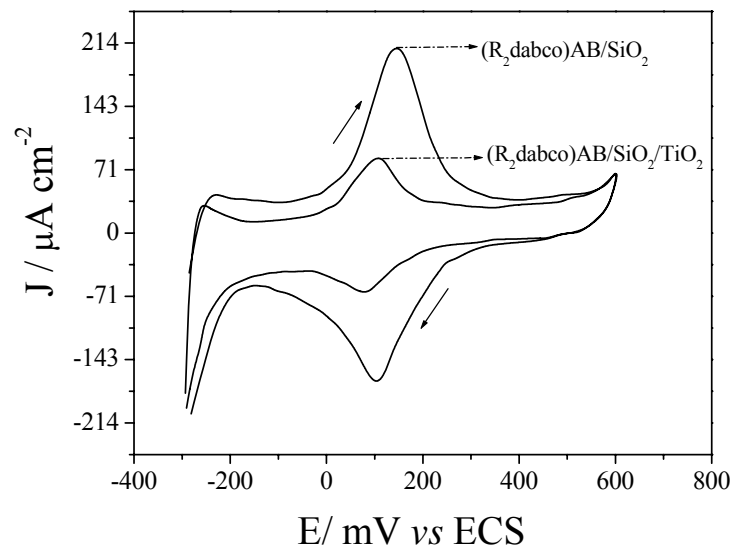


Figure 8

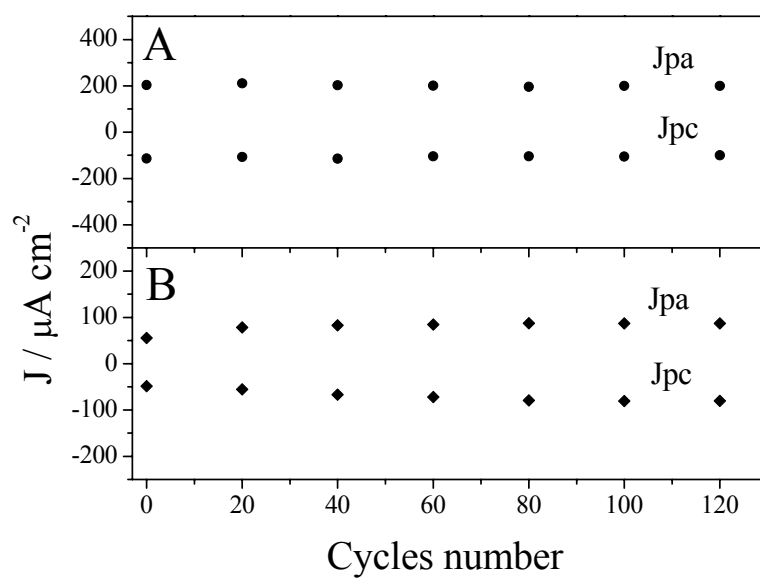


Figure 9

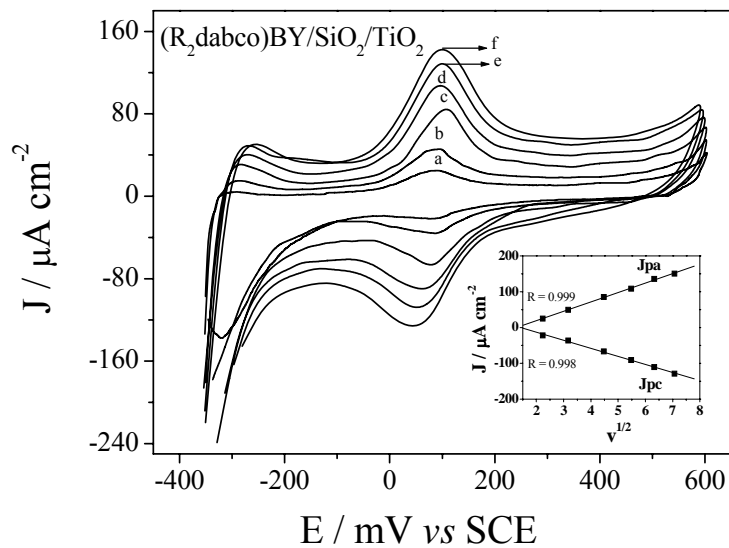
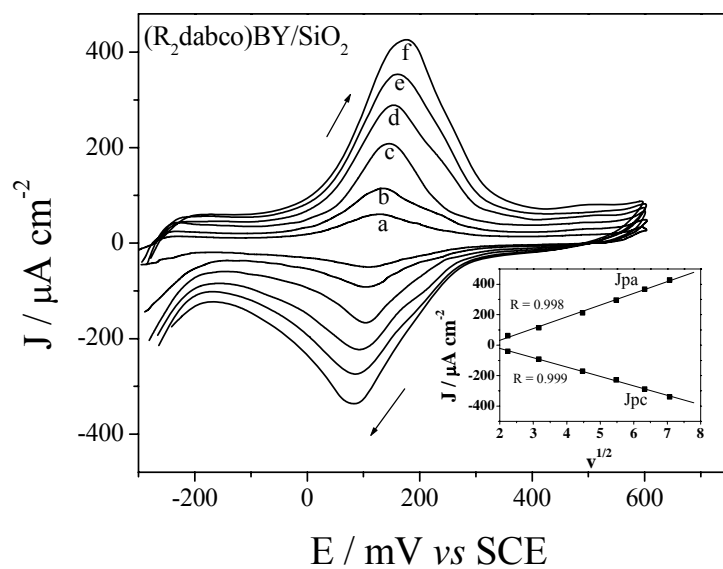


Figure 10

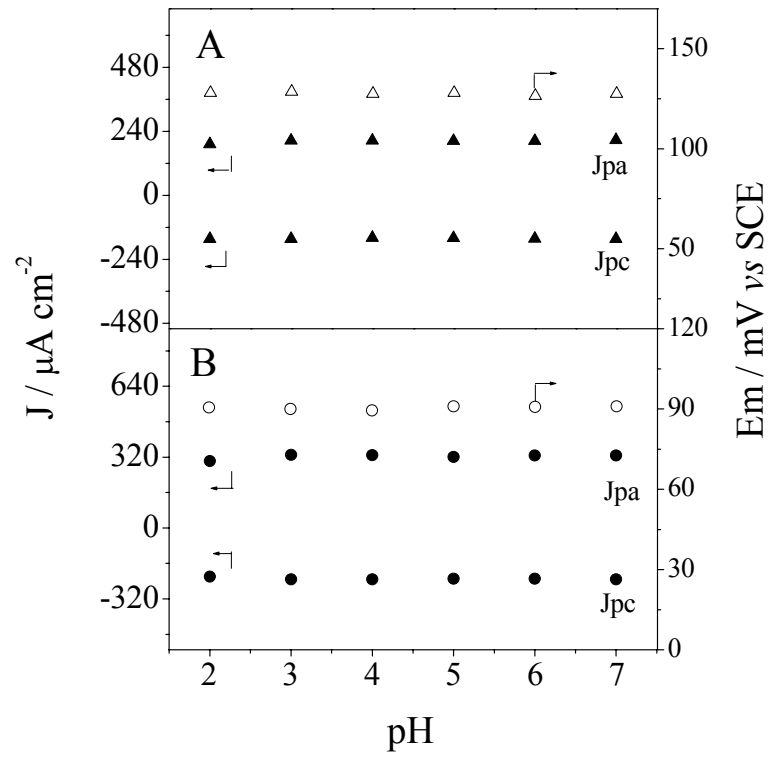


Figure 11

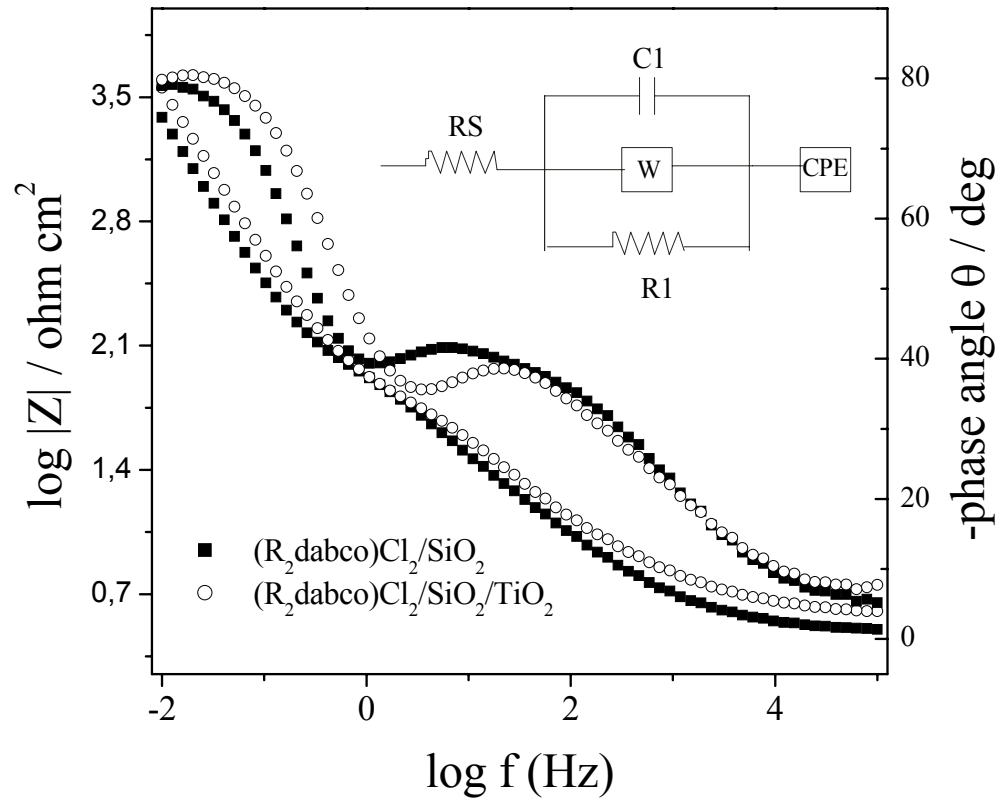


Figure 12

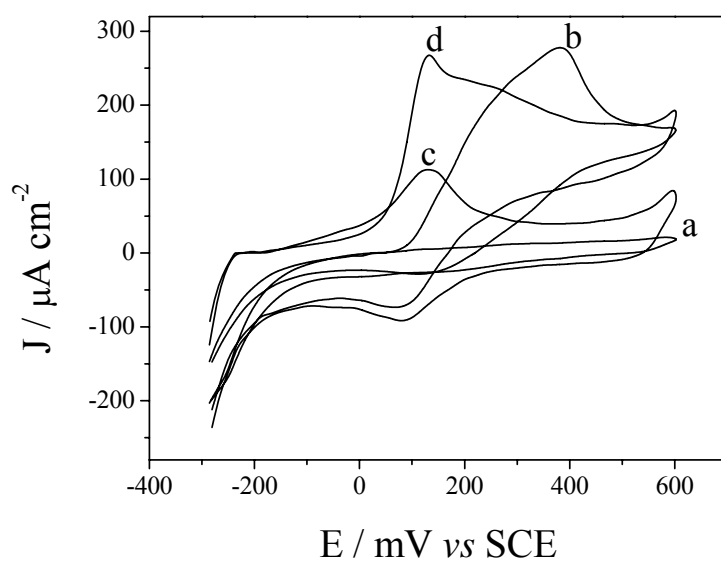


Figure 13

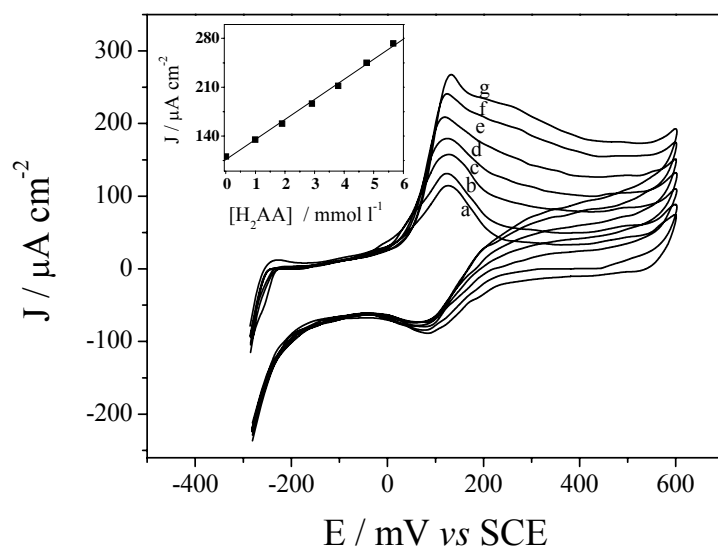


Figure 14

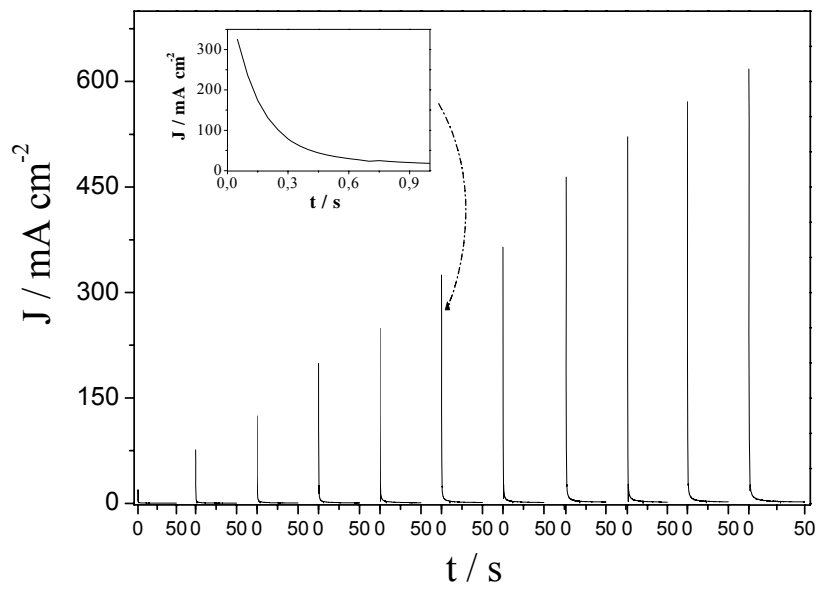
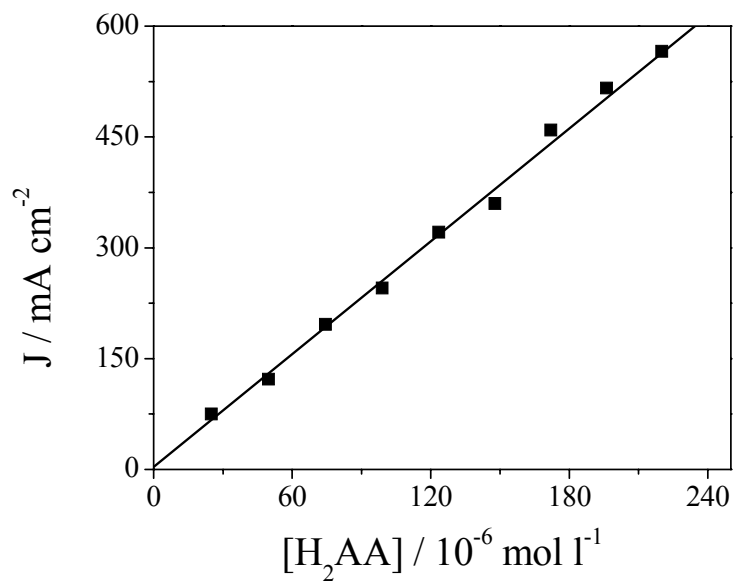


Figure 15



- 4.5- Arenas, L. T.; Simon, N. M.; Gushikem, Y.; Costa, T. M. H.; Lima, E. C.; Benvenuti, E. V. A water soluble 3-n-propyl-1-azonia-4-azabicyclo[2.2.2]octane chloride silsesquioxane grafted onto Al/SiO₂ surface. Chromium adsorption study. *Eclética. Química*, **2006**, 31, 53.

A water soluble 3-n-propyl-1-azonia-4-azabicyclo[2.2.2]octanechloride silsesquioxane grafted onto Al/SiO₂ surface. Chromium adsorption study

L. T. Arenas¹, N. M. Simon¹, Y. Gushikem², T. M. H. Costa¹, E. C. Lima^{1*}, E. V. Benvenutti¹

¹Instituto de Química, Universidade Federal do Rio Grande do Sul, CP 15003, 91501-970
Porto Alegre - RS, Brazil.

²Instituto de Química, UNICAMP, Caixa Postal 6154, 13083-970 Campinas-SP, Brazil.

*Corresponding author: e-mail: ederlima@iq.ufrgs.br

Abstract: The water soluble material, 3-n-propyl-1-azonia-4-azabicyclo[2.2.2]octanechloride silsesquioxane (dabcosil silsesquioxane) was obtained. The dabcosil silsesquioxane was grafted onto a silica surface, previously modified with aluminum oxide. The resulting solid, dabcosil-Al/SiO₂, presents 0.15 mmol of dabco groups per gram of material. The product of the grafting reaction was analyzed by infrared spectroscopy and N₂ adsorption-desorption isotherms. The dabcosil-Al/SiO₂ material was used as sorbent for chromium (VI) adsorption in aqueous solution.

Keywords: dabco; sol-gel; chromium (VI).

Introduction

In the last two decades a considerable attention has been devoted to the preparation of immobilized organic groups on silica gel surfaces that can be used as sorbent materials. The primary grafting reaction has been well studied [1-4]. This technique involves the immobilization of the organic group using an organosilane as a coupling reagent [5-7]. The resulting solids present a strong covalent bonded organic phase [7]. However, in the last decade hybrid materials obtained by using the sol-gel method became as an alternative to obtain organofunctionalized silicas [8-10]. The sol-gel synthesis for this kind of materials is based on the hydrolysis and polycondensation of organosilanes in the presence of tetraethylorthosilicate or tetramethylorthosilicate [11]. The hybrids obtained present also a strongly bonded organic phase [12,13] and they show some advantages when compared with

the grafted materials, since the synthesis can be performed at room temperature and the resulting solids have good homogeneity and purity. Additionally some properties like organic content, surface area, pore size and particle size can be controlled starting from the choice of the synthesis conditions [13,14]. Among the sol-gel silica based materials the silsesquioxanes are an interesting class of materials that contain a high degree of pendant or bridged organic groups [15,16].

In previous papers, the preparation of a silsesquioxane water soluble material was reported [17]. It was obtained by using n-propylpyridinium chloride as pendant group. Besides its high water solubility, a very important characteristic of this material was its capacity for forming a stable thin film on surfaces containing aluminum oxide [18]. Recently, we have obtained another water soluble material, the 3-n-propyl-1-azonia-4-azabicyclo[2.2.2]octanechloride silsesquioxane

(dabcosil silsesquioxane) [19,20]. It was observed that this material is constituted by oligomeric species and its solubility is a consequence of the ion dipole interactions between the azonia salt with water molecules [20].

In the present work we have combined the sol-gel method and the grafting technique in the preparation of new hybrid materials. The dabcosil silsesquioxane was synthesized by using the sol-gel process and subsequently it was grafted onto a silica gel surface, previously modified with aluminum oxide. The resulting material was characterized by using infrared spectroscopy, N_2 adsorption-desorption isotherms and its sorption capacity was evaluated for chromium (VI) uptake in aqueous solution.

Experimental

Synthesis of 3-n-propyl-1-azonia-4-azabicyclo[2.2.2]octanechloride silsesquioxane (dabcosil)

An amount of 2.244 g (10 mmol) of 1,4-diazabicyclo[2.2.2]octane (dabco, Acros), previously sublimed, were dissolved in 40 ml of an ethanol:acetone (Merck) solution (1:1), and 20 mmol (3.8 ml) of 3-cloropropyltrimethoxysilane (CPTMS, Acros) were added. This mixture was refluxed, in argon atmosphere under stirring, at near 90 °C for 48 h. The product of reaction, 3-n-propyltrimethoxysilane-1-azonia-4-azabicyclo[2.2.2] octanechloride was used as organic precursor in the sol-gel synthesis. In the previous solution it was added, under stirring, tetraethylorthosilicate (TEOS, Acros) (3.7 ml), twice distilled water (3.9 ml) and HF (0.1 ml). The mixture was stored for 15 days, just covered without sealing. The gel was then washed with acetone and dried at 90 °C for 1.5 h.

Synthesis of aluminum oxide grafted onto silica gel surface (Al/SiO₂)

Aluminum isopropoxide (Aldrich) (1.24 g) were dissolved in 50 ml of hot toluene (Merck). An amount of 10 g of silica gel (Merck) was previously activated in vacuum at 150 °C. The silica was added to aluminum isopropoxide solution. The mixture was stirred for 24 h, in argon atmosphere, under reflux conditions. The resulting product was filtered, washed with

toluene, ethanol, ethyl ether and evaporated in vacuum at 110 °C. To promote the hydrolysis, the product was immersed in twice distilled water and promptly filtrates, washed with water and finally dried in vacuum at 120 °C.

Synthesis of dabcosil silsesquioxane grafted onto Al/SiO₂ surface (dabcosil-Al/SiO₂)

The dabcosil silsesquioxane (300 mg) was dissolved in twice distilled water (100 ml) and soon it was added to 5 g of Al/SiO₂. The mixtures were shaken for 15 min and the water was then evaporated, in vacuum, at temperature of 120 °C.

Elemental analysis

The organic phase content on dabcosil silsesquioxane was obtained using a CHN Perkin Elmer M CHNS/O Analyzer, model 2400. The analysis was made in triplicate, after heating the material at 100 °C, under vacuum, for 1 hour. The amount of dabcosil groups presents on the dabcosil-AlSiO₂ surface was estimated as follows: the material was immersed in HNO₃ solution, under stirring, the acid solution was then submitted to chloride potentiometric titration with silver nitrate, using calomel electrode, as reference. The aluminum content in the Al/SiO₂ was estimated employing EDS (electron dispersive spectroscopy) analysis using a Noran detector in JEOL equipment, model JSM 5800, with 20 kV and acquisition time of 100 s and 800x of magnification.

FTIR analysis

Samples of silica gel, aluminum oxide grafted onto silica gel (Al/SiO₂) and dabcosil silsesquioxane grafted onto Al/SiO₂ materials were submitted to transmission FTIR using an IR cell described elsewhere in detail [7]. Self-supporting disks of materials with an area of 5 cm², weighing ca. 100 mg, were prepared. The disks were heated for 1 hour at 150 °C, under vacuum of 1 Pa (near 10⁻² torr). The spectra were obtained using a Shimadzu equipment model FTIR 8300, with 4 cm⁻¹ of resolution and 100 scans.

Pore size distribution

The pore size distribution was obtained by the N_2 adsorption-desorption isotherm, determined at liquid nitrogen boiling point, using a homemade

volumetric apparatus, connected to turbo molecular Edwards vacuum line system, employing a Hg capillary barometer. The apparatus is frequently checked with alumina standard reference. The hybrid material was previously degassed at 150 °C, in vacuum, for 2 h. The data analysis was made using the BJH (Barret, Joyner, and Halenda) method [21].

Surface area

The specific surface area of the previous degassed solid at 150 °C, under vacuum, was determined by the BET (Brunauer, Emmett and Teller) multipoint technique [22], in the volumetric apparatus cited above, using nitrogen as probe, in triplicate.

Chromium (VI) uptake by the dabcosil-Al/SiO₂

An aliquot of 20.00 ml of 20.00 – 1000.0 mg l⁻¹ Cr (VI) (in CrO₄²⁻ form at pH 6.0) was added to a conical plastic tube (117mm height, 30 mm diameter) containing 50.0 mg of dabcosil-Al/SiO₂. The flasks were capped, in poured horizontally in a horizontal shaker and agitated for 3 h. Afterwards the flasks were filtered, using glass filter provided with Whatman filter paper, in order to separate the adsorbent from the aqueous solution, and aliquots of 1-5 ml the supernatant were properly diluted to 50-100 ml in calibrated flasks using water. The chromium final concentrations were spectrophotometrically determined using diphenylcarbazide at 540 nm [23], after multiplying the measured concentration value found in the solution after the adsorption procedure, by the proper dilution factor.

The amount of Cr (VI) uptaken by the adsorbent is given by the equation 1.

$$Nf = \frac{(C_0 - C_f) \cdot V}{m} \quad (1)$$

Where Nf is the amount of metallic ion uptaken by the adsorbent (mmol g⁻¹); C₀ is the initial Cr (VI) concentration put in contact with the adsorbent (mmol l⁻¹), C_f is the Cr (VI) concentrations (mmol l⁻¹) after the batch adsorption procedure, m is the mass of adsorbent (g) and V is the volume of Cr (VI) solution put in contact with the adsorbent (l).

Results and discussion

The synthesis of the dabcosil silsesquioxane was carried out in two steps. Firstly the 3-n-propyltrimethoxysilane-1-azonia-4-azabicyclo[2.2.2]octanechloride was obtained from a presumable SN₂ reaction of dabco with CPTMS. In a second step, this compound was added to a TEOS solution to gelation, as already reported [19]. The product of the gelation reaction, 3-n-propyltrimethoxysilane-1-azonia-4-azabicyclo[2.2.2]octanechloride silsesquioxane (dabcosil silsesquioxane) was submitted to CHN elemental analysis and the estimated organic phase content was 3.3 mmol of dabcosil groups per gram. Considering the high water solubility of the dabcosil silsesquioxane [20] it could be immobilized on the Al/SiO₂ matrix having an Al/Si atomic ratio of 0.21, determined by EDS analysis. The dabcosil groups present on dabcosil-Al/SiO₂, estimated by using chloride potentiometric titration, was 0.28 mmol of dabcosil pendant groups per gram of AlSiO₂ matrix.

The infrared spectra of the pure silica (SiO₂), aluminum oxide grafted onto silica surface (Al/SiO₂) and dabcosil grafted onto Al/SiO₂ surface (dabcosil-Al/SiO₂) are shown in the Figure 1. It is possible to observe in the pure

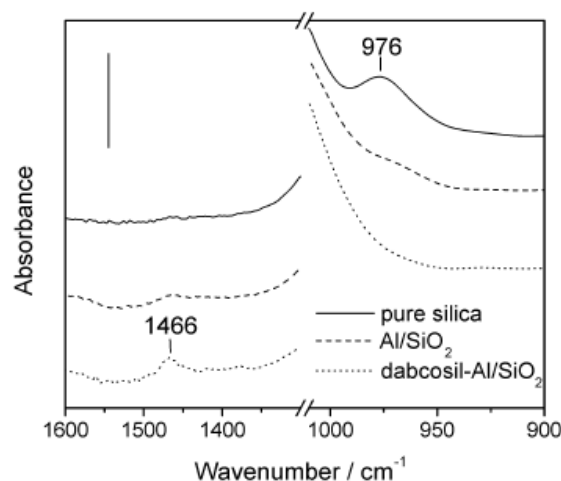


Figure 1. Infrared absorbance spectra obtained at room temperature after being heated at 150 °C, in vacuum, for two hours. a) SiO₂; b) Al/SiO₂; c) dabcosil-Al/SiO₂. The bar value is 0.5.

were available on the surface of the material that were able for ion exchange. On the other hand, in previous reports of synthesis of dabco by the sol-gel method [14], the dabco groups were not completely available for adsorption that resulted in a decrease in the maximum amount of metallic ion uptake by the adsorbent.

Conclusion

The water soluble 3-n-propyl-1-azonia-4-azabicyclo[2.2.2]octanechloride silsesquioxane was immobilized on silica previously modified with aluminum oxide in a highly dispersed form. The dabcosil-Al/SiO₂ material showed to be a

good adsorbent for Cr (VI) uptake from aqueous solution, where for each two mmol dabcosil group grafted at the Al/SiO₂ matrix was able to adsorb one mmol of Cr (VI) as chromate from aqueous solution, suggesting an ion exchange mechanism.

Acknowledgement

We thank to Capes, CNPq and FAPERGS for financial support and grants.

Recebido em: 05/04/2006

Aceito em: 31/05/2006

L. T. Arenas, N. M. Simon, Y. Gushikem, T. M. H. Costa, E. C. Lima, E. V. Benvenutti. Silsesquioxano solúvel em água, cloreto de 3-n-propil-1-azônia-4-azabicyclo[2.2.2]octano, enxertado sobre a superfície de Al/SiO₂. Estudo da adsorção de cromo.

Resumo: O material octanocloreto de 3-n-propil-1-azonia-4-azabicyclo[2.2.2] silsesquioxano (dabcosil silsesquioxano) solúvel em água foi obtido. O dabcosil silsesquioxano foi enxertado na superfície da sílica, previamente modificada com óxido de alumínio. O material sólido resultante dabcosil-Al/SiO₂, apresentou 0,15 mmol de grupamentos dabco por grama do material. O produto enxertado foi caracterizado por espectroscopia de infravermelho, e isotermas de adsorção-dessorção de N₂. O material dabcosil-Al/SiO₂ foi utilizado como sorvente para a adsorção de chromium(VI) em soluções aquosas.

Palavras-chave: dabco; sol-gel; cromo (VI).

References

- [1] U. Deschler, P. Kleinschmit, P. Panster, *Angew. Chem. Int. Ed. Engl.* 25 (1986) 236.
- [2] M. Petro, D. Berek, *Chromatographia* 37 (1993) 549.
- [3] M. Zougagh, J. M. C. Pavon, A. G. de Torres, *Anal. Bioanal. Chem.* 381 (2005) 1103.
- [4] E. M. Soliman, M. E. Mahmoud, S. A. Ahmed, *Talanta* 54 (2001) 243.
- [5] N. H. Arakaki, C. Airolti, *Quim. Nova* 22 (1999) 246.
- [6] M. A. Lazarin, Y. Gushikem, *J. Braz. Chem. Soc.* 13 (2002) 88.
- [7] J. L. Foschiera, T. M. Pizzolato, E. V. Benvenutti, *J. Braz. Chem. Soc.* 12 (2001) 159.
- [8] Y. Khoroshevskiy, S. Komeev, S. Myerniy, Y. V. Kholin, F. A. Pavan, J. Schifino, T. M. H. Costa, E. V. Benvenutti, *J. Colloid Interface Sci.* 284 (2005) 424.
- [9] J. Seneviratne; J. A. Cox, *Talanta*, 52 (2000) 801.
- [10] M. C. Burleigh, S. Dai, E. W. Hagaman, J. S. Lin, *Chem. Mater.* 13 (2001) 2537.
- [11] A. A. S. Alfaya, L. T. Kubota, *Quim. Nova* 25 (2002) 835.
- [12] S. V. M. de Moraes, M. T. Laranjo, M. Z. Tania M. H. Costa, M. R. Gallas, E. V. Benvenutti, *Appl. Phys. A* 81 (2005) 1053.
- [13] D. S. F. Gay, Y. Gushikem, C. C. Moro, T. M. H. Costa, E. V. Benvenutti, *J. Sol-gel Sci. Technol.* 34 (2005) 189.
- [14] L. T. Arenas, J. C. P. Vaghetti, E. C. Lima, C. C. Moro, E. V. Benvenutti, T. M. H. Costa, *Mater Lett* 58 (2004) 895.
- [15] K. J. Shea, D. A. Loy, *Chem. Mater.* 13 (2001) 3306.
- [16] R. G. J. Curriu, D. Leclercq, *Angew. Chem. Int. Ed. Engl.* 35 (1996) 1420.
- [17] R. V. S. Alfaya, Y. Gushikem, A. A. S. Alfaya, *J. Braz. Chem. Soc.* 11 (2000) 281.
- [18] S. T. Fujiwara, Y. Gushikem, R. V. S. Alfaya, *Colloids*

- Surf A: Physicochem. Eng. Aspects 178 (2001) 135.
- [19] L. T. Arenas, T. A. S. Aguirre, A. Langaro, Y. Gushikem, E. V. Benvenutti, T. M. H. Costa, *Polymer* 44 (2003) 5521.
- [20] L. T. Arenas, A. Langaro, Y. Gushikem, C. C. Moro, E. V. Benvenutti, T. M. H. Costa, *J. Sol-Gel Sci. Technol.* 28 (2003) 51.
- [21] E. P. Barret, L. G. Joyner, P. P. Halenda, *J. Am. Chem. Soc.* 73 (1951) 373.
- [22] S. Brunauer, P. H. Emmett, E. Teller, *J. Am. Chem. Soc.* 60 (1938) 309.
- [23] J. L. Brasil, R. R. Ev, C. D. Milcharek, L. C. Martins, F. A. Pavan, A. A. dos Santos Jr., S. L. P. Dias, J. Dupont, C. P. Z. Noreña, E. C. Lima, *J. Hazard. Mater.* 133, (2006) 143.
- [24] A. Fidalgo, L. M. Ilharco, *J. Non-Cryst. Solids* 283 (2001) 144.
- [25] J. M. D. Cónsul, I. M. Baibich, E. V. Benvenutti, D. Thiele, *Quim. Nova* 28 (2005) 393.
- [26] C. J. Pouchert, *The Aldrich Library of Infrared Spectra*, Aldrich Chem. Comp., Edition III, Wisconsin, 1981.

- 4.6- Synthesis of silica xerogels with high surface area using acetic acid as catalyst. *Journal of the Brazilian Chemical Society*. Aceito, **2007**.

Synthesis of Silica Xerogels with High Surface Area Using Acetic Acid as Catalyst

Leliz T. Arenas^a, Carolina W. Simm^a, Yoshitaka Gushikem^b, Silvio L. P. Dias^a,
Celso C. Moro^a, Tania M. H. Costa^a*, Edilson V. Benvenutti^a

^a Instituto de Química, Universidade Federal do Rio Grande do Sul, CP 15003, 91501-970
Porto Alegre - RS, Brasil.

^b Instituto de Química, Universidade Estadual de Campinas CP 6154, 13084-971 Campinas -
SP, Brasil

- Corresponding Author

Edilson V. Benvenutti
benvenutti@iq.ufrgs.br
Phone: 55 51 3316 7209
Fax: 55 51 33167304

Tania M. H. Costa
taniaha@iq.ufrgs.br
Phone: 55 51 33166279
Fax: 55 51 33167304

Abstract

The influence of acetic acid on the pore structure and surface area of silica prepared by the sol-gel method was investigated. Experimental conditions of synthesis such gelation temperature and solvents were also studied. N₂ adsorption isotherms of the samples were type 1, typical of microporous materials, explaining the high surface area values (BET) observed. The simultaneous addition of acetic and hydrochloric acids as catalysts, acetone as solvent, and using gelation temperature of 20 °C, made possible to prepare amorphous silica materials with surface area values up to 850 m² g⁻¹. The high surface area value of these samples could be explained mainly by the microporosity and also by the nanometric size of particles.

Nesse trabalho foi estudada a influência do ácido acético na estrutura de poros e na área superficial em sílicas preparadas pelo método sol-gel. Condições experimentais de síntese tais como temperatura de policondensação e solventes também foram estudadas. Isotermas de adsorção de N₂ das amostras foram classificadas como do tipo 1, típicas de materiais microporosos, o que explica os altos valores de área superficial obtidos. A adição simultânea dos catalisadores, ácidos acético e clorídrico, acetona como solvente, e temperatura de policondensação de 20 °C possibilitaram preparar sílicas amorfas com valores de área superficial de até 850 m² g⁻¹. O alto valor de área superficial dessas amostras pode ser explicado principalmente pela microporosidade e também pelo tamanho nanométrico das partículas.

Keywords

Silica, microporous materials, high surface area, acetic acid

Introduction

Inorganic materials possessing high surface area have been very studied due to its possible application as sorbents, catalysts, sensors, molecular sieves, etc.¹⁻⁴ In general, these materials were formed mainly by silicon and aluminum oxides, with ordered structures like those presented by zeolites and clays. Starting from the nineties, with the appearance of a new class of highly ordered silica mesopore materials called MCMs, the interest in high surface area silicas was renewed.⁵⁻⁸ Several synthesis methods aiming to obtain materials with high surface area and tailored pore size in the micro, meso and macropore range have been proposed. Among the proposed methods the sol-gel synthesis appears as an interesting alternative process to obtain these materials.⁹⁻¹¹ This method that is based on hydrolysis and polycondensation of silicon or metals alcoxides, allows the preparation of materials with different morphological characteristics varying the experimental synthesis conditions like pH, solvent, temperature and catalyst.^{9,12,13} The reaction medium can be acid, neutral or basic, depending on the inorganic catalyst added, like HCl, HF or NH₃.¹⁴ Organic catalysts as citric and acetic acids have been also used.¹⁵⁻¹⁷ Anionic and cationic surfactants, as well as water soluble polymers have been also added to sol-gel system to obtain materials with controlled porosity.^{18,19}

It was reported the use of acetic acid as catalyst in several sol-gel systems, like the synthesis of high purity dense silica glass microspheres^{20,21} photoluminescence lanthanide doped silica microspheres with controllable size,²² silica based hybrid materials^{17,23} and titania based systems.^{24,25} Although the mechanism of the acid acetic action is not completely known, it was already well studied in several works as follows. It was firstly proposed by Pope and Mackenzie²⁶ that the acetic acid solvolysis occurs by a two steps mechanism involving the formation of ester as intermediate. In sequence, it was established a consent about the formation of intermediate metal acetate species.^{15,17,24} For pure silica systems, besides to produces acid catalysis, the acetic acid can influence in the kinetic of policondensation, decreasing the speed of reaction and consequently influencing in the primary particle growing of the gel, or causing a narrow particle diameter distribution.^{15,16} In previous work of our research group,²⁷ we had observed that in silica/cellulose sol-gel systems, the presence of acetic acid produced high surface area hybrid materials and as far as we know this fact was not been reported yet. Thus, we believe that the acetic acid can be more explored as an important factor in the sol-gel synthesis for controlled pores size and high surface area materials.

In this work, it was investigated the effects of the acetic acid presence on the pore structure and surface area of silica xerogels. Some experimental conditions such solvent used and gelation temperature were studied.

Experimental

Synthesis of silica xerogels

Two sample series of silica xerogel were prepared by the sol-gel method based on the hydrolysis and polycondensation of tetraethylorthosilicate (TEOS) in acid medium. The Table 1 summarizes the synthesis conditions of the silica xerogel samples of the first series. They were obtained starting from 22 mmol of TEOS dissolved in the solvent specified in the Table 1. Afterwards, the catalyst and water, in stoichiometric ratio with Si $r = 4/1$ (1.6 ml), were added to the precursor solutions, under stirring, except the sample A that was synthesized without water. The samples were left for gelation and solvent evaporation, just covered without sealing, for two weeks at 20 ± 5 °C. The xerogels obtained were comminuted in an agate mortar, washed with 10 mL of water and ethanol and dried in an oven at 100 °C. Nine samples were prepared, varying the solvent and the used catalyst, glacial acetic acid and HCl solution 0.1 mol L^{-1} , according to Table 1.

The second series was obtained using the experimental conditions of the sample E, varying the gelation temperature. It was used 5, 15, 20, 25, 30 and 50 ± 1 °C. The more precise temperature used in this sample series was attained using thermostated system containing water or oil bath. The same gelation and washing procedures above explained were used for this sample series.

N₂ adsorption-desorption isotherms

The nitrogen adsorption-desorption isotherms of previous degassed xerogels, at 150 °C, were determined at liquid nitrogen boiling point in a homemade volumetric apparatus, connected to a vacuum line system employing a turbo molecular Edward vacuum pump. The

pressure measurements are made using capillary Hg barometer. The specific surface areas of hybrid materials were determined from the BET (Brunauer, Emmett and Teller) multipoint method²⁸ and the pore size distribution was obtained using BJH (Barret, Joyner, and Halenda) method.²⁹

SAXS analyses

Small angle X-ray scattering (SAXS) data were obtained on a Shimadzu XD3A equipment, using the Cu K α radiation source. The average pore radii of the samples were obtained by using the Guinier law.^{30,31} This law establish that the scattering intensities $I(q)$ are described as $\ln I(q) = \ln I_0 - (RG^2 q^2) / 3$, where RG is the gyration radii and q is defined as $q = (4\pi \sin\theta) / \lambda$, where θ is the scattering angle and λ the wavelength of the x-ray used. The gyration radii could be calculated by the equation $RG = (3p)^{1/2}$, where p is the slope of the Guinier plot, ($\ln(q)$ vs q^2). Considering spherical pores the pore radii were obtained by the equation $R_p = (5/3)^{1/2} RG$.

TEM analyses

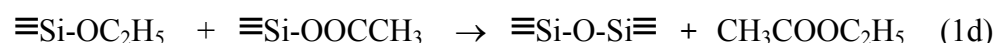
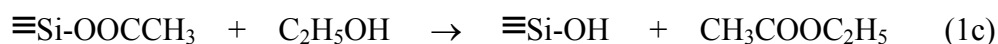
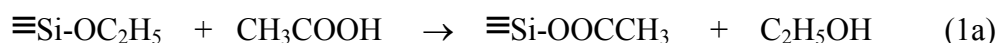
Transmission Electron Microscopy images were obtained in a JEOL apparatus, model JEM 2010 with acceleration voltage of 200 kV, using powdered samples. The magnification used was up to 500,000 times. The samples were ground as very fine powder in an agate mortar, dispersed in isopropyl alcohol and ultrasonicated for 20 minutes. The samples were settled over a copper grid for analysis.

Results and discussion

The results of surface area, pore volume and gelation time of the first sample series are showed on Table 2. In a general way, in the present work, the samples catalyzed only with acetic acid, samples B, C and D of the Table 1, present higher surface area values, near twice, than those catalyzed only by hydrochloric acid, samples G, H and I, (near 370 m² g⁻¹). One exception is the sample A which was synthesized with acetic acid but without initial water

addition, for which the surface area obtained was $440 \text{ m}^2 \text{ g}^{-1}$. For all the other samples, it was added an initial water amount. The highest surface area value was obtained for sample E, when both acid catalysts were used at the same time, and acetone as solvent, being this value $825 \text{ m}^2 \text{ g}^{-1}$. Additionally, it can be observed in the Table 1 that for the samples E and F, where hydrochloric and acetic acids were simultaneously used, the gelation time was lower than those observed for samples catalyzed by acetic acid only.

It was already reported that the use of acetic acid in silica sol-gel systems can produces changes in the microstructure and final characteristics of the materials, such as control in the particle size distribution.^{15,16} The silica sol-gel films obtained are crack-free and show optical transparency.^{16,17} Although the mechanisms which govern the materials formation are not well known, there is a general consensus about the formation of the species $\equiv\text{Si-OOCCH}_3$ and $\text{CH}_3\text{COOC}_2\text{H}_5$ in TEOS/ethanol systems. The $\equiv\text{Si-OOCCH}_3$ species were identified by infrared spectroscopy.^{15,20} It was proposed that in the presence of acetic acid several reactions steps could occur, which are showed in the Scheme 1.^{15,17}



It was observed that the addition of acetic acid in sol-gel silica systems produces a reduction on the gelation kinetics in comparison when inorganic acids are added. This effect can be overcome by the addition of water, however the water also influences the microstructure of the materials.^{13,17,32} Based on results obtained in previous works, the water/TEOS molar ratio used was 4:1, since the use of this molar ratio resulted in hybrid or pure silica xerogels having high surface area.^{5,13,32}

Figure 1 shows the N_2 adsorption isotherms for the first sample series. It can be seen that all curves are type 1 isotherms, typical of microporous materials.³³ This result can explain the high surface area values observed for this sample series.

Considering that the high surface area value of the silica xerogels was obtained for sample E, where acetone was used as solvent and acetic and hydrochloric acids as catalysts we decided to study this xerogel sample preparation in a more detailed way. In previous

works it was observed for silica based hybrid systems that the gelation temperature is an important parameter in determining surface area values.^{12,34} In those papers, it was reported a decreasing in surface area values with the increasing of temperature from room up to 50 °C, being this fact accompanied by an increasing in organic incorporation of the xerogels. In the present paper it was prepared a second series of pure silica maintaining the experimental conditions of the sample E and varying the gelation temperature in a more controlled way. The used values were 5, 15, 20, 25, 30 and 50 ± 1 °C. For this new sample series, the samples obtained were named E5, E15, E20, E25, E30 and E50, respectively. The surface area values for these samples are presented in Table 3. The highest surface area value attained was of 850 m² g⁻¹ for the sample submitted to gelation temperature of 20 °C (sample E20). For lower temperatures occurred a decreasing in surface area and for higher temperatures there is also a slight decreasing according to the results cited above, already reported for silica based hybrid materials.^{12,34}

For the sample E20, that present the higher surface area value, we decided to improve the characterization. The pore size was determined by using SAXS analysis. From the Guinier plot it was possible to adjust the curve with a linear fitting presenting slope of -0.2598. The radii value obtained was 1.1 nm. It was also obtained transmission electron microscopic images showed in the Figure 2. It is possible to see that, at this magnification, the silica xerogel sample E20 present particles with diameter lower than 50 nm.

Although the high specific surface area value for this sample is mainly due to the microporosity contribution as observed from the N₂ isotherms (Figure 1 and Tables 2 and 3), there is also a contribution of external area of the nanometric size of the xerogel particles, observed on TEM images. Additionally, these observed nanostructures could be agglomerates presenting internal structures, and the surface area contribution of these presumable primary particles can not be discarded.

Considering morphological aspects, the main papers published about the silica/acetic acid system report the preparation of microspheres with controlled size and shape.^{15,20-22} In our case the materials presented different characteristics not observed up to now, like very high surface area and nanometric particle size with diameter between 20 and 50 nm. Although the ratios water / acetic acid / TEOS used were the same, 4:4:1 there are important experimental differences in synthesis method as follows: in cited papers it was not used solvents and the reaction was performed under vigorous stirring. On the other hand, in the

present work it was used ethanol and acetone as solvents to promote homogeneity considering that water and TEOS are immiscible.

Conclusions

The use of acetic acid in sol-gel silica systems was satisfactory to obtain high surface area microporous materials without addition of any template. The simultaneous addition of acetic and hydrochloric acids as catalysts and acetone as solvent, made possible to prepare amorphous silica materials with surface area values up to $850 \text{ m}^2 \text{ g}^{-1}$, taking a gelation time of two days. The gelation temperature also influences the surface area, being the highest value attained at gelation temperature of $20 \text{ }^\circ\text{C}$. For this material, the estimated micropore radius, obtained by SAXS, was 1.1 nm and the observed particle size was below 50 nm. The high surface area value of this sample could be explained mainly by the microporosity and also by the nanometric size of particles.

Acknowledgements

We thank to FAPERGS (Fundação de Amparo à Pesquisa no Estado do Rio Grande do Sul, Brasil) and CNPq (Conselho Nacional de Desenvolvimento Científico e Tecnológico, Brasil), for financial support and grants. We thank to CME – Centro de Microscopia Eletrônica -UFRGS for the use of the TEM.

References

1. Schuth, F.; *Annu. Rev. Mater. Res.* **2005**, *35*, 209.
2. Corma, A.; *Chem. Rev.* **1997**, *97*, 2373.
3. Adebajo, M. O.; Frost, R. L.; Klopogge, J. T.; Carmody, O.; Kokot, S.; *J. Porous Mater.* **2003**, *10*, 159.
4. Valdes, M. G.; Perez-Cordoves, A. I.; Diaz-Garcia, M. E.; *Trends Anal. Chem.* **2006**, *25*, 24.
5. Kato, M.; Shigeno, T.; Kimura, T.; Kuroda, K.; *Chem. Mater.* **2005**, *17*, 6416.
6. Xiao, F. S.; *Top. Catal.* **2005**, *35*, 9.
7. Su, B. L.; Léonard, A.; Yuan, Z. Y.; *Chimie* **2005**, *8*, 713.

8. Kresge, C. T.; Leonowicz, M. E.; Roth, W. J.; Vartuli, J. C.; Beck, J. S.; *Nature* **1992**, 359, 710.
9. Shea, K. J.; Loy, D. A.; *Chem. Mater.* **2001**, 13, 3306.
10. Burleigh, M. C.; Dai, S.; Hagaman, E. W.; Lin, J. S.; *Chem. Mater.* **2001**, 13, 2537.
11. Kato, M.; Sakai-Kato, K.; Toyooka, T.; *J. Sep. Sci.* **2005**, 28, 1893.
12. Gay, D. F. S.; Gushikem, Y.; Moro, C. C.; Costa, T. M. H.; Benvenutti, E. V.; *J. Sol-Gel Sci. Technol.* **2005**, 34, 189.
13. Azolin, D. R.; Celso, C. C.; Costa, T. M. H.; Benvenutti, E. V. B.; *J. Non-Cryst. Solids* **2004**, 337, 201.
14. Brinker, C. J.; Scherer G. W.; *Sol-Gel Science*, Academic Press; London, 1990.
15. Karmakar, B.; De, G.; Kundu, D.; Ganguli, D.; *J. Non-Cryst. Solids* **1991**, 135, 29.
16. Liu, Y.; Ren, W.; Zhang, L.; Yao, X.; *Thin Solid Films*, **1999**, 353, 124.
17. Stathatos, E.; Lianos, P.; Orel, B.; Vuk, A. S.; Jese, R.; *Langmuir*, **2003**, 19, 7587.
18. Raman, N. K.; Anderson, M. T.; Brinker, C. J.; *Chem. Mater.* **1996**, 8, 1682.
19. Xiao, F. S.; *Current Opinion in Colloid Interface Sci.* **2005**, 10, 94.
20. Karmakar, B.; De, G.; Ganguli, D.; *J. Non-Cryst. Solids*, **2000**, 272, 119.
21. Moran, C. E.; Hale, G. D.; Halas, N. J.; *Langmuir*, **2001**, 17, 8376.
22. De, G.; Karmakar, B.; Ganguli, D.; *J. Mater. Chem.*, **2000**, 10, 2289.
23. Bekiari, V.; Lianos, P.; *Chem. Mater.*, **1998**, 10, 3777.
24. Ivanda, M.; Music, S.; Popovic, S.; Gotic, M.; *J. Mol. Struct.*; **1999**, 480-481, 645.
25. Birnie, D. P.; *J. Mater. Sci.*, **2000**, 35, 367.
26. Pope, E. J. A.; Mackenzie, J. D.; *J. Non-Cryst. Solids*, **1986**, 87, 185.
27. Arenas, L. T.; Correa, C. P.; Gushikem, Y.; Dias, S. L. P.; Costa, T. M. H.; Benvenutti, E. V. *Abstracts of the Congresso Latino Americano de Química*, Salvador, Brazil, 2004.
28. Brunauer, S.; Emmett, P. H.; Teller, E.; *J. Am. Chem. Soc.* **1938**, 60, 309
29. Barret, E. B.; Joyner, L. G.; Halenda, P. P.; *J. Am. Chem. Soc.* **1951**, 73, 373.
30. Guinier, A.; Fournet, G.; *Small-Angle Scattering of X-Ray*, Wiley, New York, 1955.
31. Glatter, O.; Kratky, O.; *Small Angle X-Ray Scattering*, Academic press, London, 1982
32. Xi, Y.; Liangying, Z.; Sasa, W.; *Sens. Actuators B* **1995**, 24-25, 347.
33. Gregg, S. J.; Sing, K. S. W.; *Adsorption, Surface Area and Porosity*, Academic Press, London, 1982.
34. Pavan, F. A.; Hoffmann, H. S.; Gushikem, Y.; Costa, T. M. H.; Benvenutti, E. V.; *Mater. Lett.* **2002**, 55, 378.

Table 1: Experimental conditions of silica xerogel syntheses of the first sample series

Sample	Solvent	Total solvent volume / mL	Catalyst	Catalyst volume / mL
A ^a	Acetone	5	acetic acid	5
B	Acetone	5	acetic acid	5
C	acetone:ethanol (1:1)	5	acetic acid	5
D	Ethanol	5	acetic acid	5
E	Acetone	5	acetic acid / HCl	5 / 0.1
F	Ethanol	5	acetic acid / HCl	5 / 0.1
G	Acetone	10	HCl	0.2
H	Ethanol	5	HCl	0.2
I	acetone:ethanol (1:1)	10	HCl	0.2

^a = without water

Table 2: Surface area and pore volume of the first xerogel series.

Sample	Surface area / $\pm 25 \text{ m}^2 \text{ g}^{-1}$	Pore volume / $\pm 0.03 \text{ cm}^3 \text{ g}^{-1}$	Gelation time / day
A	440	0.24	3
B	750	0.18	2
C	680	0.18	4
D	785	0.31	3
E	825	0.19	2
F	620	0.11	2
G	335	0.10	1
H	425	0.12	< 1
I	355	0.10	< 1

Table 3: Surface area and pore volume of the second xerogel series.

Sample	Temperature / °C	Surface area / $\pm 25 \text{ m}^2 \text{ g}^{-1}$	Pore volume / $\pm 0.03 \text{ cm}^3 \text{ g}^{-1}$	Gelation time / day
E0	0	520	0.13	14
E15	15	700	0.16	3
E20	20	850	0.24	2
E25	25	670	0.17	2
E30	30	630	0.15	1
E50	50	630	0.15	< 1

Figure captions

Figure 1: N₂ adsorption isotherms for the first sample series.

Figure 2: Transmission electron microscopic images of the sample E20.

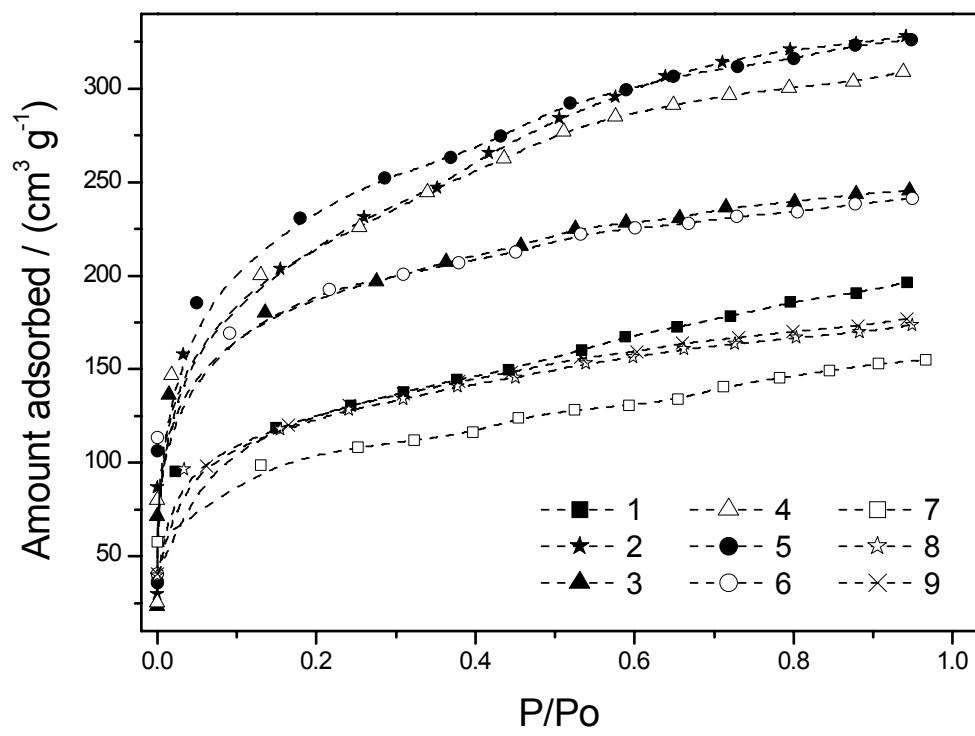


Fig 1

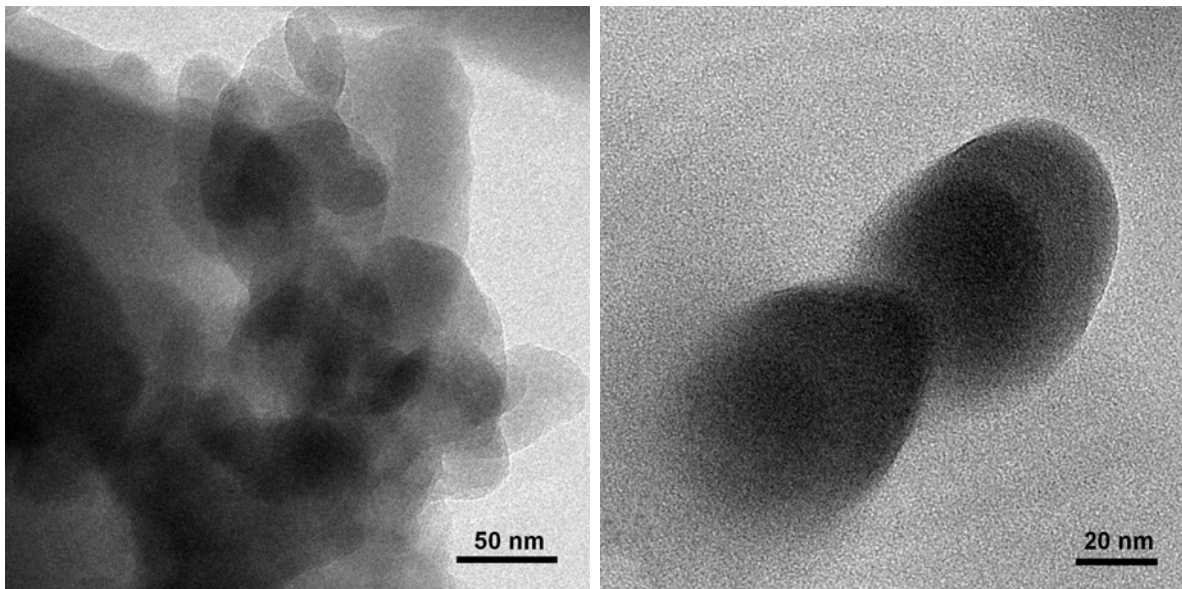


Fig 2